CRC Report No. AVFL-13

Fuel Chemistry Impacts in Gasoline HCCI

Final Report

December 2006

Updated Report, Distributed September 2007

COORDINATING RESEARCH COUNCIL, INC.
3650 MANSELL ROAD·SUITE 140·ALPHARETTA, GA 30022

COORDINATING RESEARCH COUNCIL, INC.
3650 MANSELL ROAD·SUITE 140·ALPHARETTA, GA 30022

47519 HALYARD DRIVE
PLYMOUTH, MI 48170-2438
PHONE: (734) 414 9618
FAX: (734) 414 9690

REPORT PEI 0310
December 2006

Fuel Chemistry Impacts in Gasoline HCCI (CRC Project No. AVFL-13)

Written by	Approved by	Approved by
Dr. Yuan Shen Project Engineer	Dr. Ulrich Pfahl Chief Engineer	Chris Cowland Technical Director

Distribution

Coordinating Research Council
3650 Mansell Road, Suite 140
Alpharetta, GA 30022

EXECUTIVE SUMMARY

Homogeneous charge compression ignition (HCCI) combustion offers the potential of producing diesel-like fuel economy combined with ultra-low NOx emissions in gasoline-fueled spark ignition engines. Since HCCI combustion occurs by auto-ignition of the fuel/air mixture, fuel parameters such as octane quality, composition, and distillation are likely to play a role in HCCI engine operation and performance. However, the precise impacts of these parameters are not presently known. Also unknown is what HCCI operating mode will dominate future HCCI engines. Therefore, it is the goal of this CRC AVFL13 project to quantify fuel effects for various conditions and modes of HCCI engine operation.

In this study, ten gasoline-like test fuels of varying octane quality, composition, and distillation were tested by AVL of Plymouth, MI on a single cylinder engine equipped with a hydraulic variable valve train (VVT) and a gasoline direct injection (GDI) system. These fuels were tested using three different HCCI operating modes:

- Re-compression early injection (RCEI),
- Re-compression split injection (RCSI), and
- Re-breathing early injection (RBEI).

For each mode, three engine operating conditions were investigated:

- 1.5 bar IMEP at 1000 rpm,
- 3 bar IMEP at 2000 rpm, and
- 5.5 bar/deg of maximum rate of pressure rise at 3000 rpm (IMEP's very near 3 bar).

These three operating conditions represent, respectively: near-idle conditions, mid-HCCI load conditions, and high-speed HCCI conditions. At higher engine loads, it is anticipated that an HCCI engine will switch to normal closed-loop spark-ignition operation.

The ten gasoline-like test fuels were blended from four common refinery streams normally used to blend commercial gasolines: (A) reformate [about 55% aromatic], (B) alkylate [about 88% iso-paraffin], (C) cat cracker gasoline [about 45% olefin], and (D) straight run gasoline [about 24% normal paraffin] (n-paraffin). Although there are other refinery streams available for gasoline blending, the four streams selected reflect the most commonly used blend stocks in finished gasoline. The only other blending component used in the test fuels was normal butane (n-C4). Normal butane was added to bring each test fuel up to a consistent, nominal 7 psi vapor pressure. This was done as a safety precaution since some of the blends had an RVP so low that there was a concern that an explosive mixture could occur in the vapor space when using the fuels.

The recipes for blending these four refinery streams to produce the ten test fuels were determined by first using a proprietary blending model to generate a set of 56 potential test fuels where the research octane quality was set at or near three levels (92, 65 to 70, and a mid level), and the composition (aromatics, olefins, n-paraffins, and iso-paraffins) and distillation temperatures were varied over as large a range as possible. The final

ten blending recipes were then selected using an experimental-design statistical procedure that maximized the spread in fuel parameters (octane, composition, and distillation) while minimizing fuels with similar properties and statistically representing all fuel candidates. The nine fuel parameters used in the statistical analysis were: research octane number, octane sensitivity, temperature at which ten percent of the fuel evaporates (T10), temperature at which ninety percent of the fuel evaporates (T90), % aromatics, % iso-paraffins, % n-paraffins without butane, % butane, and % olefins. The following table summarizes the measured values of the nine key fuel properties for each of the ten fuels tested.

Table ES.1: Summary of Key Measured Fuel Properties for Ten Tested Fuels[1]

Fuel / Fuel Properties	A100	B100	C100	B50D50	C85D15	B77D23	B30D70	A79D21	C50D50	A33D67
RON	95.53	89.07	91.45	58.93	87.68	81.04	64.73	84.01	77.96	65.50
Sensitivity	10.69	-0.18	11.13	-2.13	10.42	-0.84	1.06	7.85	6.45	2.70
T10 (F)	174.6	153.5	133.7	187.0	138.6	158.9	172.8	181.9	146.7	191.1
T90 (F)	327.2	338.4	255.7	420.8	297.1	337.1	344.1	329.5	319.8	338.5
Aromatics	55.0%	2.8%	10.8%	7.9%	16.7%	3.0%	10.6%	41.0%	18.2%	25.9%
Iso Paraffins	27.3%	88.1%	30.1%	42.4%	28.7%	77.1%	50.9%	31.0%	31.3%	29.2%
Normal Paraffins without Butane	10.2%	0.6%	4.1%	20.6%	6.0%	5.9%	16.0%	14.3%	12.2%	19.6%
Butane	2.3%	4.4%	0.2%	8.0%	0.9%	6.6%	6.3%	3.6%	4.0%	6.2%
Olefins	2.1%	0.8%	44.7%	1.1%	36.9%	0.9%	1.4%	1.8%	18.2%	2.1%

[1] The test fuels are blends of refinery streams A, B, C, and D. For example, B50D50 is 50/50 blend of streams B and D.

The first step in the engine testing was to determine the baseline engine operating conditions (valve timings, fuel-rail pressure, single injection timing, split injection timings and quantities, and overall fueling quantities). These baseline tests were conducted for each HCCI mode and for each of the three operating conditions for each mode. Indolene was used as the fuel for these baseline tests. These baseline engine-operating conditions were the starting conditions for testing each of the test fuels and then only the valve timings were changed to achieve the required operating conditions (primarily combustion phasing and engine load). Four repeatability tests with indolene were interspersed in the test fuel matrix to assure the engine operation remained consistent throughout testing. The engine parameters of interest in both the baseline testing and test fuel testing were: indicated specific fuel consumption (g/kWh), NO_x emissions (ppm), indicated specific hydrocarbon emission (g/kWh), indicated specific carbon monoxide emission (g/kWh), filter smoke number (size), combustion duration (degrees), combustion noise (dB), coefficient of variance of IMEP (%), peak cylinder pressure (bar), and exhaust valve closing angle (degrees).

RESULTS -

The repeatability tests with indolene showed test-to-test variability correlated with engine operating parameters which were measured but could not be precisely controlled. To account for variations in operating conditions, a backward, step-wise multiple regression analysis was performed on the indolene data to develop normalization models to adjust each relevant engine parameter for every test fuel prior to further data analysis. This normalization procedure was found to reduce the overall variability in the test-fuel data. This procedure assumes that the test fuel response to minor changes in engine operating conditions is the same as is indolene's response.

It was desired to perform a statistical analysis for each of the ten engine performance

parameters listed previously as a function of the nine fuel parameters for each of the nine engine test conditions (1000 rpm, 2000 rpm, and 3000 rpm each tested at the three HCCI modes: RCEI, RCSI, and RBEI) examined. Because of the limited number of test fuels (10) compared to the number of fuel parameters of interest (9), it was not feasible to construct a statistical model to estimate the effects of all nine fuel properties and their interactions on each performance measure. Instead, regression models were fit to all 36 possible combinations of two fuel properties and their interaction. Separate models were fit for each of the nine combinations of engine speed and mode. This approach uses four degrees of freedom for estimating model parameters and leaves six for estimating the error variances.
The model results were reviewed to identify the "best" model. The first step in this process was to identify only models with an overall F-Test p-value of 0.1 or less. These may be considered potentially explanatory of the observed variability in the performance parameter. Then these models within each speed and mode condition were ranked from lowest to highest R^2 value and the two-factor model with the highest sum of ranks across the nine speed and mode conditions was identified as "best". This method placed strong weight on a two-factor model that was both highly explanatory of observed variability (i.e., high R^2) and consistently explanatory across all speeds and modes (i.e., high sum of ranks).

For all ten engine parameters there was no universally "best" model in which all individual speed/mode regressions were highly statistically significant ($p < 0.05$). However, there were several cases where subgroups of speed/mode conditions did exhibit statistically significant results. These were further evaluated to determine if they showed consistency in level of significance and form of relationship (i.e., increase in fuel property produces same response in different models). The most important and significant of these parameters are discussed individually below. Following that discussion is a summary table with the results for these parameters and a summary of the statistical modeling results for the remaining parameters.

Indicated Specific Fuel Consumption

The "best" two-factor statistical model to predict indicated specific fuel consumption (ISFC) was for the fuel properties percent aromatic content and percent iso-paraffin content. This two-factor model with interaction had the highest R^2 of any two-factor model in five of the six speed/mode combinations at 2000 and 3000 rpm. In three of these six cases, the overall model p-value was less than 0.05 and in all six cases, the overall model p-value was less than 0.2. Furthermore, the coefficients of the model parameters were generally consistent among the six conditions.

Increases in both aromatics and iso-paraffins in the model were associated with poorer ISFC in the range of the fuel properties for the ten test fuels. The magnitude of this effect varied depending on the particular speed/mode model and on the joint distribution of aromatic and iso-paraffin values. From the statistical models and within the range of the ten fuels tested:

- Lowest ISFC was seen for fuels with low aromatics (<30%) and low iso-paraffin (<50%), averaging about 203 g/kWh. In this region, an increase of 1 percentage point in aromatics results in poorer ISFC by 0.1 to 0.8%. An increase of 1 percentage point in iso-paraffins results in poorer ISFC by 0.2 to 1.1%.

- Highest ISFC was seen for fuels with high aromatics (>30%) and low iso-paraffin (approximately 30%), averaging about 218 g/kWh. This region shows greater sensitivity to changes in iso-paraffins. An increase of 1 percentage point in aromatics results in poorer ISFC by 0.1 to 0.4%. An increase of 1 percentage point in iso-paraffins results in poorer ISFC by 0.9 to 2.0%.
- The remaining fuels fit into a range with simultaneously low aromatics (<15%) and high iso-paraffins (>50%), with average ISFC about 216 g/kWh. This region shows greater sensitivity to changes in aromatics. A 1 percentage point increase in aromatics increases fuel consumption by 0.4 to 2.3%. A 1 percentage point increase in iso-paraffins increases fuel consumptions by less than 0.5%.

The ISFC relationship with aromatics and iso-paraffins was further linked to engine operational parameters. Fuels with either high aromatics or high iso-paraffins generally exhibited earlier exhaust valve close, increasing the amount of residual gas in the cylinder at the beginning of compression. These same fuels produced smaller average lambdas (air/fuel ratio). These facts may help explain the poorer fuel efficiency for fuels with high aromatics or iso-paraffins.

The results for indicated specific fuel consumption at 1000 rpm were much less clear. No two-factor model was statistically significant for the RCEI mode and the models that were significant for the 1000 rpm RBEI and RCSI modes were not consistent with each other or with the 2000 or 3000 rpm results.

NOx

The “best” two-factor statistical model to predict NOx emissions was based on percent n-paraffins (excluding butane) and the temperature at which 10% of the fuel distills (T10). Five of the six regression models for the 2000 and 3000 rpm speeds and the three operating modes provided strong statistical evidence (p-value < 0.05) that n-paraffin and T10 levels were related to NOx levels in the tested fuels.

According to the models, increases in the n-paraffin content were associated with lower NOx (except for T10 below 150, where the effect of n-paraffin is not as well characterized). The magnitude of this effect varied depending on the particular speed/mode and on the joint distribution of n-paraffin and T10 levels. The largest level observed was for simultaneously high n-paraffins (~20%) and T10 (~190F), where the models show a one percentage point increase in n-paraffins resulting in as much as a 2.6 ppm drop in NOx.

Increases in T10 were associated with higher average NOx (except for n-paraffins above about 20% where limited data were available on the effect of T10). The magnitude of this effect varied depending on the particular speed/mode and on the joint distribution of n-paraffin and T10 levels. The largest levels observed were for low n-paraffins (<5%), where the models show a one degree increase in T10 resulting in as much as a 1.0 ppm increase in NOx.

The evaluation of NOx and fuel properties at 1000 rpm did not yield statistically significant and consistent results. However, the measured NOx levels at this low power condition were all 2 ppm or lower. Any real impact due to fuel properties may have been masked by the natural variability in the testing results. Also at this low a level, real

differences in emissions levels by fuel property could be statistically significant but might be of no practical significance.

Indicated Specific Carbon Monoxide (CO)

The "best" two-factor statistical model to predict CO emissions was for the fuel properties percent aromatics and percent iso-paraffins. However, even this best model yielded statistically significant results (p-value < 0.05) for only one of the six 2000 and 3000 rpm speeds and modes. Consequently, the conclusion is that CO emission levels at these speeds cannot be accurately modeled from the fuel property data collected on the ten test fuels. This result may be attributable to low overall CO emission levels, averaging about 4 ppm for most fuels at 2000 rpm and about 3 ppm for most fuels at 3000 rpm. The variability in the data may have been too large to identify statistically significant effects over such a small range of the response.

At idle (1000 rpm), the aromatics and percent iso-paraffins model was statistically significant (p-value < 0.05) in explaining the observed CO levels for the ten test fuels at all three modes. Furthermore, the coefficients of the model parameters were consistent among the three conditions.

Increases in both aromatics and iso-paraffins in the model were associated with lower CO in
the range of the fuel properties for the ten test fuels. The magnitude of this effect varied depending on the particular mode model and on the joint distribution of aromatic and iso-paraffin values. It was possible to generalize that:

- Lowest CO at idle was seen for fuels with high aromatics (>30%) and low iso-paraffin (approximately 30%), averaging about 31 ppm. In this region, an increase of 1 percentage point for aromatics reduces CO by less than 1.0 ppm, while an increase of 1 percentage point for iso-paraffins reduces CO by 2.8 to 4.5 ppm.
- Highest CO at idle was seen for fuels with low aromatics (<30%) and low iso-paraffin (<50%), averaging about 53 ppm. In this region, an increase of 1 percentage point in aromatics is associated with lower CO by 0.7 to 1.8 ppm. An increase of 1 percentage point in iso-paraffins results in lower CO by 0.8 to 2.3 ppm.
- The remaining fuels fit into a range with simultaneously low aromatics (<30%) and high iso-paraffin (>50%), averaging about 39 ppm. In this region, an increase of 1 percentage point in aromatics is associated with lower CO by 2.2 to 5.4 ppm. An increase of 1 percentage point in iso-paraffins results in lower CO by 0.4 to 1.1 ppm.

Filter Smoke Number

The "best" two-factor statistical model to predict filter smoke number (smoke) was for the fuel properties percent aromatic content and RON. In six of the nine speed/mode combinations, this model had a p-value less than 0.05 and in all nine cases, the overall model p-value was less than 0.2. Furthermore, the coefficients of the model parameters were generally consistent among the six conditions.

Fuels in the range of less than 20 percent aromatics and greater than 75 RON showed lowest average smoke across all speed/modes at 0.04. Fuels with either higher aromatics or lower RON (there were no fuels with both), displayed an average smoke level of 0.23. Because of the strong interaction effect in these models and the variability in the model parameters from one speed/mode to another, there was no simple

generalization on the sensitivity in the models with changes to the fuel properties. Both the magnitude and direction of the effect of a change in one variable depended on the particular speed/mode model and on the joint distribution of aromatic and RON values.

A table of statistical modeling results is provided below. It summarizes the most important results from the detailed discussions above. It also provides results for other engine parameters studied. Note that in most of these cases, no consistent or strong statistical models emerged to explain the observed engine performance as a function of the measured fuel properties. This does not necessarily mean that no such relationships exist, only that they could not be identified based on probabilistic analysis of the data collected.

Table ES.2: Summary of Statistical Analysis for Engine Parameters as a Function of Fuel Properties

Engine Performance Parameter	Speed (rpm)	Average[1]	Range[2]	Fuel Property[3] (Effect)[4] (Range)[5]		Comments
Indicated Specific Fuel Consumption (g/kWh)	2000	207	(189,221)	Aromatics (+)	i-Paraffins (+)	
	3000	214	(189,235)	Aromatics (+) (3%, 55%)	i-Paraffins (+) (27%, 88%)	
NOx (ppm)	2000	9	(3,19)	n-Paraffins w/o C4 (-[a])	T10 (+[b])	[a] Model sign may reverse for low T10 (<150 F). [b] Model sign may reverse for high T10 (>185 F).
	3000	24	(9,64)	n-Paraffins w/o C4 (-[a]) (1%, 21%)	T10 (+[b]) (134 F, 191 F)	
Indicated Specific Hydrocarbons (HC) (g/kWh)	No two-factor with interaction model showed statistically significant alignment with measured data across a range of speeds and modes. The "Best" two factor model with i-Paraffins and Sensitivity was only statistically significant (p< 0.05) for two of the nine tested speed and mode conditions.					
Indicated Specific Carbon Monoxide (CO) (g/kWh)	1000	44	(24,71)	Aromatics (-) (3%, 55%)	i-Paraffins (-) (27%, 88%)	
Filter Smoke Number (sz)	1000	0.02	(0.00, 1.08)	Aromatics (m)	RON (m)	Despite mixed sign of influence of fuel properties on the response, the two-factor Aromatics/RON models are statistically significant in six of the nine speed/mode combinations
	2000	0.08	(0.00, 0.52)	Aromatics (m)	RON (m)	
	3000	0.31	(0.00, 3.04)	Aromatics (m) (3%, 55%)	RON (m) (59, 96)	
Combustion Duration (CA)	No two-factor with interaction model showed statistically significant alignment with measured data across a range of speeds and modes. The "Best" two factor model with n-Paraffins excluding C4 and T10 was only statistically significant (p< 0.05) for three of the nine tested speed and mode conditions.					
Combustion Noise (dB)	No two-factor with interaction model showed statistically significant alignment with measured data across a range of speeds and modes. The "Best" two factor model with Aromatics and n-Paraffins excluding C4 was not statistically significant (p< 0.05) for any of the nine tested speed and mode conditions.					
Coefficient of Variance of IMEP (%)	This stability response was evaluated only at Idle as this is the only operating range where its effects are of concern in HCCI combustion. No two-factor with interaction model showed statistically significant alignment with measured data across all modes at Idle. The "Best" two factor model with RON and T10 was only statistically significant (p< 0.05) for one of the three modes.					
Peak Cylinder Pressure (bar)	No two-factor with interaction model showed statistically significant alignment with measured data across a range of speeds and modes. The "Best" two factor model with Olefins and i-Paraffins was only statistically significant (p< 0.05) for three of the nine tested speed and mode conditions.					
Crank Angle at Exhaust Valve Close (deg)	1000	234	(226,242)	i-Paraffins (m)	Sensitivity (m)	"-" for RBEI but "mixed" for RCEI and RCSI modes
	2000	248	(240,260)	i-Paraffins (-[c])	Sensitivity (-[d])	[c] model sign may reverse for low sensitivity (~ -2) [d] model sign may reverse for low i-Paraffins (~ 27%), high sensitivity (~ 11)
	3000	277	(260,294)	i-Paraffins (-[c]) (27%, 88%)	Sensitivity (-[d]) (-2,11)	

[1] Average of mean responses of ten test fuels

[2] (Minimum,Maximum) of mean responses of ten test fuels

[3] Fuel properties that represent best two-factor statistical model of response

[4] Effect of increase in effect on response; positive (+), negative (-), or mixed (m) across the three modes tested within each speed
Note: The magnitude of the effect of one predictor may vary considerably based on the level of the other predictor

[5] (Minimum, Maximum) of measured values for the response predictors across the ten test fuels. Note that ten tested fuels do not necessarily represent all regions of the two predictor variables (e.g., the maximum level of both or the minimum of one and the maximum of the other)

In summary, this study provided no strongly definitive associations between fuel properties and HCCI engine performance in general. However, it did identify some important and statistically meaningful results. Among these:

1. For speeds above idle, specific fuel consumption performance appeared statistically related to fuel aromatic and iso-paraffin content. Best specific fuel consumption was associated with fuels having low aromatic and iso-paraffin content. Increases in either fuel property were associated with decreased SFC performance.
2. For speeds above idle, NOx emissions appeared statistically related to n-paraffin content (excluding butane) and the temperature at which 10 percent of the fuel distils. Lowest NOx was associated with fuels having low n-paraffins and high

T10. Though not completely consistent, increases in n-paraffins were generally associated with lower NOx and increases in T10 with higher NOx.

3. At idle, CO emissions appeared statistically related to fuel aromatic and iso-paraffin content. Lowest CO was associated with fuels having high aromatics and low iso-paraffins. Increases in either fuel parameter were associated with decreased CO emission levels.
4. At all speed and mode conditions, smoke appeared statistically related to aromatic content and RON. Lowest smoke was associated with low aromatics and RON of at least 75.

Recommendations for future work have included:

- Examining the effects of ethanol as a component of the test fuels
- Testing additional fuels with intermediate compositions to fill in blank spaces in the fuel property matrix
- Performing additional statistical analyses such as three parameter regressions (maybe eliminating three-way interactions to give one more degree of freedom to estimate the error) and/or quadratic regressions

All these recommendations have been accepted and the testing for the additional fuels has begun in AVFL 13B.

Table of Contents

1 Introduction

The use of homogeneous charge compression ignition (HCCI) combustion in internal combustion engines is of interest because it has the potential to produce low NOx and low particulate matter (PM) emissions while providing diesel-like efficiency. In HCCI combustion, a premixed charge of fuel and air auto-ignites at multiple points in the cylinder near top dead center (TDC), resulting in rapid combustion with very little flame propagation. Since ignition occurs in an HCCI engine by auto-ignition of the fuel/air mixture, the choice of fuel will have a significant impact on both engine design and control strategies. The start of ignition depends on the temperature, pressure, and concentration history during the compression stroke, and the unique reaction kinetics of the fuel/air mixture. To control the temperature, pressure, and concentration of fuel/air mixture, different dilution strategies, valve timings, and injection schemes are proposed for HCCI engines.

In this study, 10 gasoline-like test fuels are tested in an AVL single cylinder engine equipped with a hydraulic variable valve train (VVT) and gasoline direct injection (GDI) system. By using VVT and GDI, three different intake charge preparation modes are implemented: re-compression early injection (RCEI), re-compression split injection (RCSI), and re-breathing early injection (RBEI). For each intake charge preparation mode, three engine operating conditions are investigated: 1.5 bar IMEP at 1000 rpm, 3 bar IMEP at 2000 rpm, and 5.5 bar/deg of maximum rate of pressure rise at 3000 rpm (IMEP's very near 3 bar). For all engine operating conditions and intake charge preparation modes, the combustion phasing, represented by the 50% mass fraction burned location (CA50), were fixed at 5 degrees after top dead center.

The fuel impacts on HCCI combustion are quantified by a multiple regression method, in which two out of nine independent fuel properties are correlated with combustion or emission related parameters. In the report, only emissions (HC, CO, NOx), fuel consumptions, and combustion stability results are presented. It is concluded that engine emissions, fuel consumptions, and combustion stability are influenced by both fuel chemistry and octane-related properties. Detailed results are reported in Section 5.

2 Selection of test fuels

Fuel chemistry, especially normal paraffins, ratios of iso-paraffins to aromatics and olefins as octane components, affects both the octane ratings and octane sensitivity of blended fuels. Paraffins, especially normal paraffins, possess a unique low-temperature chemistry which can lead to knock in spark ignited engines and can assist ignition in HCCI engines. Aromatics and many olefins do not possess this low temperature chemistry, are often rated conservatively in octane tests, and can inhibit knock in spark ignited engines to a greater extent that their octane numbers suggest. In HCCI, we wish to enhance the pre-flame reactions of the fuel in order to ensure ignition, while allowing control of combustion phasing and rate of burning over a wide range of speeds and loads.

The relationship of these HCCI characteristics to fuel chemistry and measured octane ratings is not well understood and is also operating condition and engine design dependent. Fuels exhibiting high octane sensitivity (aromatic or olefin derived) are

expected to behave differently than fuels with low octane sensitivity (paraffin derived). Refineries today are optimized to produce high octane components for spark ignited gasoline (aromatic, iso-paraffin, olefin) while minimizing low octane components (normal paraffin). Fuel volatility in the normal range for gasoline is not expected to affect HCCI mixing, although large changes in volatility such as between gasoline and distillate fuels would be expected to have an effect.

In this study, ten fuels are blended and evaluated. The most prevalent refinery streams used for gasoline blending are reformate (about 50% aromatic), alkylate (about 100% iso-paraffin), cat cracker gasoline (about 25% olefin), and straight run gasoline (about 100% normal paraffin). Therefore, these four streams are used to blend the test fuels. The following characteristics and ranges of fuel properties are the most relevant for this fuel matrix:

1. Using 4 blending streams (reformate, alkylate, cat cracker gasoline, and straight run gasoline) to manufacture the 10 test fuels considerably simplifies fuel blending while emphasizing refinery based fuel blends. Fuel property blend modeling will be more accurate and efficient because of the use of well characterized full boiling range components and eliminate the need for iterative hand blending in achieving the final fuels.

2. Adjust all 4 blending streams as much as possible for a full gasoline boiling range equivalent to American Society for Testing and Materials (ASTM) gasoline distillation class A. For gasoline range fuels, it is not expected that volatility will play a large role in mixture preparation. The Reid vapor pressure (RVP) of all fuels will be adjusted to 7 psi with butane.

3. Blend fuels to three research octane number (RON) targets of about 92, 65, and a mid point between. A RON of 92 represents the average RON in unleaded regular grade gasoline today (NIPER survey). It is very unlikely that going higher than this will be of benefit to HCCI combustion. A RON of 65 is about the lowest value which can be achieved using full boiling range straight run gasoline and is therefore recommended as a lower limit for this study. A mid point octane stresses the importance of octane as a variable for correlating combustion and knock performance and also for relating to current gasoline and refinery practices. Blending to exact RON values is not critical since the actual octane values achieved will be independent variables for the data analysis.

4. The three target ranges of RON can be achieved with multiple combinations of the blending streams and it is expected that motor octane number (MON) and octane sensitivity will vary with each blend formula. This will allow correlation of engine performance to octane values, octane sensitivity, and to fuel chemistry. Three variations of fuel chemistry should be attempted for each RON level.

In summary, it is recommended that a parametric blending study be undertaken to determine multiple blend formulas which can achieve the target RON values of approximately 92, mid value, and 65 by using the four blending streams. These multiple blend formulas will then be screened for maximum variation in MON and fuel chemistry in order to select the final 3 fuel blends per RON target (There will be 4 fuel blends for one RON target). Design of experiments methods will be used to ensure proper selection of the final ten blends.

2.1 Fuel properties and chemistry

Based on a review of relevant literature and Oak Ridge National Laboratory (ORNL) fuels testing expertise, it is expected that HCCI combustion in a gasoline engine will be affected by fuel research octane number (RON), fuel motor octane number (MON), their average (R+M)/2, their difference (R-M), boiling point distribution, and fuel chemistry.

Octane number is known to affect knock and pre-ignition in conventional spark ignited engines and is a basic specification for the production control of commercial gasoline. RON and MON are measured under different conditions and correlate to different types of engine operation. It is common to refer to an averaged octane number ((R+M)/2) and an octane sensitivity number (R-M). The main way of varying octane numbers and their relationship is to vary fuel chemistry.

Fuel volatility controls fuel evaporation and mixing and in conventional gasoline is varied seasonally to aid cold starting (high volatility desired) in cold weather and to prevent HC evaporative emissions and vapor lock in hot weather (low volatility desired). Volatility is controlled by a combination of the fuel boiling point distribution (T10, T50, and T90), Reid vapor pressure, and Vapor/Liquid (V/L) ratio. The boiling point distribution describes the complete fuel with minor emphasis on the high volatility components and the RVP and V/L ratio describe the highly volatile front end of the fuel in more detail. In this project, RVP will be adjusted to 7 psi with the addition of n-butane for every fuel to eliminate volatility as an independent variable.

Gasoline is composed of hydrocarbon molecules such as paraffins (normal paraffin, iso-paraffin, or cyclo-paraffin), aromatics, olefins, and oxygenated compounds such as alcohols or ethers. Fuel chemistry is not restricted except in emissions non-attainment areas, and refineries are allowed to blend as desired to maximize gasoline yield while meeting other performance specifications such as octane and volatility requirements. Other gasoline quality standards include corrosion, gum, and oxidation stability.

It is the desire of this project to correlate engine performance variables to fuel variables, both fuel properties and fuel chemistry. Table 2.1 lists the recommended properties and fuel chemistry for this study.

Table 2.1: Recommended fuel properties and fuel chemistry

1	API
2	Research octane number (RON)
3	Motor octane number (MON)
4	(R+M)/2
5	(R-M)
6	T10
7	T50
8	T90
9	% Aromatics
10	% Olefins
11	% N-paraffins
12	% Iso-paraffins
13	% All paraffins
14	% Naphthenes

2.2 Fuel candidates

AVL received 56 candidate blends of four blending streams referred to as A, B, C, and D from ConocoPhillips. Fuel properties of 56 candidate blends were estimated by a blending model, which was verified by the gas chromatography data of 15 fuels, including pure streams A, B, C, and D. The 56 fuel candidates are shown in Table 2.2.

Table 2.2: Fuel candidates

Number	Name	% A	% B	% C	% D	% EXTRA	% n-C4
1	SPLASH87E10	48	8	37	6	10	2.3
2	B100	0	100	0	0	0	4.4
3	A50B50	50	50	0	0	0	3.1
4	A33B33C33	33.33	33.33	33.33	0	0	2.4
5	B50C50	0	50	50	0	0	2.8
6	ROAD87E10	48	8	37	6	10	2.3
7	A100	100	0	0	0	0	1.9
8	A33B33C33D4	32	32	32	4	0	2.8
9	A50C50D6	47	0	47	6	0	2.1
10	A50C50	50	0	50	0	0	1.6
11	C100	0	0	100	0	0	1.2
12	SPLASH84E10	37	7	47	9	10	2.5
13	SPLASH84E20	37	7	47	9	20	2.5
14	SPLASH25E33	25	25	25	25	33	4.4
15	B47C47D6	0	47	47	6	0	3.2
16	A47B47D6	47	47	0	6	0	3.6
17	A98D2	98	0	0	2	0	2.0
18	C99D1	0	0	99	1	0	1.4
19	ROAD87	48	8	37	6	0	2.3
20	ROAD84	37	7	47	9	0	2.5
21	SPLASH25E20	25	25	25	25	20	4.4

Table 2.2: Fuel candidates - continued

22	SPASH25E10	25	25	25	25	10	4.4
23	SPLASH84K10	47	7	37	9	10	2.6
24	A25B25C25D25	25	25	25	25	0	4.4
25	A75D25E10	75	0	0	25	10	4.0
26	B80D20	0	80	0	20	0	5.5
27	SPLASH17E20	17	17	17	49	20	6.2
28	B33C33D34	0	33	33	34	0	5.2
29	A33C33D34	33	0	33	34	0	4.5
30	C85D15	0	0	85	15	0	2.6
31	A79D21	79	0	0	21	0	3.7
32	B77D23	0	77	0	23	0	5.7
33	A22B22C22D34	22	22	22	34	0	5.1
34	SPLASH84K20	47	7	37	9	20	2.6
35	A33B33D34	33	33	0	34	0	5.4
36	C83D17	0	0	83	17	0	2.7
37	A75D25	75	0	0	25	0	4.0
38	SPLASH17E10	17	17	17	49	10	6.2
39	SPLASH22K10	22	22	22	34	10	5.1
40	SPLASH9E20	9	9	9	73	20	8.1
41	C50D50	0	0	50	50	0	5.7
42	A17B17C17D49	17	17	17	49	0	6.2
43	B50D50	0	50	0	50	0	7.3
44	A50D50	50	0	0	50	0	6.0
45	SPLASH9E10	9	9	9	73	10	8.1
46	A30D70E10	30	0	0	70	10	7.6
47	SPLASH22K20	22	22	22	34	20	5.1
48	C25D75	0	0	25	75	0	8.0
49	B35D65	0	35		65	0	8.2
50	C23D77	0	0	23	77	0	8.2
51	A33D67	33	0	0	67	0	7.4
52	A9B9C9D73	9	9	9	73	0	8.1
53	B30D70	0	30	0	70	0	8.4
54	A30D70	30	0	0	70	0	7.6
55	SPLASH22K30	22	22	22	34	30	5.1
56	D100	0	0	0	100	0	10.2

Note:

1. Vapor pressure has been adjusted to 7 psi RVP for all blends except splash blends.
2. Splash blends are volume percent additional (e.g. E10 is 10 ml ethanol into 100 ml sample) and are not corrected for changes in vapor pressure.
3. Blends are made up of only refinery blend stocks A, B, C, D and n-C4, unless otherwise noted in %EXTRA column (E=ethanol, K=kerosene splash blended).
4. Steam A: High aromatic content.
5. Steam B: High iso-paraffin content.
6. Stream C: High olefins content.
7. Stream D: Light Straight Run (LSR) gasoline.

2.3 Fuel selection method

A statistical selection method was developed by Battelle (AVL subcontracted Battelle to statistically select the test fuels and analyze the engine data). Pairwise plots of the 14 fuel properties revealed that several sets of fuel properties are so highly correlated that subsequent analyses of the relationships between engine performance and fuel properties could not distinguish between the effects of properties within each set. Thus, unless additional candidate fuels were prepared in a way that would reduce the correlation of those properties, it is necessary to choose only one of the properties to serve as a surrogate for all properties in the set. This resulted in the seven "target" fuel properties shown in Table 2.3. The pairwise plots of the seven "target" properties are shown in Figure 2.1a – Figure 2.1c.

Table 2.3: Target fuel properties used in the experimental design

Target Fuel Property	Highly Correlated Properties[1]
RON	Road ((R+M)/2), MON, NAPH
R-M	
T10	
% Aromatics	API
% Olefins	
% N Paraffins	T50, T90
% Iso Paraffins	All Paraffins

[1] It is not possible to differentiate among the effects of highly correlated fuel properties on engine performance measures.

Following the CRC committee's decision to exclude D100 and splash blends containing ethanol or kerosene, a total of 37 candidate fuels were considered for the project. A statistical design approach was used to select 10 test fuels whose properties are statistically representative of the distribution of properties among the 37 candidate fuel blends. Orban et. al. (2003) [2] applied these methods in a similar type of research project (APBF-DEC 2004) in which a set of diesel lubricants was selected from a larger set of candidates. The sampled lubricants were used in engine tests to establish the relationship between diesel emissions and lubricant properties.

The statistical design method for selecting the test fuels used principal component analysis (Morrison 1976) [1] to transform the seven estimated fuel properties into seven new properties called principal components (PCs). The value of each principal component for a given fuel is called a principal component score. The PC score is calculated by taking a weighted average of the standardized properties (value minus the mean divided by the standard deviation) for that fuel. Unlike the original variables, which tend to be highly correlated, the principal component scores are uncorrelated. Furthermore, they are sorted according to amount of the total variability that each explains. Typically, a large portion (e.g., 90% or 95%) of the total variability of the data can be explained by the first few principal components.

The advantage of using principal component analysis is that experimental design techniques that are appropriate for uncorrelated variables can be applied. The final design is evaluated relative to both the principal components as well as the original properties. The PRINCOMP procedure in the Statistical Analysis System (SAS©) software package was used to perform this analysis.

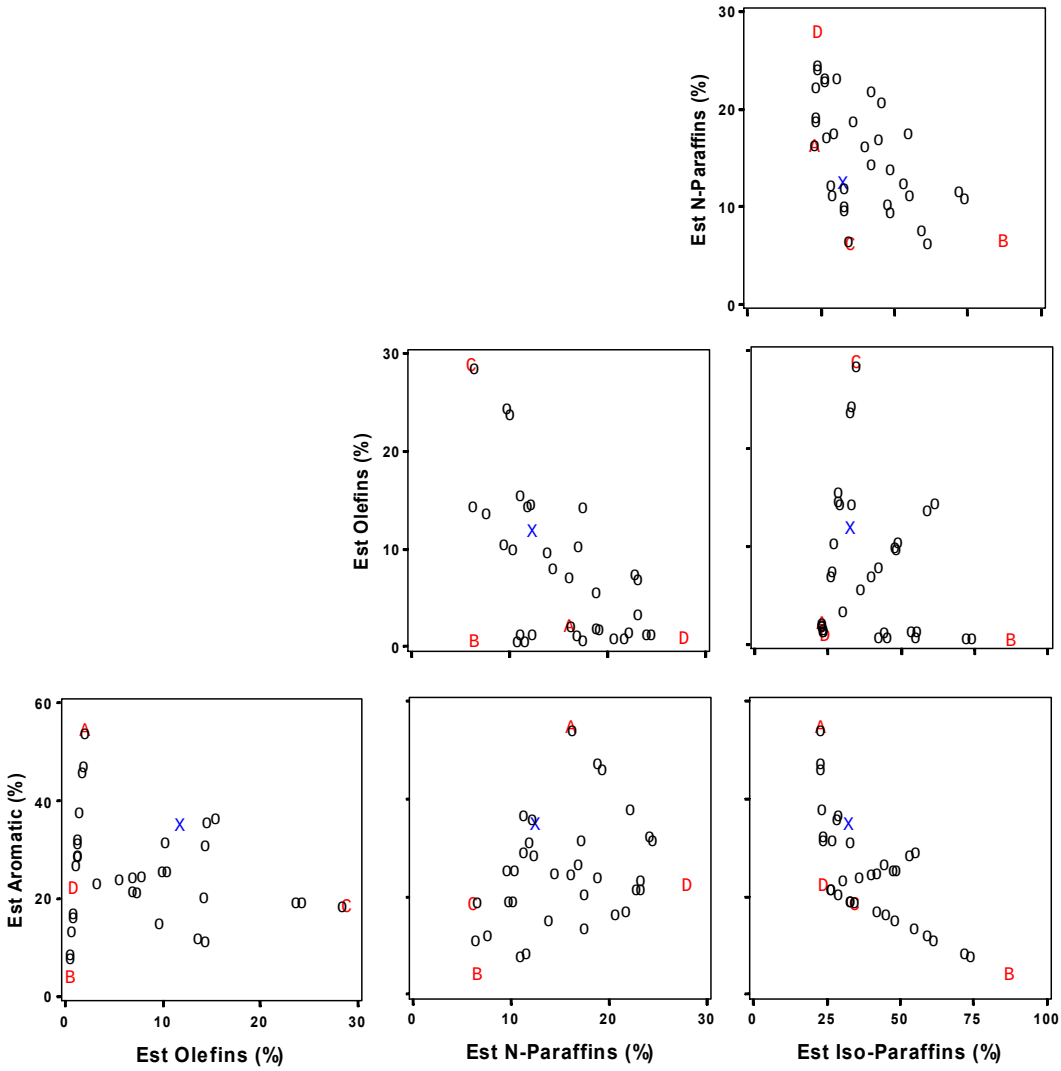

Figure 2.1a: Pairwise plots of fuel properties for 37 Candidate fuels (Including A, B, and C). Blending stock D100 (D) and ROAD87 (X) shown for reference

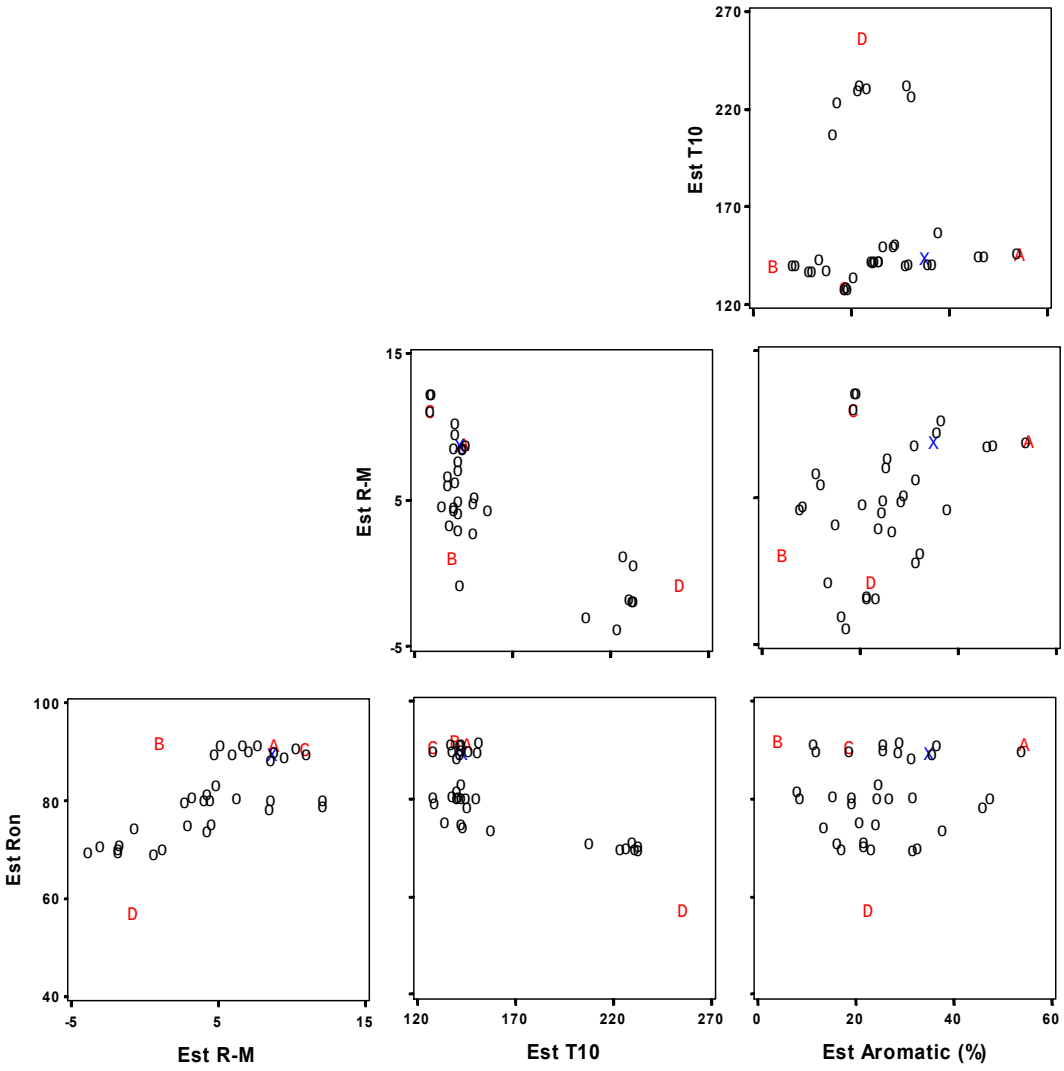

Figure 2.1b: Pairwise plots of fuel properties for 37 Candidate fuels (Including A, B, and C). Blending stock D100 (D) and ROAD87 (X) shown for reference

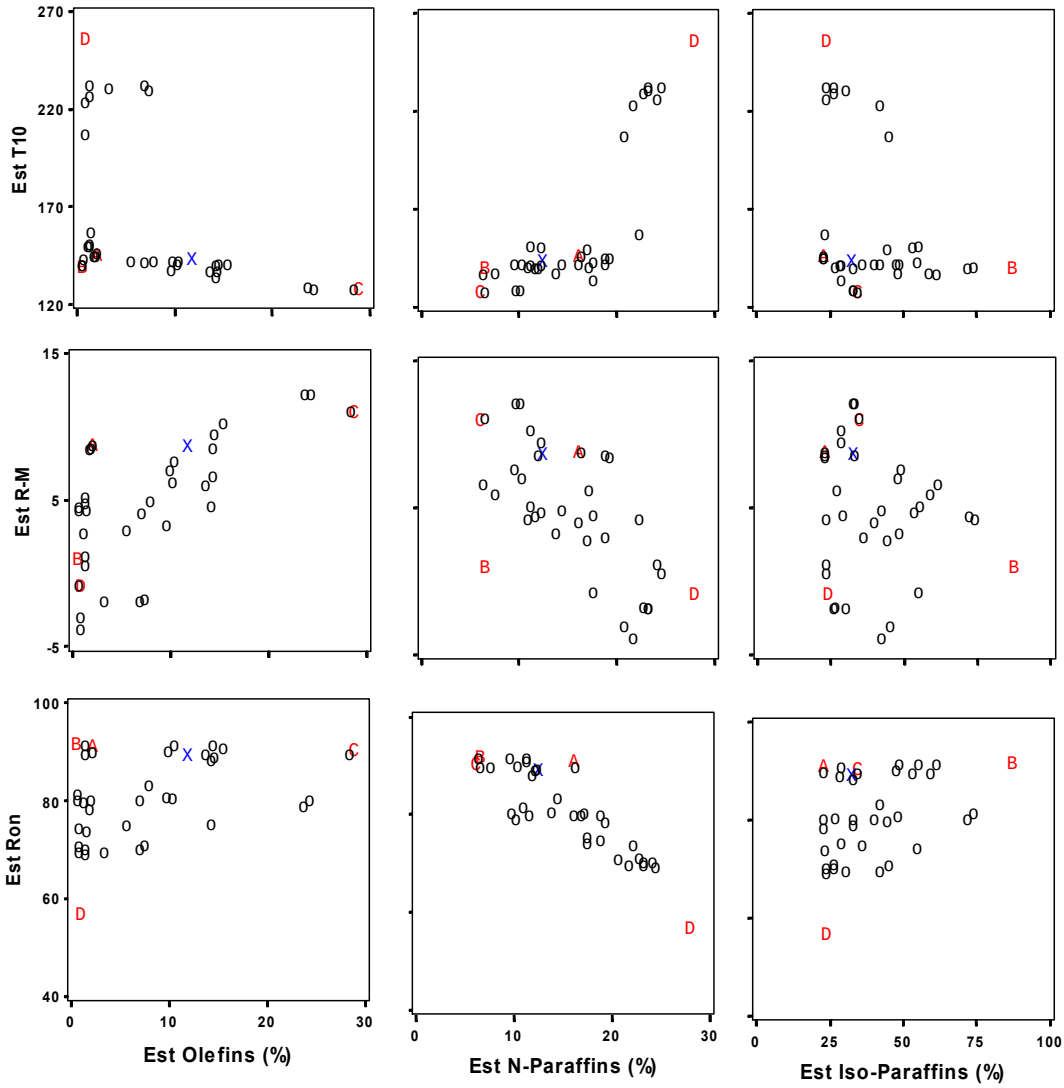

Figure 2.1c: Pairwise plots of fuel properties for 37 Candidate fuels (Including A, B, and C). Blending stock D100 (D) and ROAD87 (X) shown for reference

Because the test fuels will be created from blends of four blending stocks, it is natural that the blending stocks will tend to produce the most extreme values of each fuel property. Therefore, almost any experimental design intended to meet the criteria of spanning the fuel properties would have selected these four blending stocks as test fuels. Thus, fuels A, B, and C are automatically included in the experimental design. Fuel D was excluded because the octane level is too low to meet the program objectives.

The statistical approach applies mathematical algorithms to select the set of 10 fuels that contain minimal redundancy (i.e., no fuels with very similar properties) while maximizing the spread (i.e., total distance) among fuels. It involves three steps.

The first step is to calculate the minimum statistical distance between any two fuels within each possible combination of 10 fuels selected from the 37 candidates. Under the constraint discussed earlier, only combinations that contain fuels A, B, and C are considered. The statistical distance between fuels F_1 and F_2 is calculated using the formula

$$\text{Distance} = \sqrt{\sum_{i=1}^{7} \frac{(x_i - y_i)^2}{s_{ii}}},$$

where $(x_1, x_2, \cdots, x_7)$ is the 7-dimensional PC scores for fuel F_1, $(y_1, y_2, \cdots, y_7)$ is the 7-dimensional PC scores for fuel F_2, and $s_{11}, s_{22}, \cdots, s_{77}$ are sample variances of PC scores.

The next step is to select the combinations of ten fuels that produce the maximum value of this minimum pairwise distance. There can be multiple combinations that achieve this maximum minimum distance. The final step is to select from these combinations the combination that has the maximum total pairwise distances between packages. This approach utilizes all seven PCs to make sure that no fuels with similar properties are chosen.

Table 2.4 lists the fuel blends that were selected using this statistical design approach. As discussed earlier, three blending stocks (A, B, and C) were automatically included in the design; however, all three – or fuels that are almost equivalent (e.g., C99D1) - would have been selected using this design approach. Figures 2.2 and 2.3 show the fuel properties and principal component values, respectively, for the 10 selected test fuels relative to the distribution of values among the 37 candidate fuels and reference fuels. In the figures, fuel properties and principal component values for 37 fuel candidates are shown at the bottom, while those of test fuels are shown on the top in red. It is shown that the selected test fuels cover the maximum variations of fuel properties for all seven fuel properties and evenly distributed on the plots for most fuel properties. Figures 2.4a – 2.5c present pairwise plots of the properties and principal components for the selected fuels relative to the values for the 37 candidate fuels.

Table 2.4: Fuel blends selected

Fuel Number	Proposed Test Fuel	Reference Fuels[1]	Plotting Symbol[2]
7	A100		A
2	B100		B
11	C100		C
56		D100	D
51	A33D67		E
31	A79D21		F
53	B30D70		G
43	B50D50		H
32	B77D23		I
41	C50D50		J
30	C85D15		K
19		ROAD87	X

[1] Reference fuels shown in selected plots. ROAD87 was a candidate fuel; but was not selected by the statistical approach. D100 was not a candidate.

[2] Plotting symbols used in Figures 2.2 through 2.5.

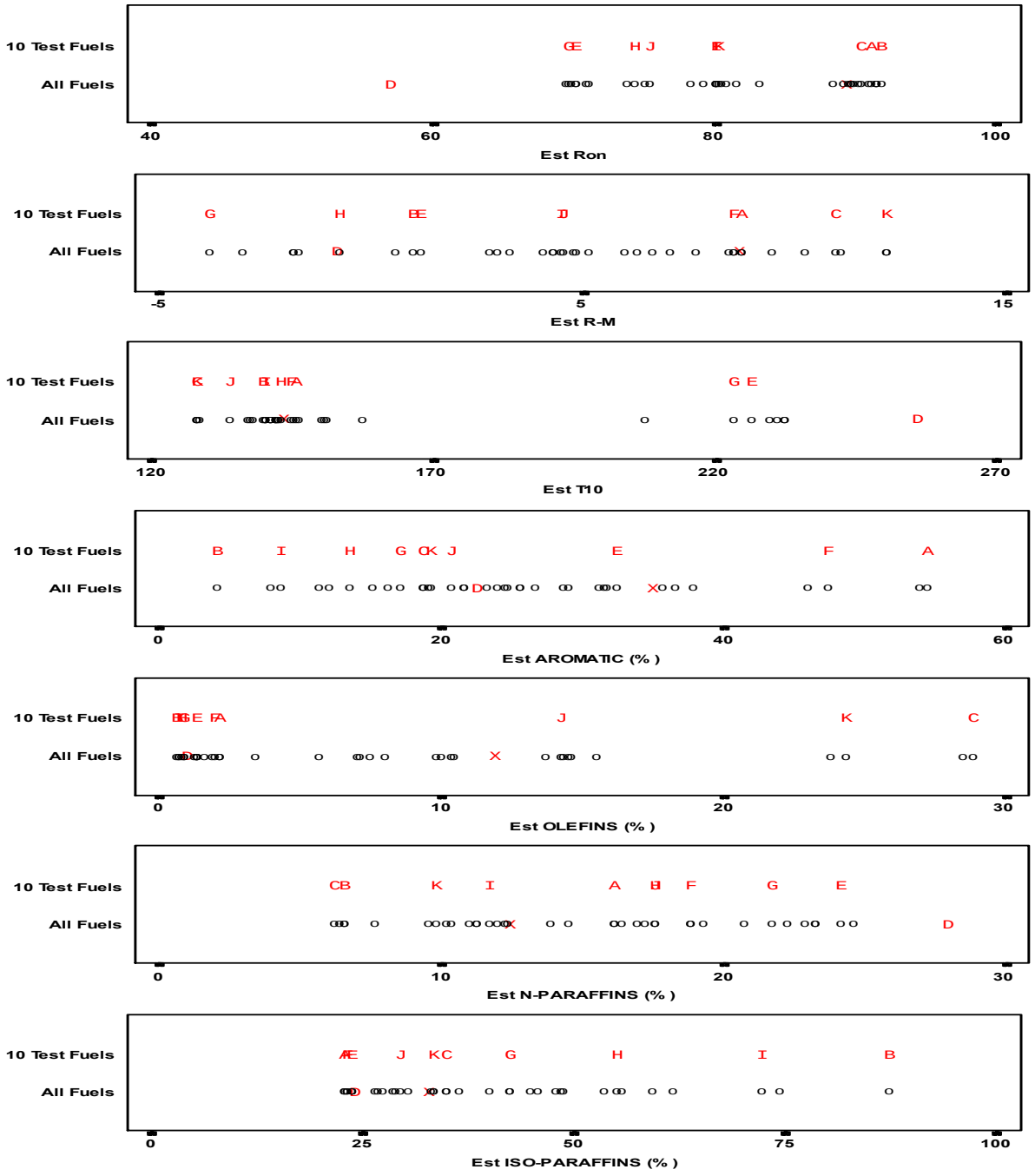

Figure 2.2: Properties of the 10 proposed test fuels relative to the range of properties for all candidate fuels. Blending stock D100 (D) and ROAD87 (X) shown for reference.

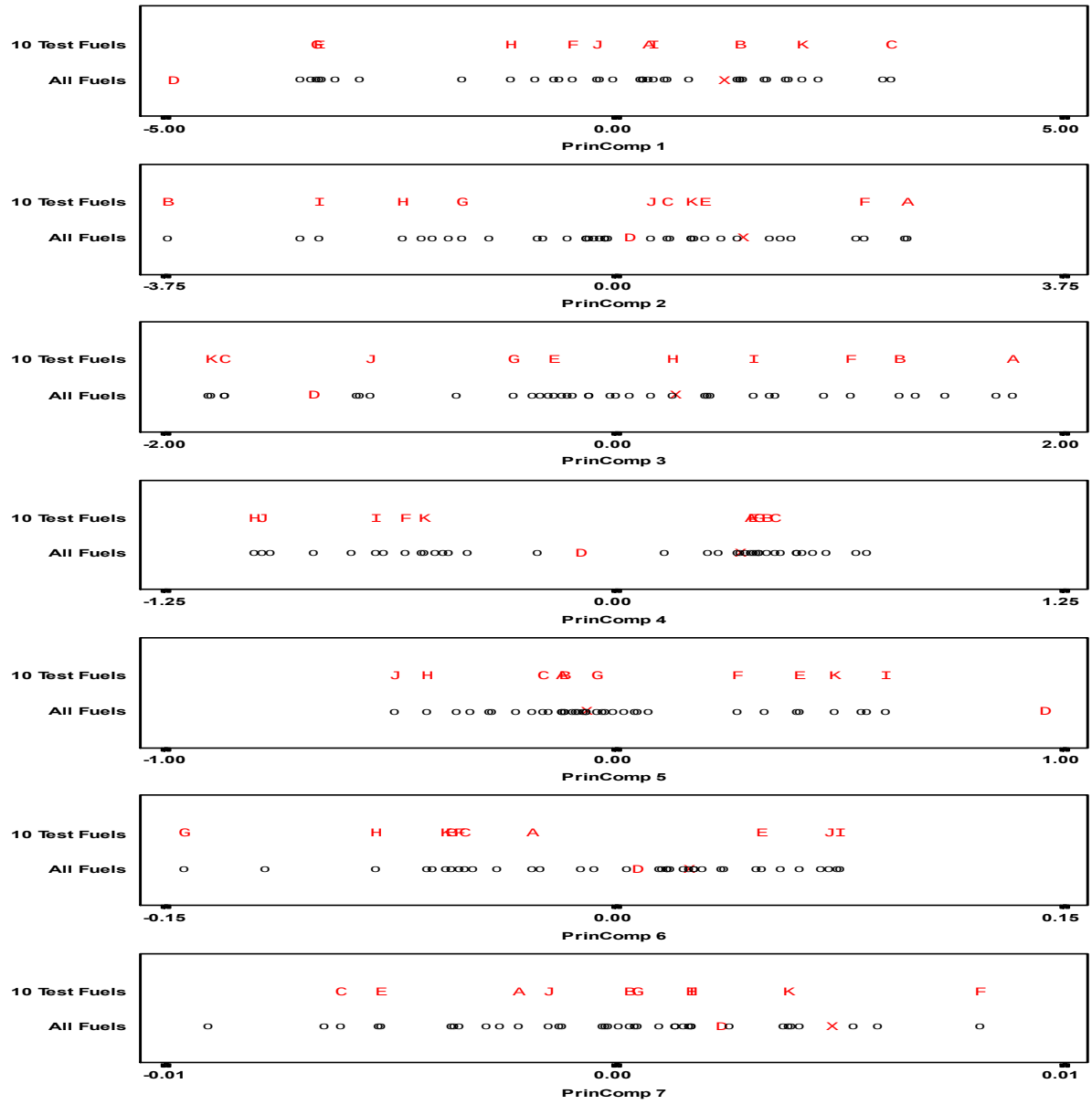

Figure 2.3: Principal component scores of the 10 proposed test fuels relative to the range of scores for all candidate fuels. Blending stock D100 (D) and ROAD87 (X) shown for reference.

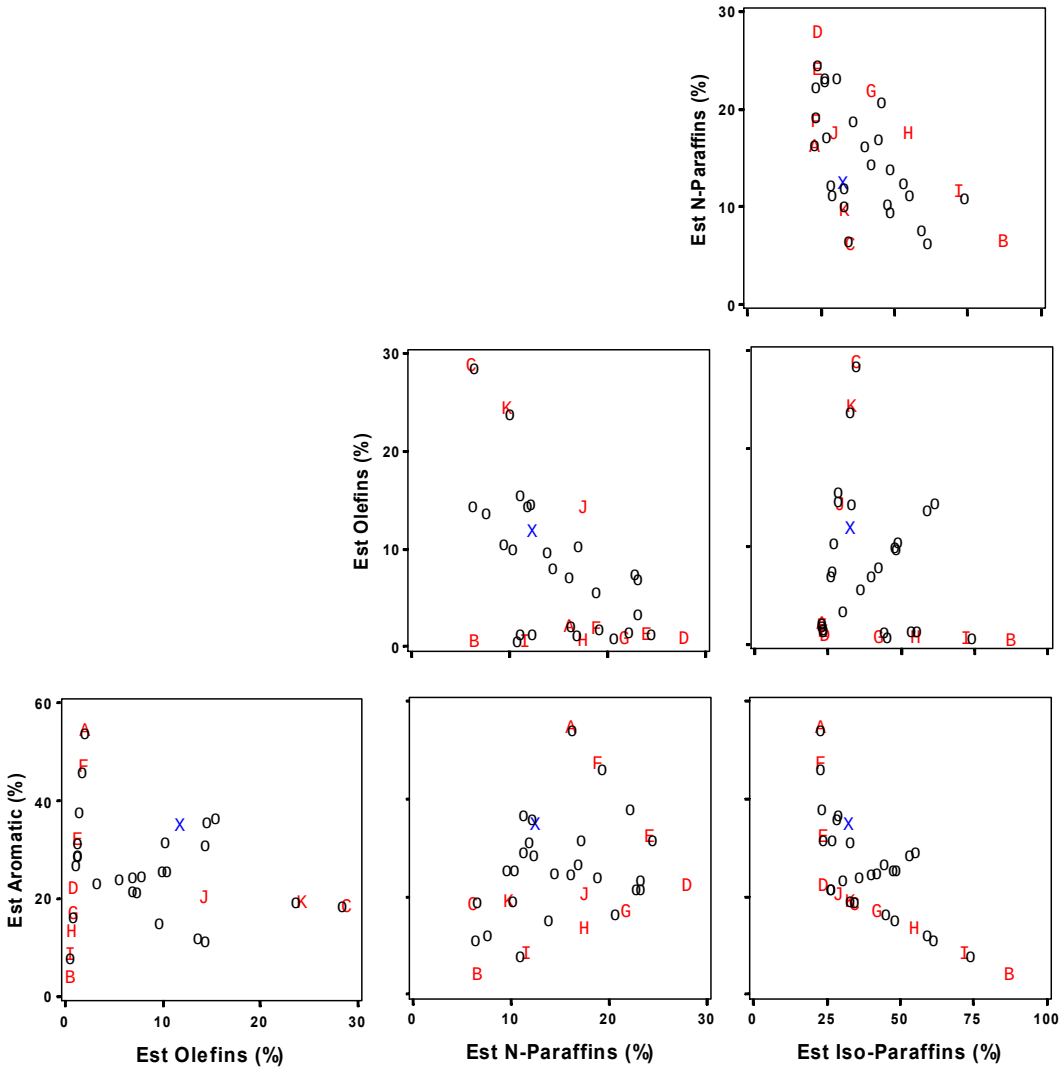

Figure 2.4a: Pairwise plots of fuel properties for the 10 proposed test fuels. Blending stock D100 (D) and ROAD87 (X) shown for reference.

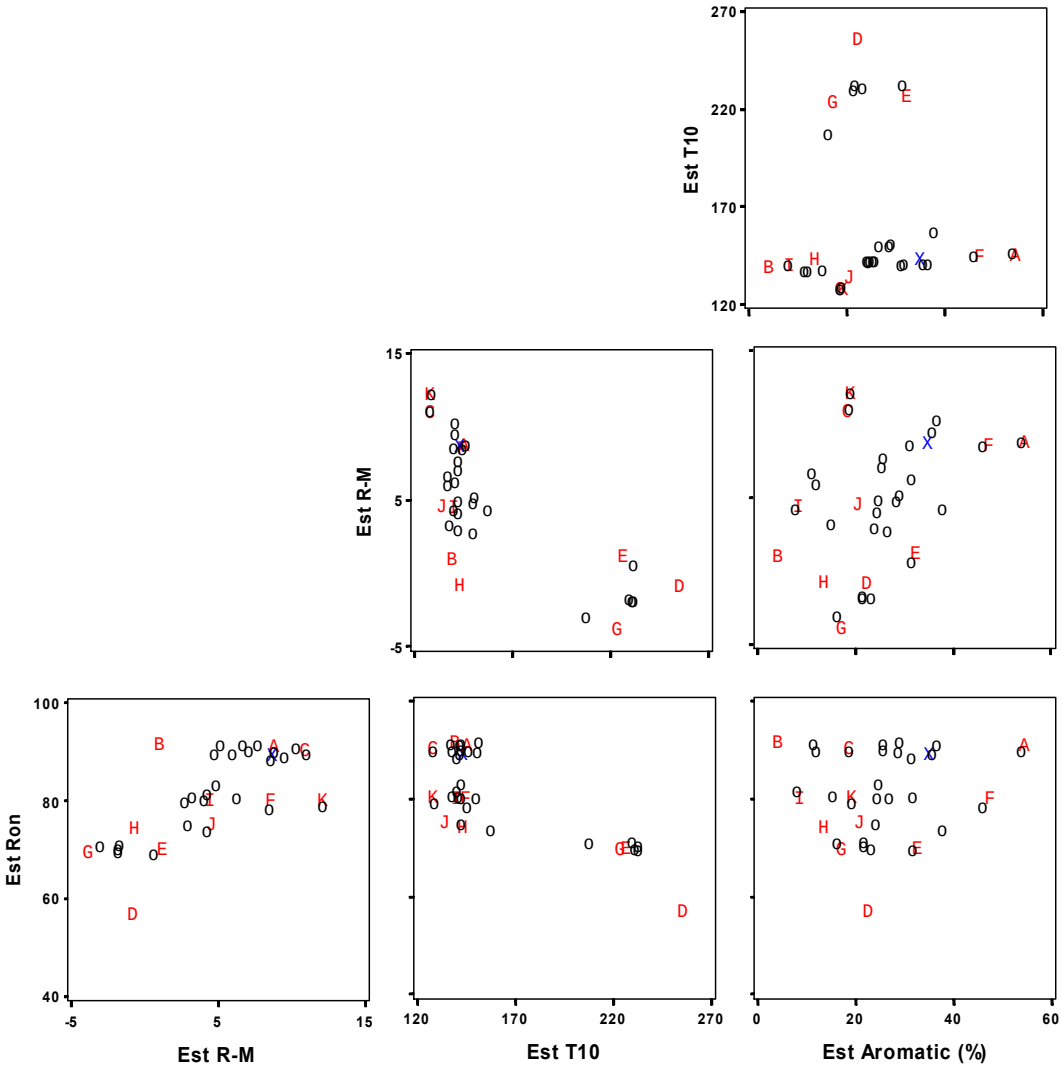

Figure 2.4b: Pairwise plots of fuel properties for the 10 proposed test fuels. Blending stock D100 (D) and ROAD87 (X) shown for reference.

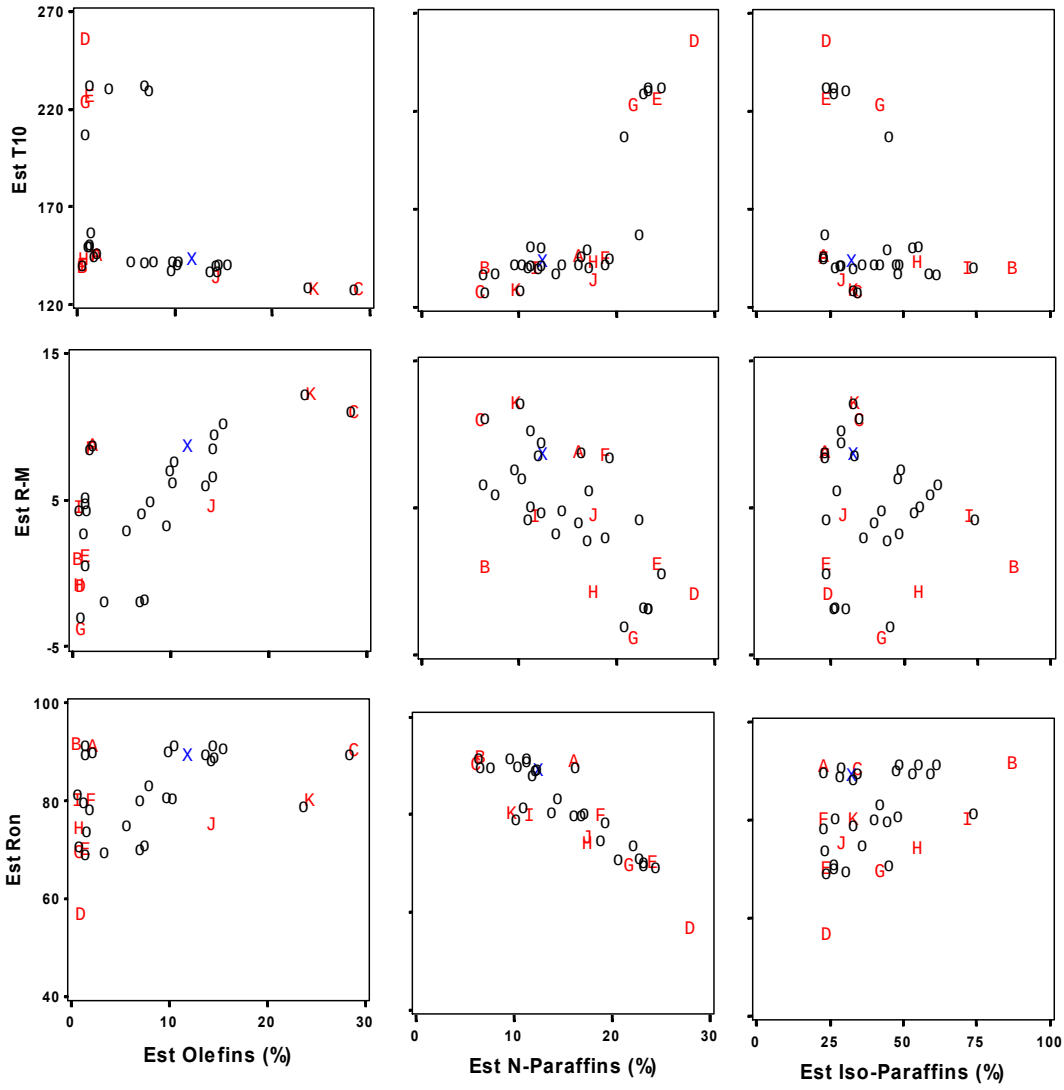

Figure 2.4c: Pairwise plots of fuel properties for the 10 proposed test fuels. Blending stock D100 (D) and ROAD87 (X) shown for reference.

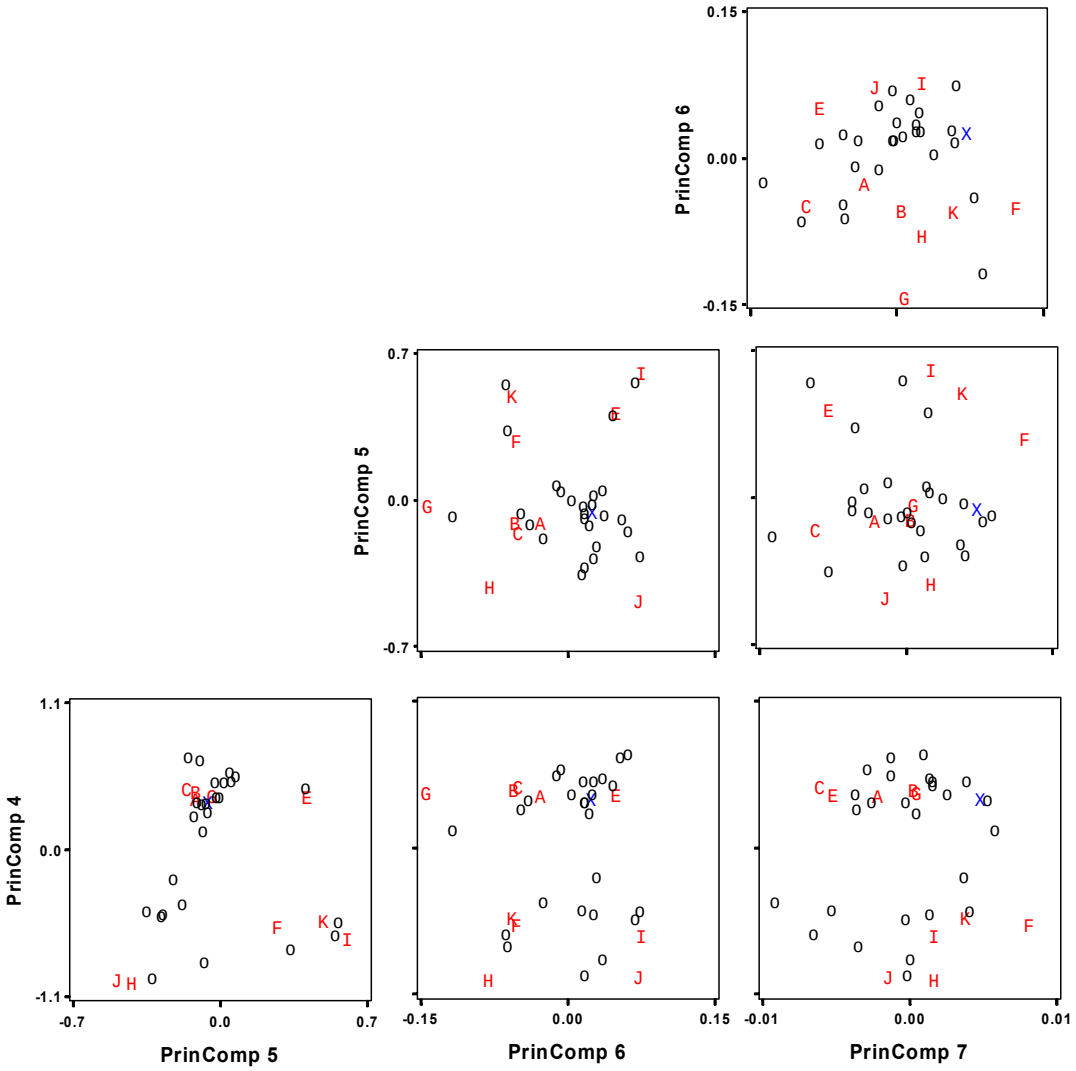

Figure 2.5a: Pairwise plots of principal component scores for the 10 proposed test fuels. Blending stock D100 (D) and ROAD87 (X) shown for reference.

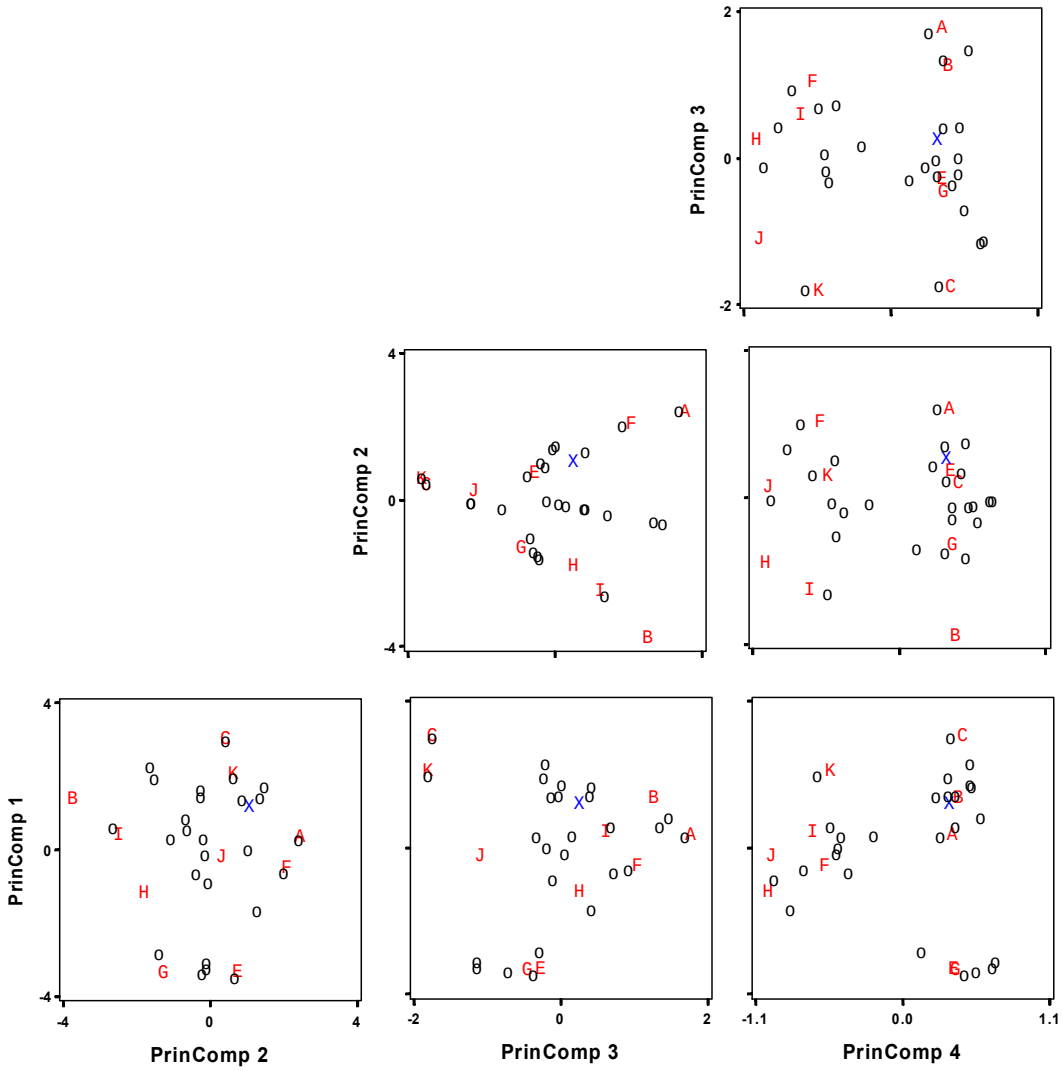

Figure 2.5b: Pairwise plots of principal component scores for the 10 proposed test fuels. Blending stock D100 (D) and ROAD87 (X) shown for reference.

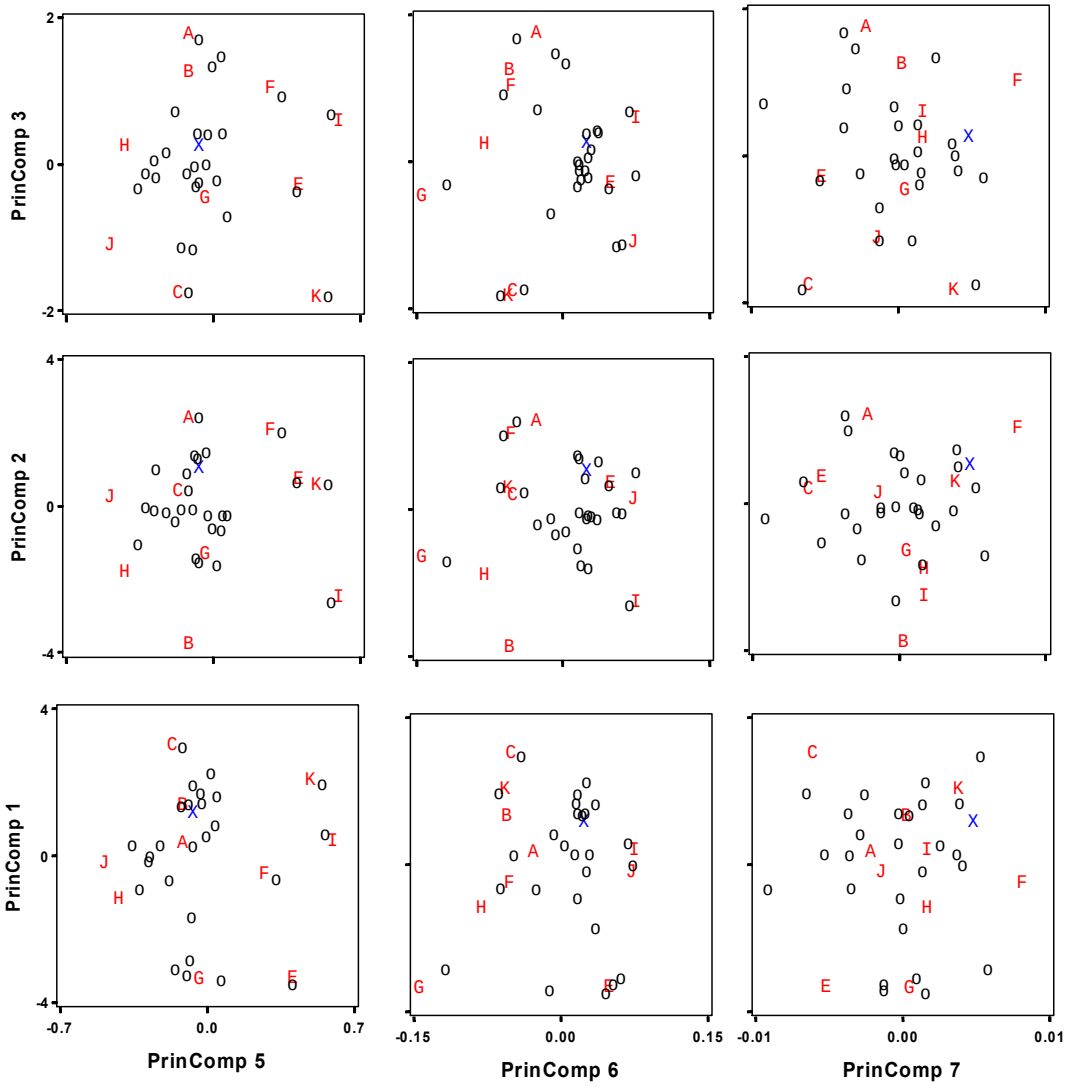

Figure 2.5c: Pairwise plots of principal component scores for the 10 proposed test fuels. Blending stock D100 (D) and ROAD87 (X) shown for reference.

The following are some observations that were considered in making the final test fuel design recommendations.

- The ten test fuels selected by the statistical approach span the ranges of the seven fuel properties, nearly achieving the minimum and maximum values of every property. Of particular importance, there are two fuels with RON values near 70, two near RON=75, three near RON=80, and three near RON=90. The only notable gap in coverage is in the 5% to 15% range of Olefins.

- The design also does a good job of selecting fuels that span the ranges of the principal component scores. There are no significant gaps in the coverage of the range of any PC score.

- The pairwise plots of fuel properties (Figure 2.4) and principal component scores (Figure 2.5) show that the proposed design includes fuels that cover the outer portions of the 2-by-2 design spaces shown in the pairwise plots; however, there are some minor gaps in the interior of these spaces.

2.4 Fuel data comparisons

The ten test fuels were blended by ConocoPhillips. All test fuels were primarily analyzed by ConocoPhillips and validation analysis were performed by BP. Shown in Figures 2.6 – 2.11 are comparisons of fuel properties (RON, MON, T10, Aromatics%, Olefins%, and total Paraffins%) evaluated by lab analyses and estimated by the blending model.

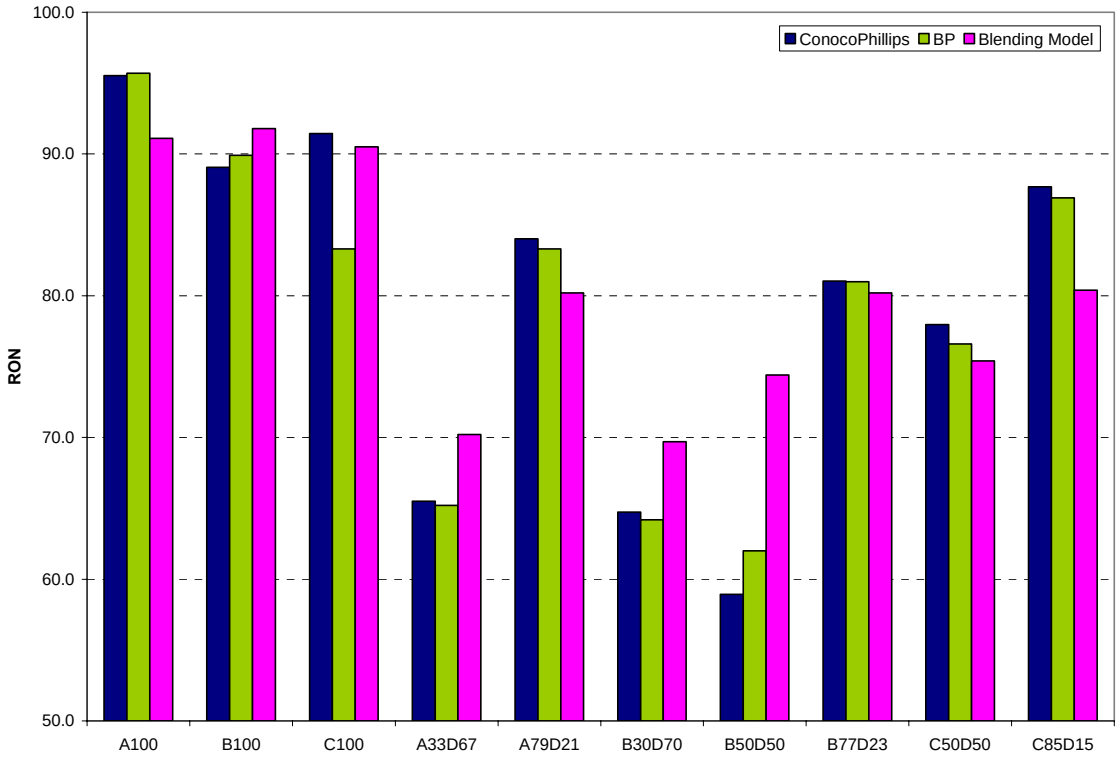

Figure 2.6: Comparisons of RONs analyzed by ConocoPhillips and BP and estimated by the blending model.

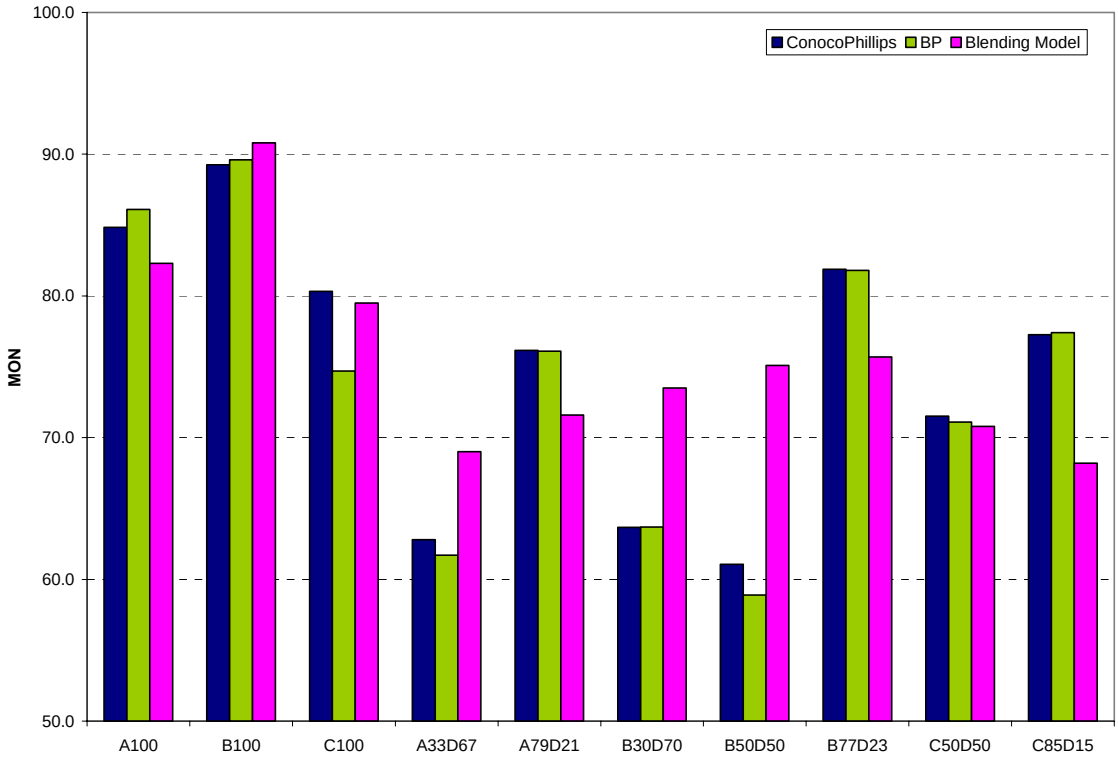

Figure 2.7: Comparisons of MONs analyzed by ConocoPhillips and BP and estimated by the blending model.

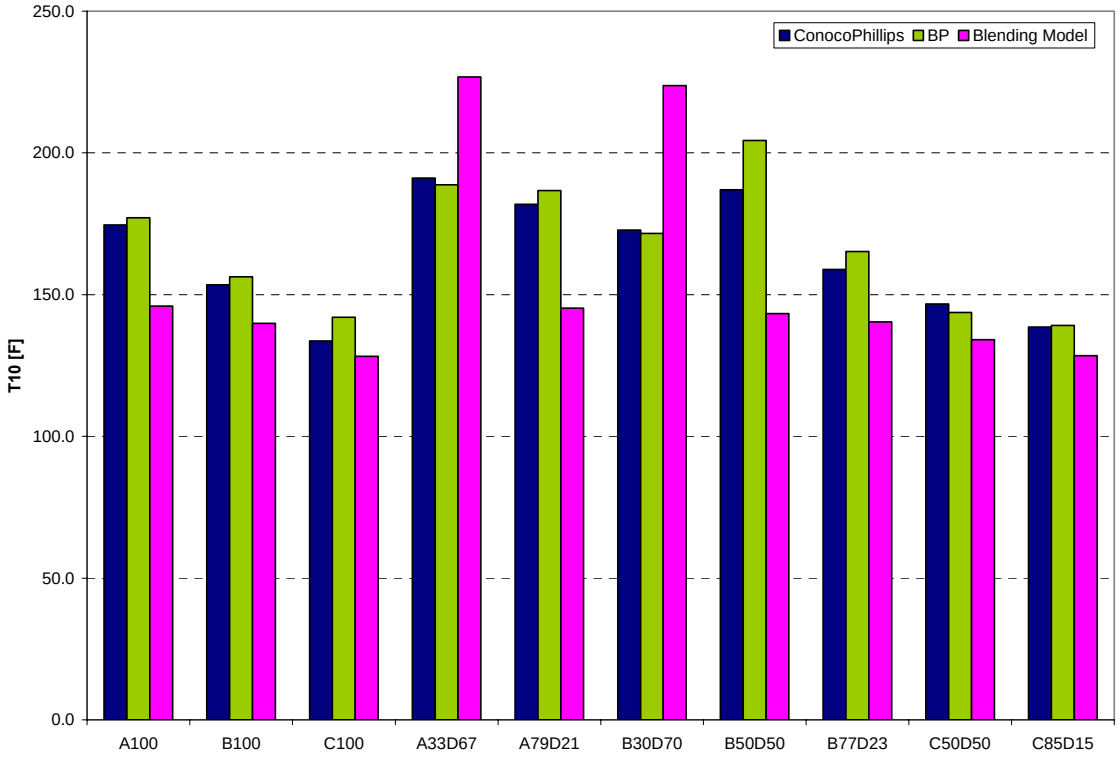

Figure 2.8: Comparisons of T10s analyzed by ConocoPhillips and BP and estimated by the blending model.

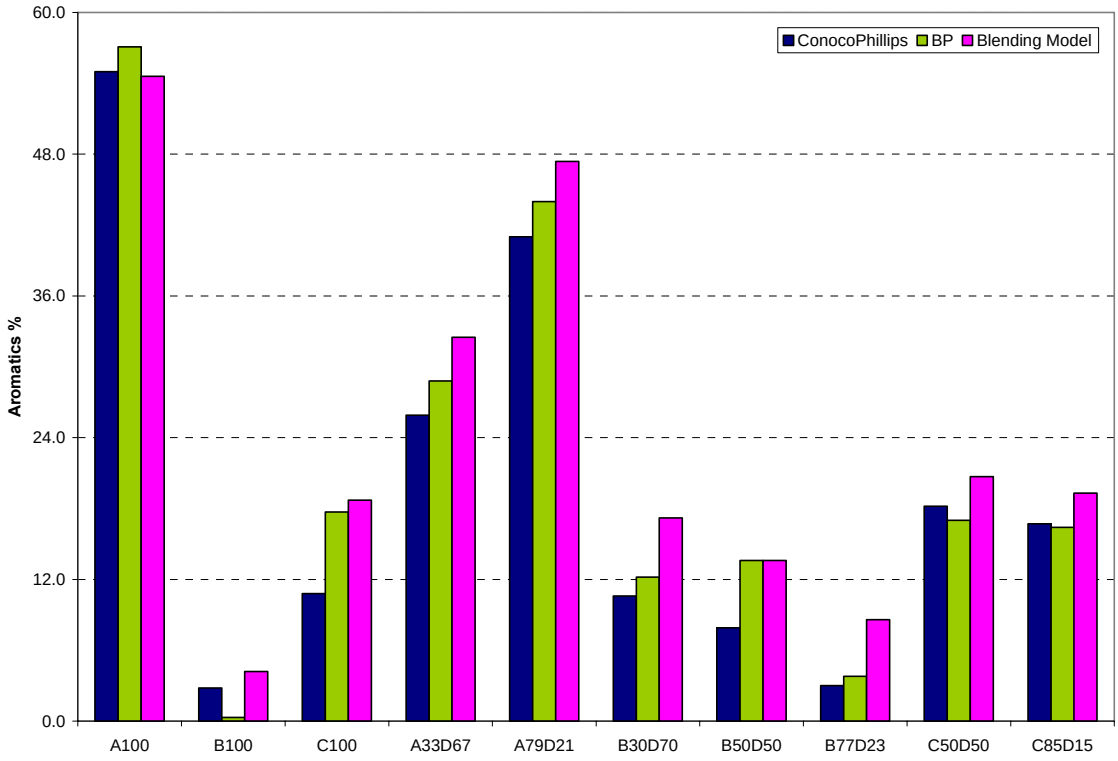

Figure 2.9: Comparisons of percentages of Aromatics analyzed by ConocoPhillips and BP and estimated by the blending model.

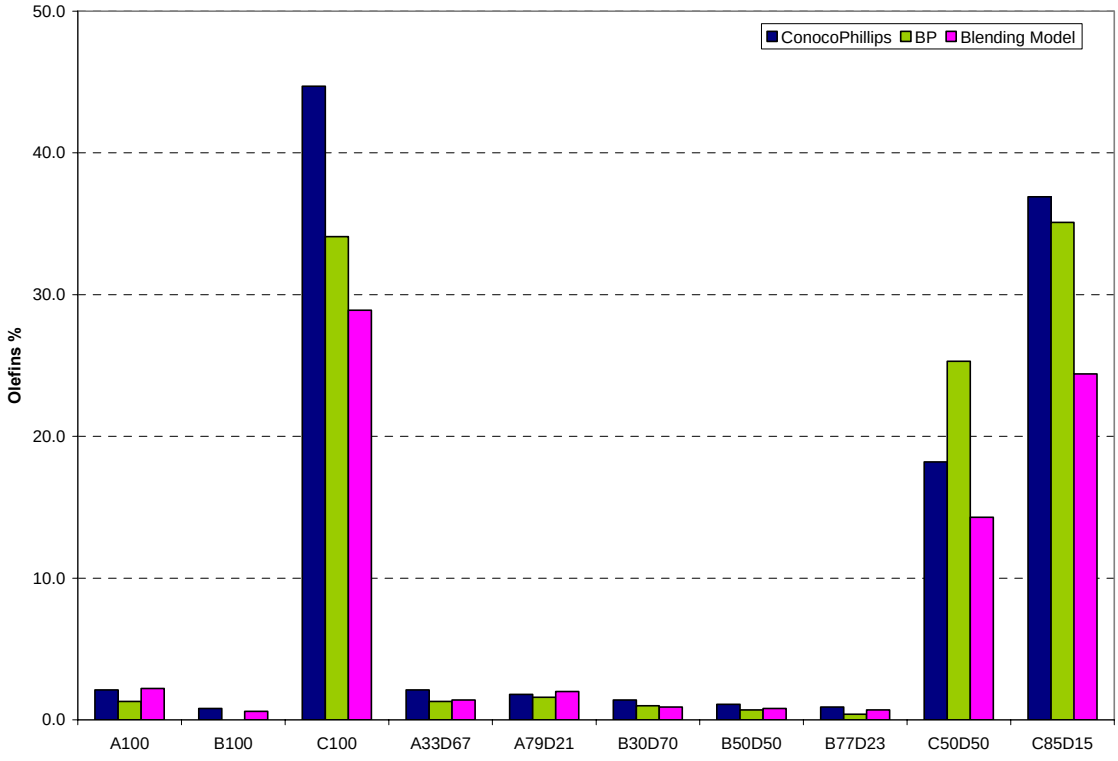

Figure 2.10: Comparisons of percentages of Olefins analyzed by ConocoPhillips and BP and estimated by the blending model.

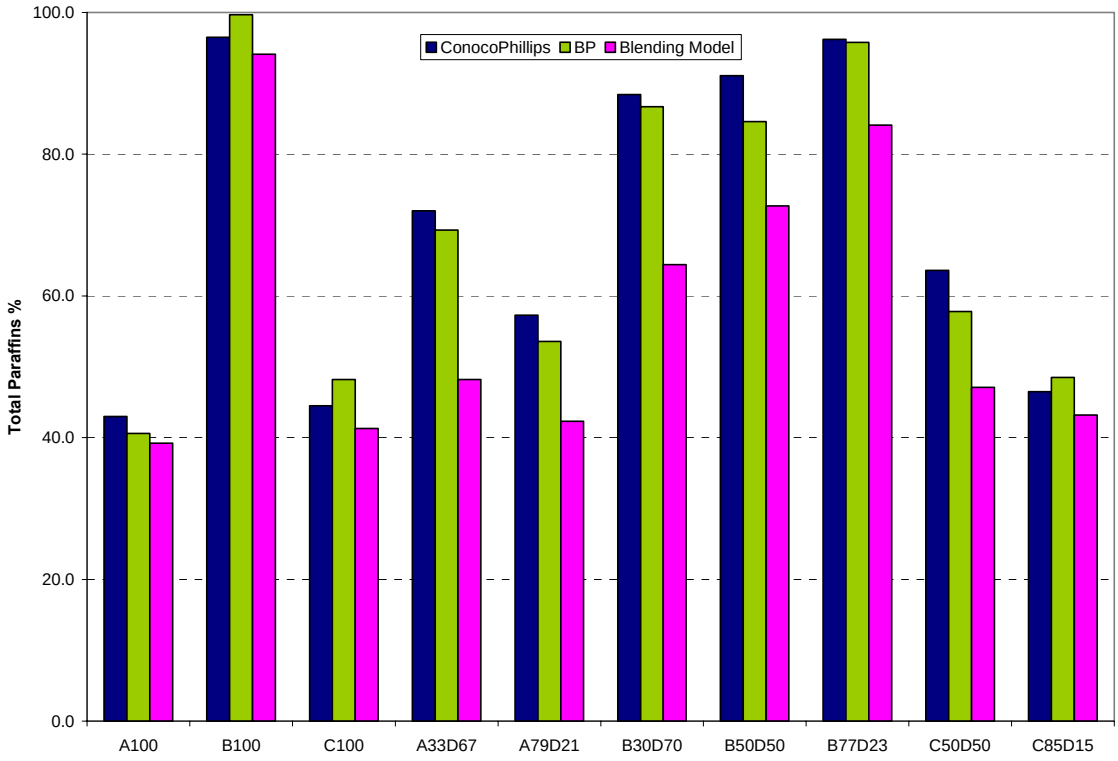

Figure 2.11: Comparisons of percentages of total Parafins analyzed by ConocoPhillips and BP and estimated by the blending model.

These figures show that the fuel properties analyzed by ConocoPhillips and BP are very close, except for fuels C100 and B50D50. Even though there were a few cases where the BP results differed from the ConocoPhillips results, no errors were found in the primary results. For statistical analysis on the fuel impacts in HCCI combustion, the ConocoPhillips data are employed.

Figures 2.6 – 2.11 present that there are big discrepancies between lab analysis results and blending model estimations. However, the discrepancies do not change the relationship between fuel properties, i.e, independent fuel properties are still independent instead of correlating to other fuel properties. Figures 2.12a – 2.12c shows the pairwise plots of lab analyzed fuel properties for the ten test fuels as well as baseline fuel indolene (represented by X in the plots).

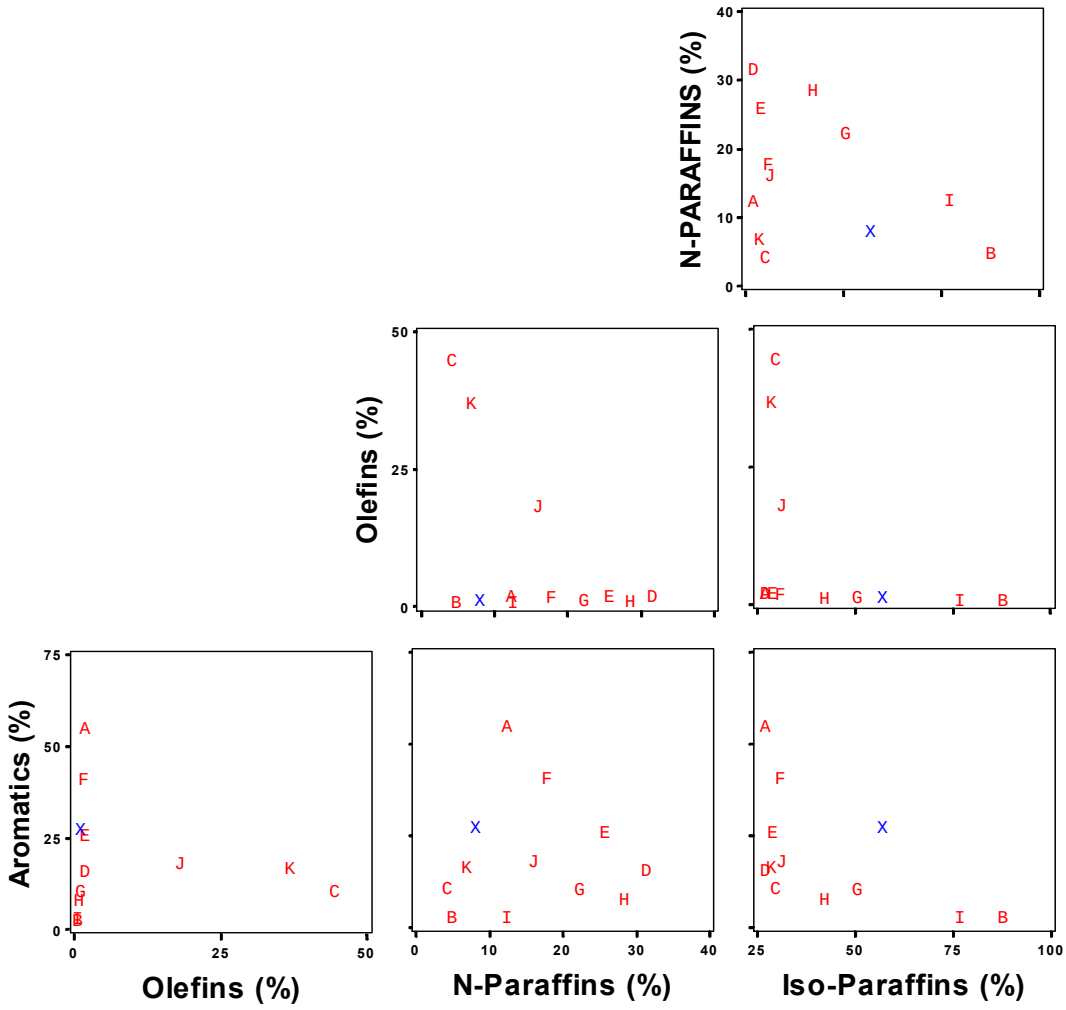

Figure 2.12a: Pairwise plots of fuel properties for the 10 test fuels. Baseline fuel indolene (X) is shown for reference.

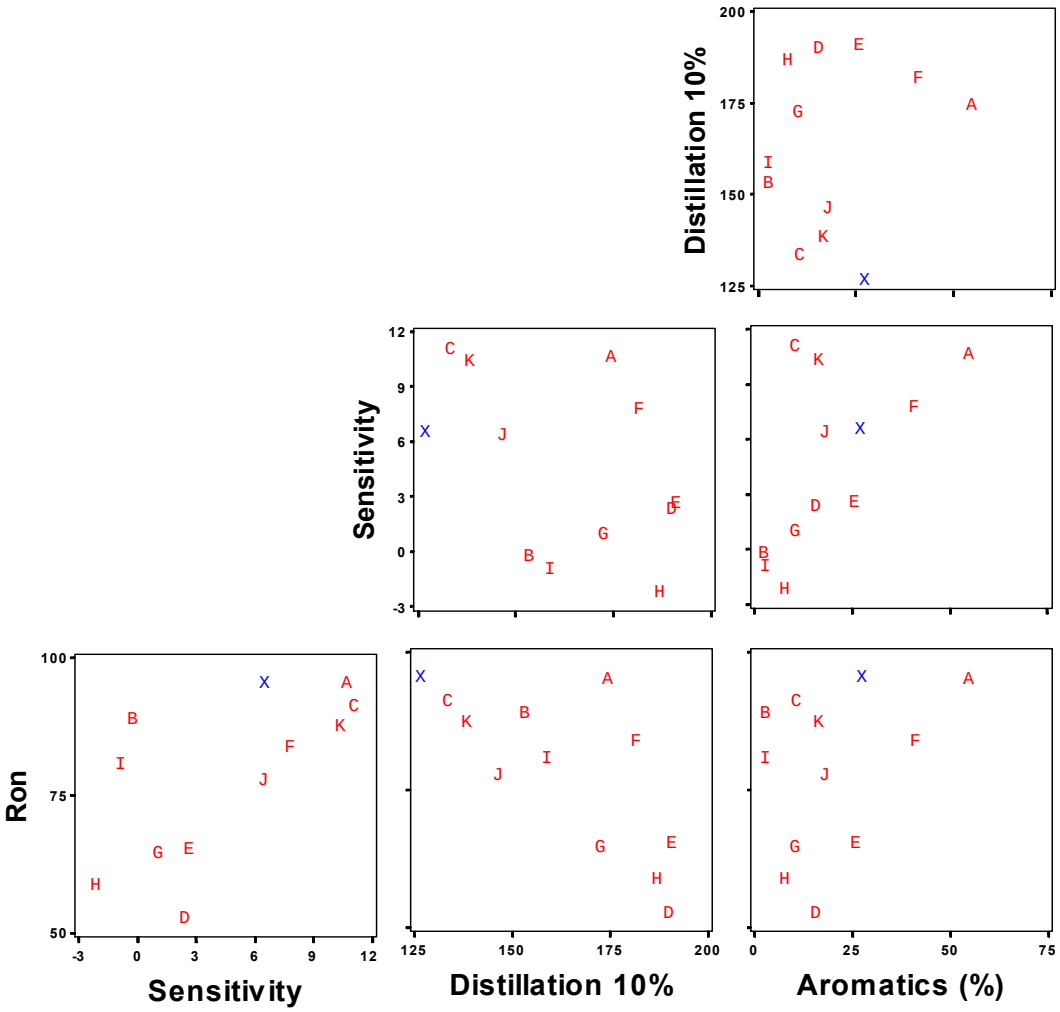

Figure 2.12b: Pairwise plots of fuel properties for the 10 test fuels. Baseline fuel indolene (X) is shown for reference.

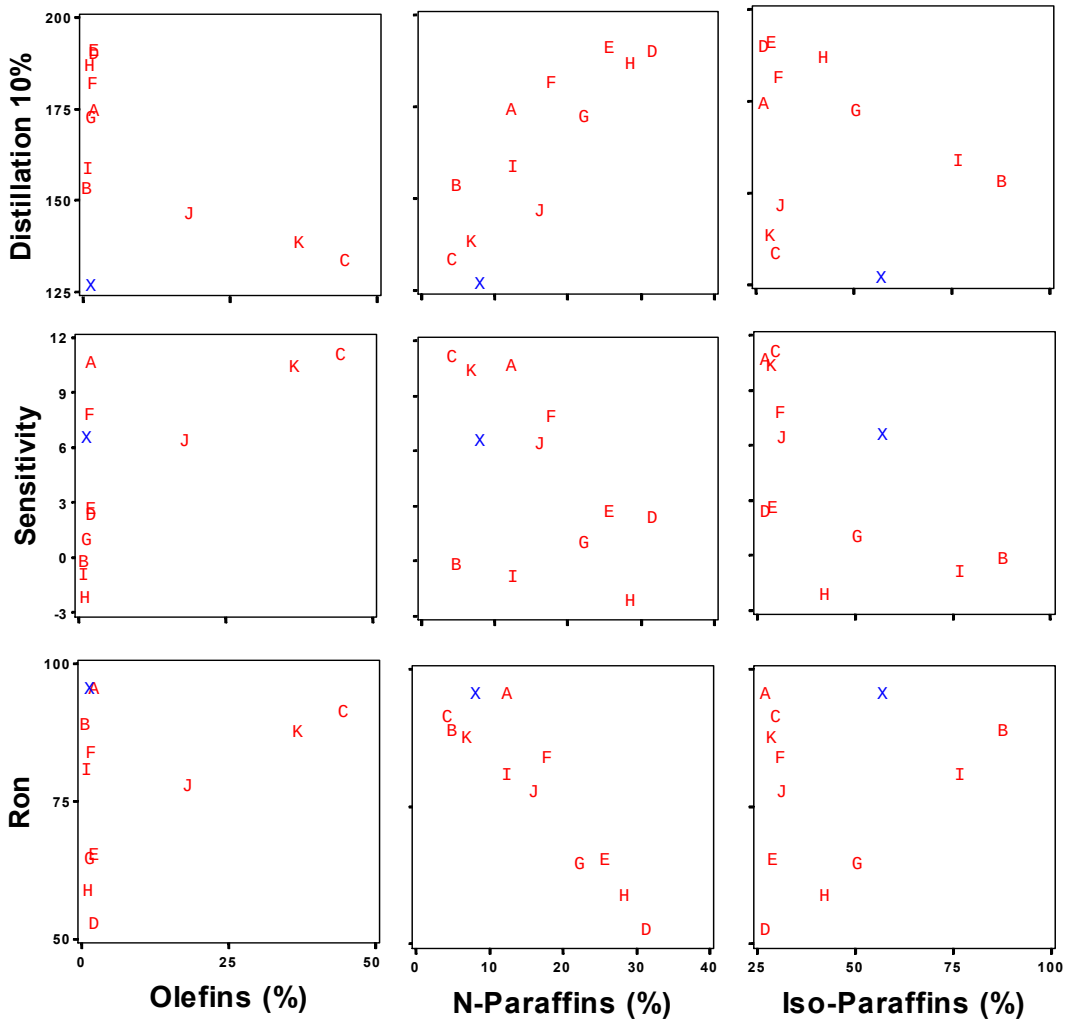

Figure 2.12c: Pairwise plots of fuel properties for the 10 test fuels. Baseline fuel indolene (X) is shown for reference.

2.5 Summary of test fuels

The selected ten test fuels meet the essential design requirement of selecting fuels that are representative of the relevant properties of the candidate fuels that were considered in the study. The ten test fuels span the values of all seven fuel properties as well as the values of all seven principal component scores, which represent the "key independent features" of the fuel properties. Furthermore, the selection does an excellent job of selecting fuels that have intermediate values of each property. This will be helpful in evaluating continuous relationships between the fuel properties and engine performance measures that will be developed during the data analysis phase of this project. Even though there are discrepancies between lab analyzed fuel data and blending model estimated data, the relationship between fuel properties does not change.

3 Baseline fuel tests

The start of combustion in HCCI engines is controlled by chemical kinetics, which is subjected to the intake charge temperature and pressure histories [3]. In general, the intake charge temperature and pressure are controlled by the fuel injection, external Exhaust Gas Re-circulation (EGR), internal EGR, and residual gas for naturally aspirated engines.

Several researchers have implemented HCCI combustion successfully with port fuel injections (PFI) [4, 5]. PFI offers good fuel/air mixing, however, there is no control of the combustion phasing. Marriott et al [6] demonstrated that the combustion phasing can be controlled by the injection timing in a direct injection engine. By sweeping the injection timing from early in the intake stroke to late in the compression stroke, optimum combustion phasings over a range of intake air temperature, engine loads, and speeds were obtained.

In HCCI engines, combustion happens spontaneously leading to high energy release rates and combustion noise. It is very important to dilute the intake charge to lower the combustion rate to protect the engine. Exhaust Gas Re-circulation (EGR) is a major method used to dilute the charge [7-9]. It is found that the higher heat capacity of the exhaust gas can cause a reduction of the end-of-compression charge temperature, which would tend to retard the auto-ignition.

With a variable valve train, two major strategies were employed to obtain the burnt gas to dilute the intake charge: re-compression and re-breathing. In the re-compression mode, the exhaust valves are closed early in the exhaust stroke, before exhaust TDC, to trap burnt gas within the cylinder [10, 11]. In the re-breathing mode, the exhaust gas re-enters the cylinder after leaving the engine through reopening the exhaust valve during the intake stroke, which is also called internal EGR [12, 13].

In this report, both re-compression and re-breathing modes were investigated with a fully variable valve train and direct injection system. Two injection strategies were employed for the re-compression mode, single injection and split injection. For the re-breathing mode, only single injection was studied.

For each intake charge preparation mode, three engine speeds/loads were investigated at the fixed combustion phasing, represented by 50% mass fraction burned location (CA50) at 5 degrees after top dead center (ATDC).

3.1 Experiment

3.1.1 Test engine

The engine used for this study is a single-cylinder research engine equipped with a hydraulic variable valve train and gasoline direct injection system. The geometric parameters of the engine are shown in Table 3.1.

Table 3.1: Engine specifications

Bore [mm]	90.2
Stroke [mm]	90.0
Displacement [l]	0.575
Compression Ratio	11.3
Valve Arrangement	2 Intake / 1 Exhaust
Valve Timing/Lift	Fully Variable
Fuel Injection System	GDI

The engine has two inlet ports, a tangential swirl port and a neutral filling port. The ports are designed to give a torque meter swirl ratio of 2.6 with only the tangential swirl port valve open and 0.1 with both valves open [14]. In this study, only the swirl valve was used to enhance swirl and improve combustion control. Swirl motion of the intake air helps the mixing of fuel and air at the beginning of the intake stroke, and then the mixing process stabilizes during the compression stroke. Near the end of the compression stroke, stabilized motion of the intake charge leads to lower maximum rate of cylinder pressure rise and combustion noise [15, 16]. For all experiments there was no intake-manifold throttling.

A Sturman fully variable Hydraulic Valve Actuation (HVA) system is used on the engine to control valve timings and lifts. It utilizes hydraulic force controlled by high-speed digital latching valves, in place of traditional mechanical camshafts, to actuate engine intake and exhaust valves. Fully variable lift, duration, and timing are independently controlled for all three engine valves [14].

A Bosch HDEV gasoline direct injector was mounted between the two intake valves in the cylinder head. The injector was controlled by a Bosch Injector Power Stage ES-HDEV1, which enables multiple injection events in a single engine cycle.

The engine is equipped with a spark plug, which is located at the center of cylinder head. The spark plug is utilized to start the engine in SI mode, then transition to HCCI mode. Figure 3.1 is a picture of the engine setup in the test cell.

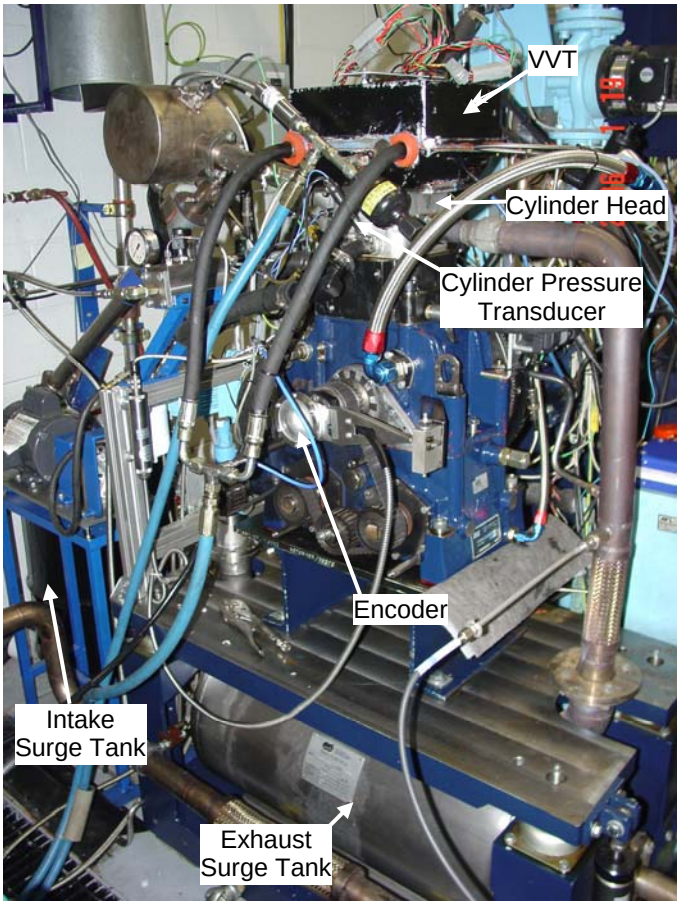

Figure 3.1: Engine setup

3.1.2 Fuel

The fuel used in the baseline engine tests is indolene. The fuel specifications are presented in Table 3.1.

Table 3.2: Fuel specifications

Fuel	Indolene
RON	96.5
MON	87.5
Heating Value [kJ/kg]	43,007
Aromatics [% vol]	30.5
Olefins [% vol]	0.2
Saturates [% vol]	69.3

3.1.3 Intake charge preparation

Three different intake charge preparation modes were tested in this study. The first mode is Re-Compression Early Injection (RCEI) mode, which employs Early Exhaust

Valve Closing (EEVC) resulting in residual burnt gas being trapped in the cylinder and re-compressed plus early fuel injection to provide a homogeneous fuel/air mixture.

The second mode is Re-Compression Split Injection (RCSI) mode, which is very similar to the first mode, trapping the burnt gas in cylinder and re-compressing it by closing the exhaust valve early. However, there are two injection events in one cycle in this mode, one happens early to provide a homogeneous fuel/air mixture, the other one happens late in the compression stroke to stratify the homogeneous charge.

The third mode is Re-Breathing Early Injection (RBEI) mode, in which the exhaust valve remains open longer than during the first two modes trapping less residual gas and re-opens during the intake stroke to induce burnt gas into the cylinder from exhaust port. In RBEI mode, there is only one early injection to provide a homogeneous fuel/air mixture.

The injection timings and valve timings for the three intake charge preparation modes are shown in Figures 3.2 – 3.4 along with the measured cylinder pressure. The optimization of the valve timings and injection timings will be discussed later.

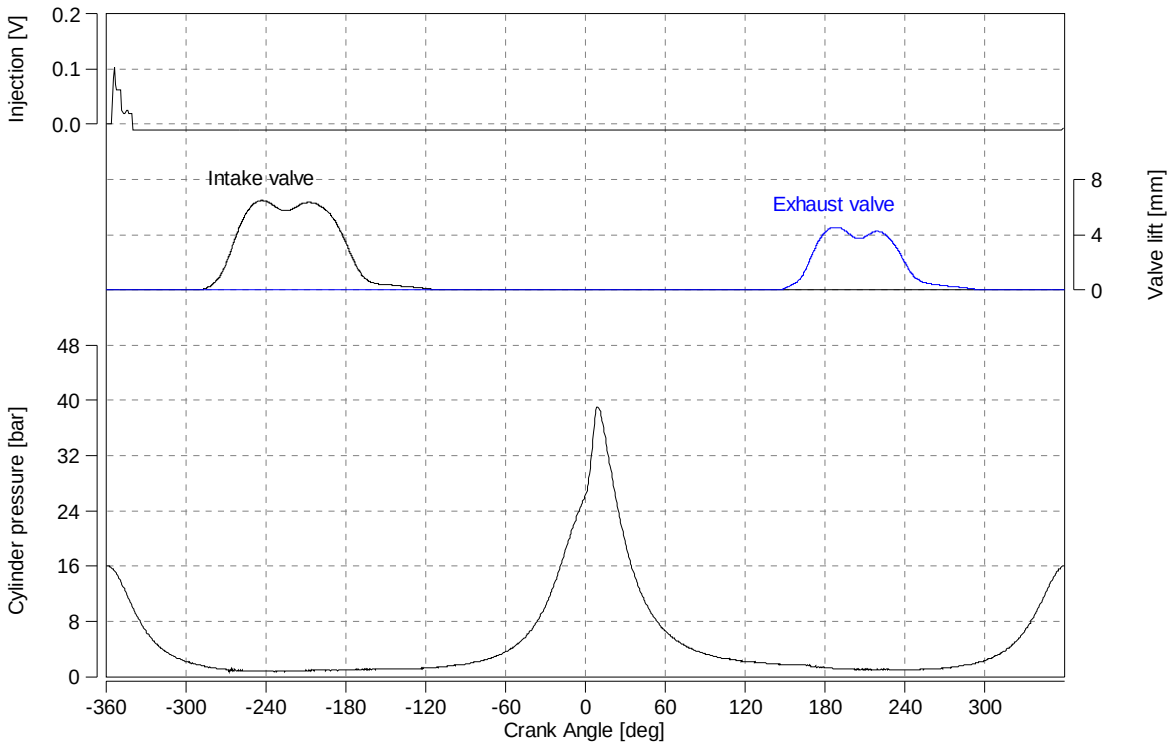

Figure 3.2: Injection event, valve traces, and cylinder pressure trace for RCEI HCCI combustions at 2000 rpm, 3 bar IMEP.

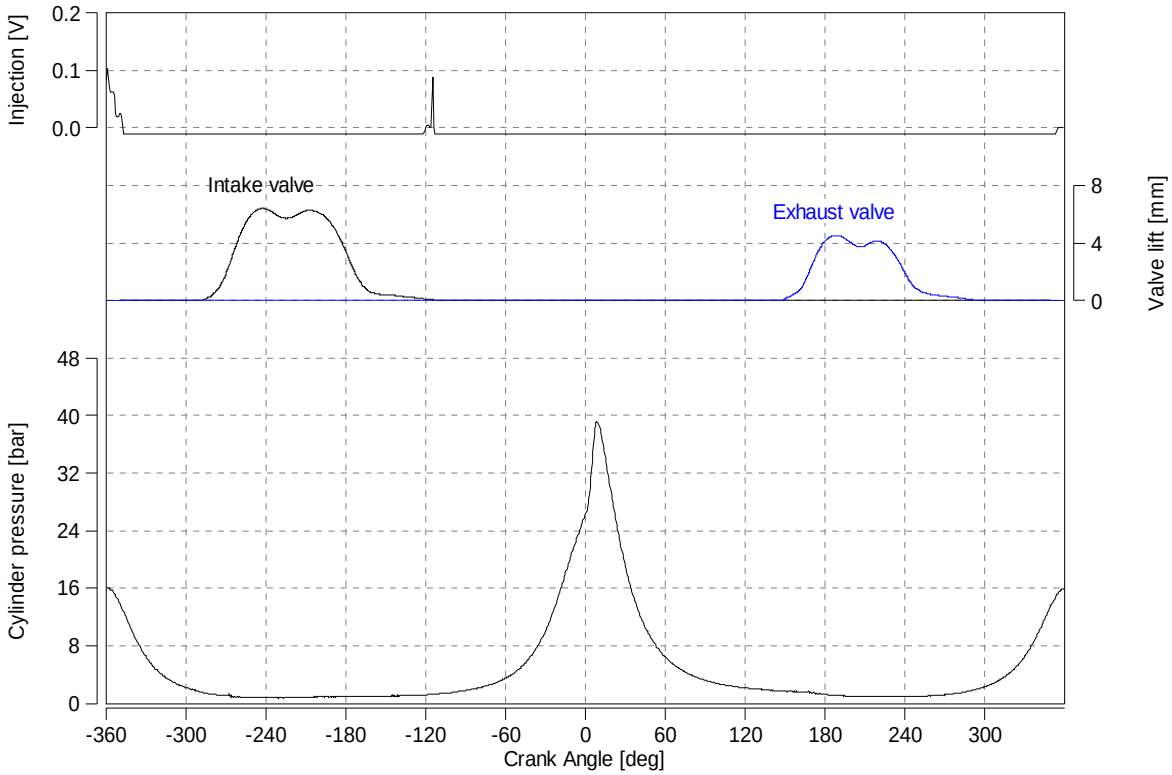

Figure 3.3: Injection event, valve traces, and cylinder pressure trace for RCSI HCCI combustions at 2000 rpm, 3 bar IMEP.

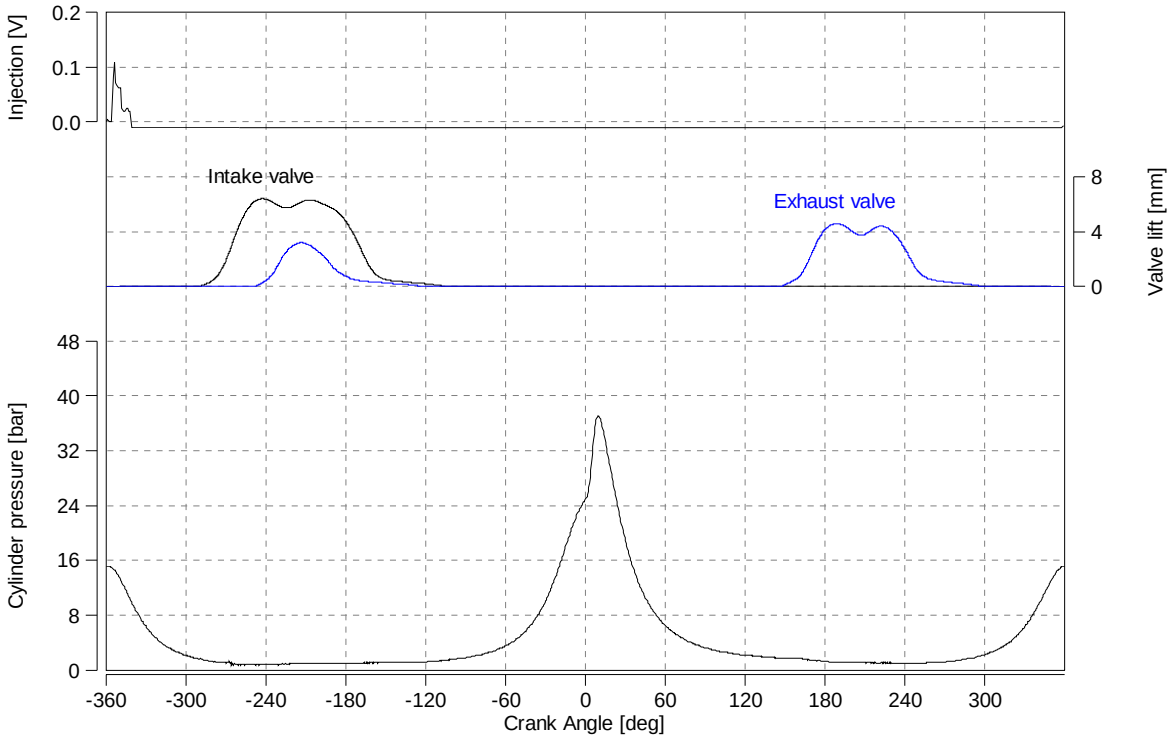

Figure 3.4: Injection event, valve traces, and cylinder pressure trace for RBEI combustions at 2000 rpm, 3 bar IMEP.

3.1.4 Engine operating conditions

Three engine operating speeds/loads were investigated in this study, which are shown in Table 3.3.

Table 3.3: Engine operating conditions

	Idle	Mid-Speed	High Speed
Speed [rpm]	1000	2000	3000
IMEP [bar]	1.5	3	N/A
CA50 [° ATDC]	5	5	5
MRPR [bar/deg]	N/A	N/A	5.5

For all three engine operating conditions, the combustion phasings were fixed, represented by 50% mass fraction burned location (CA50), at 5 degrees ATDC. At 1000 rpm and 2000 rpm, the engine loads were controlled by IMEP, while controlled by the maximum rate of pressure rise (MRPR) at 3000 rpm.

3.2 Results – baseline testing

3.2.1 Valve timing

Single Exhaust Event – RCEI and RCSI

Base valve timings and lifts were optimized in the Re-Compression Early Injection (RCEI) mode at 2000 rpm, 3 bar IMEP. Two criteria for the optimization are (1) CA50 at 5 degrees ATDC and (2) coefficient of variation (COV) of IMEP lower than 3%.

With the base valve timings and lifts shown in Table 3.4, the combustion phasing is well controlled (CA50 = 5.2 °ATDC) and the COV of IMEP is less than 2% (COV of IMEP = 1.72%). The actual valve timings and lifts used at the other speeds and loads will change slightly from the base timings and lifts, depending on the engine operating conditions.

Table 3.4: Base valve timings and lifts

Intake Valve Open [deg. BTDC]	268
Intake Valve Close [deg. BTDC]	168
Intake Valve Lift [mm]	6
Exhaust Valve Open [deg. ATDC]	166
Exhaust Valve Close [deg. ATDC]	247
Exhaust Valve Lift [mm]	4

Dual Exhaust Events - RBEI

The base timings of the second exhaust valve event were optimized by sweeping the second exhaust valve opening with a fixed valve open duration of 50 degrees and valve lift of 3 mm at 2000 rpm and 3 bar IMEP for the Re-Breathing Early Injection (RBEI)

mode. Figure 3.5 shows that the optimum second exhaust valve opening is at 240 °BTDC and second exhaust valve closing at 190 °BTDC in terms of CA50 and lowest COV of IMEP. The actual second exhaust valve timings and lifts for RBSI HCCI will be dependent on engine speed and load. In general, the open duration of the second exhaust valve falls in the middle of intake valve open period.

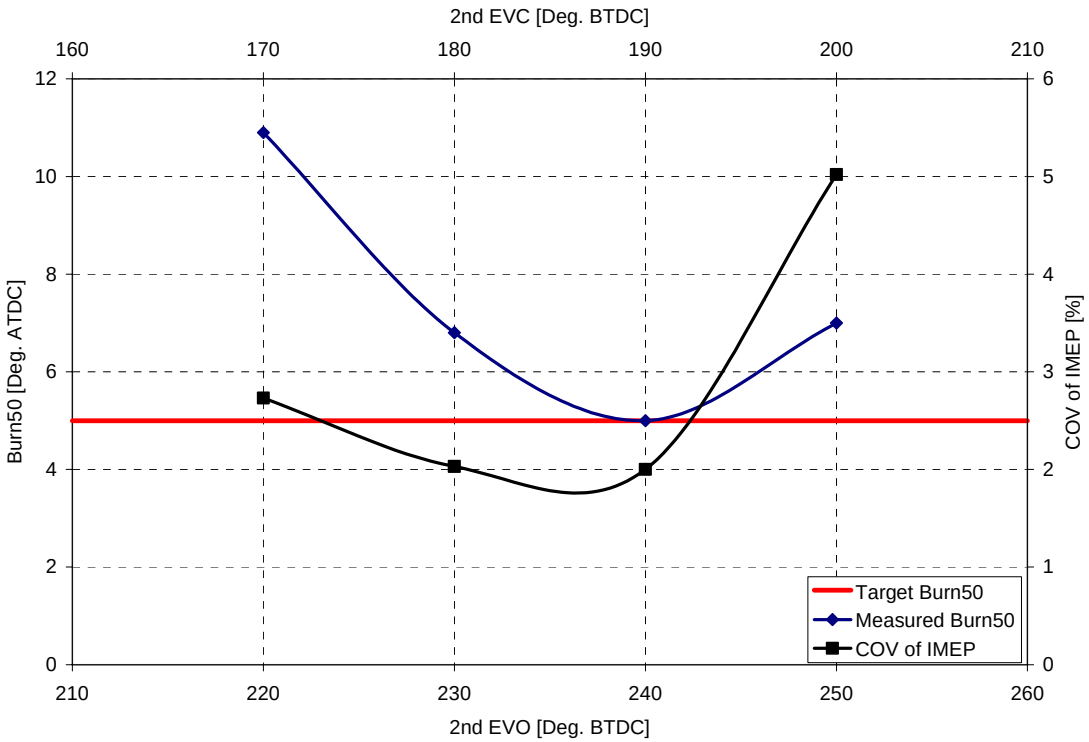

Figure 3.5: CA50s and COVs of IMEP with different second valve timings in RBEI mode at 2000 rpm, 3 bar IMEP

3.2.2 Fuel injection

Rail Pressure

The rail pressure for the Bosch HDEV gasoline direction injection (GDI) system was investigated in RCEI mode at the 2000 rpm and 3 bar IMEP to find the optimum rail pressure for HCCI combustion. It is shown in Figure 3.6 that a higher rail pressure leads to lower COV of IMEP. Fuel penetration and atomization affect the mixing process of air and fuel. Fuel penetration and atomization are better at higher rail pressure, which leads to more homogeneous air and fuel mixing, less cycle-to-cycle variations, and lower COV of IMEP. In this study, a rail pressure of 60 bar was used for all tests, except Re-Compression Split Injection (RCSI) mode at 1000 rpm due to the minimum injection pulse width limit.

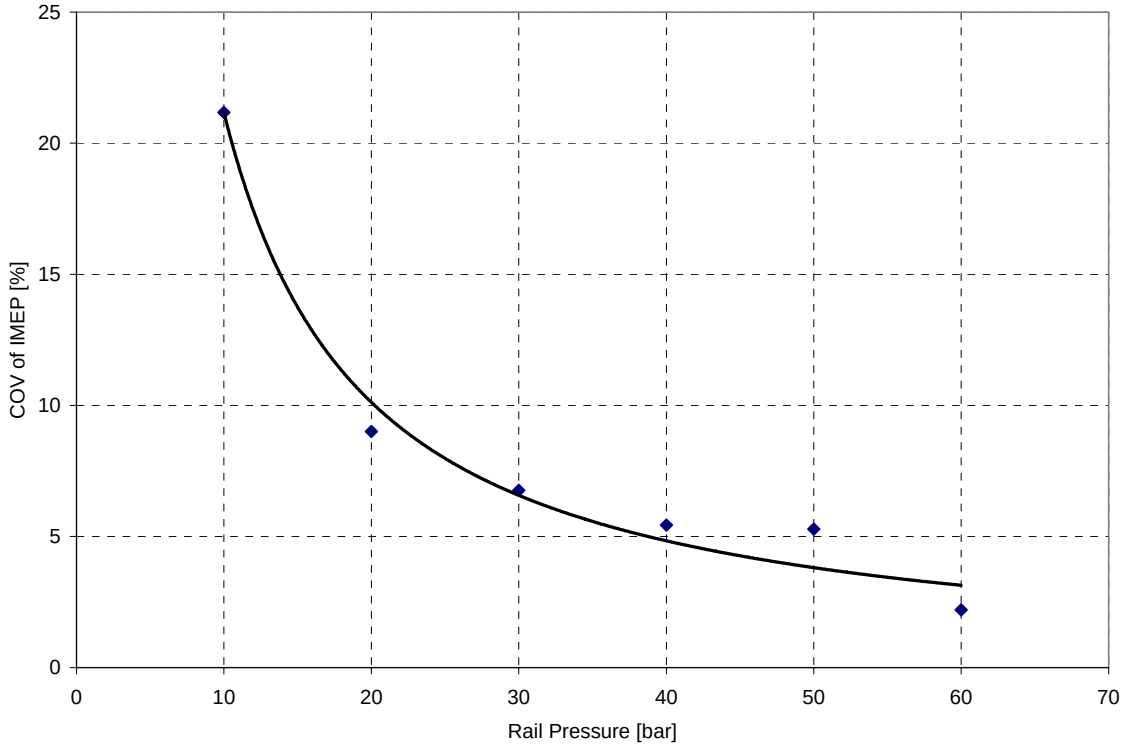

Figure 3.6: The influence of rail pressure on the COV of IMEP in RCEI mode at 2000 rpm and 3 bar IMEP.

Single Injection Timing

The injection timings for RCEI and RBEI modes for the GDI system at the rail pressure of 60 bar were investigated in RCEI mode at 2000 rpm and 3 bar IMEP. It is found in Table 3.5 that HCCI combustion could not be maintained when fuel was injected near intake valve opening or during the intake valve open period (456 degrees through 554 degrees). When fuel was injected after the intake valve closed, only spark-assisted HCCI combustions could be maintained. Therefore, an injection timing of 360 was used for most of tests in this study.

Table 3.5: Combustion characteristics with different injection timings in RCEI mode at 2000 rpm, 3 bar IMEP

Injection Timing	Combustion Mode	CA 50
[° ATDC]	[-]	[°ATDC]
300	Pure HCCI	-2
-360	Pure HCCI	5
-300	No combustion	N/A
-240	No combustion	N/A
-180	No combustion	N/A
-150	Spark-assisted HCCI	5
-120	Spark-assisted HCCI	5

Note: 0 degree is defined as compression TDC, see Figure 2.

Split Injections Timing and Amount

For the Re-Compression Split Injection (RCSI) mode, both the injection timing and pulse width of the second injection were investigated at 2000 rpm and 3 bar IMEP. The first injection timing was carried over from the RCEI mode, which is around top dead center of the exhaust stroke. With the first injection around exhaust TDC, it is found that CA50 at 5 degrees ATDC can only be achieved by injecting fuel around 240 ATDC for the second injection event.

The relationship between the COV of IMEP with the amount of fuel in the second injection is shown in Figure 3.7. It is shown that smaller amounts of the second fuel injection lead to lower COV of IMEP. In general, smaller amounts of the second fuel injection introduce less stratification of fuel in the combustion chamber, which leads to more homogeneous fuel/air mixing, less cycle-to-cycle variations, and lower COV of IMEP. In this study, the amount of the second fuel injection was around 35% of the total fuel injection to maintain a low COV of IMEP.

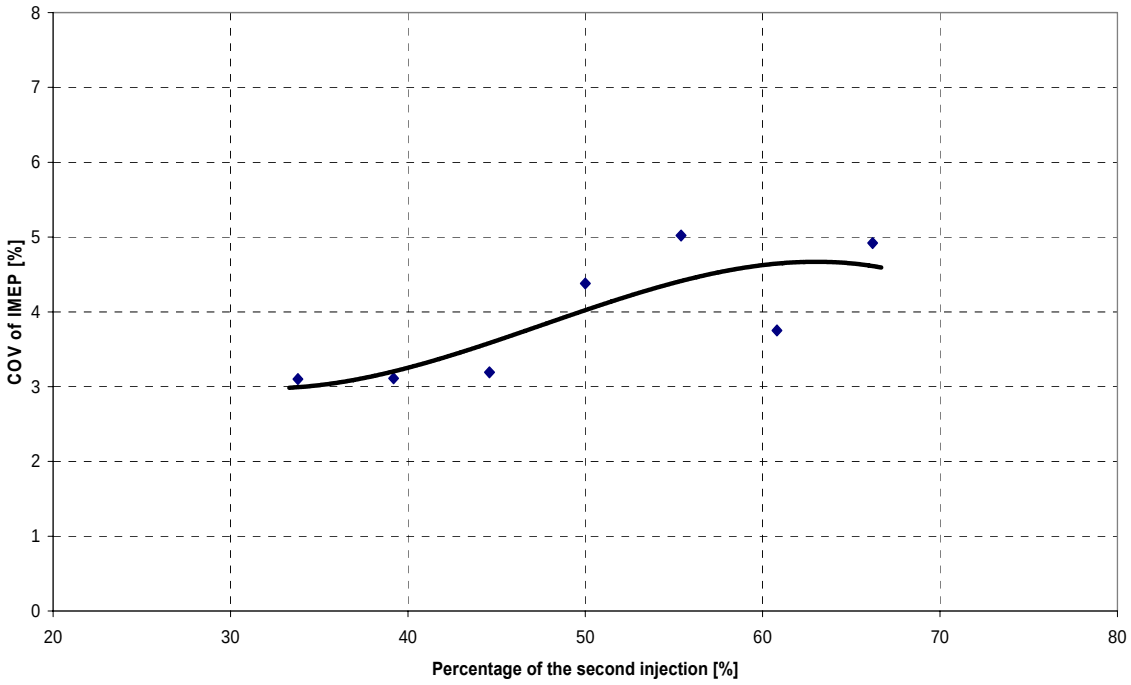

Figure 3.7: The influence of the amount of the second injection on the COV of IMEP in RCSI mode at 2000 rpm and 3 bar IMEP.

3.2.3 Combustion characteristics

Indicated Thermal Efficiency

The indicated thermal efficiency is defined as the ratio of net work (calculated from measured cylinder pressure trace) generated in the cylinder from combustion to the total amount of energy released from burning the fuel [17], which is

$$\eta_f = \frac{W_c}{m_f Q_{HV}} = \frac{P}{\dot{m}_f Q_{HV}} = \frac{1}{ISFC \times Q_{HV}} \qquad (3.1)$$

where W_C is the net work generated in the cylinder per cycle, m_f is the mass of fuel inducted per cycle, Q_{HV} is the heating value of the fuel, P is the indicated power, $\dot{m}_f$ is the fuel flow rate, and $ISFC$ is the indicated specific fuel consumption.

The Indicated thermal efficiencies for the three HCCI combustion modes are shown in Figure 3.8. It is shown that all three intake charge preparation modes have similar indicated thermal efficiencies at 1000 rpm/1.5 bar IMEP and 2000 rpm/3 bar IMEP. At 3000 rpm/2.9 bar IMEP, RCEI has the highest indicated thermal efficiency, while RCSI has the lowest. At higher engine speed, there is less fuel and air mixing time. The second injection in RCSI mode and second exhaust event in RBEI mode introduce more inhomogeneous mixture in the cylinder than those at lower engine speed, which lower the indicated thermal efficiencies in these two intake charge preparations modes.

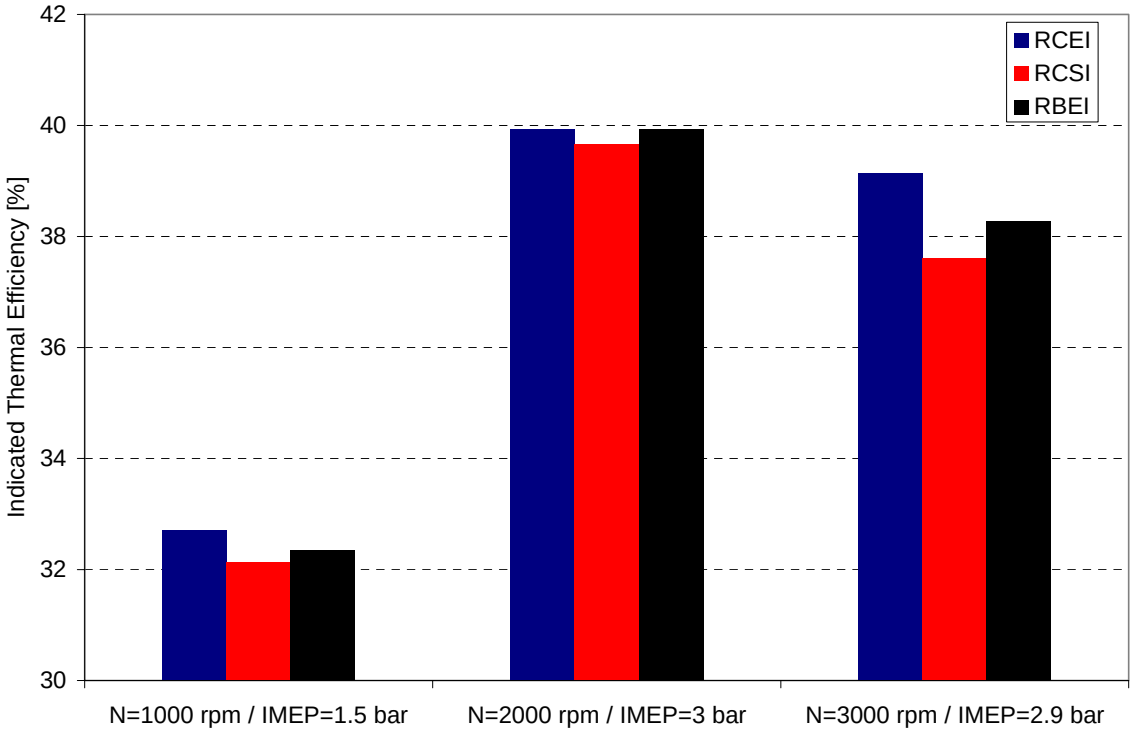

Figure 3.8: The indicated thermal efficiencies of HCCI combustion at the three different speed/load points.

It is also shown in Figure 3.8 that the indicated thermal efficiencies at idle (1000 rpm/1.5 bar IMEP) are the lowest among three engine operating conditions, which is due to unstable HCCI combustion. Figure 3.9 presents COVs of IMEP for the three different speed/load points. It is shown that the COVs at idle for all three charge preparation modes are higher than those at the higher speeds, due to different controls of start of combustion at idle. Another factor that produces lower indicated thermal efficiencies at idle is the longer time available for heat transfer to the cylinder walls.

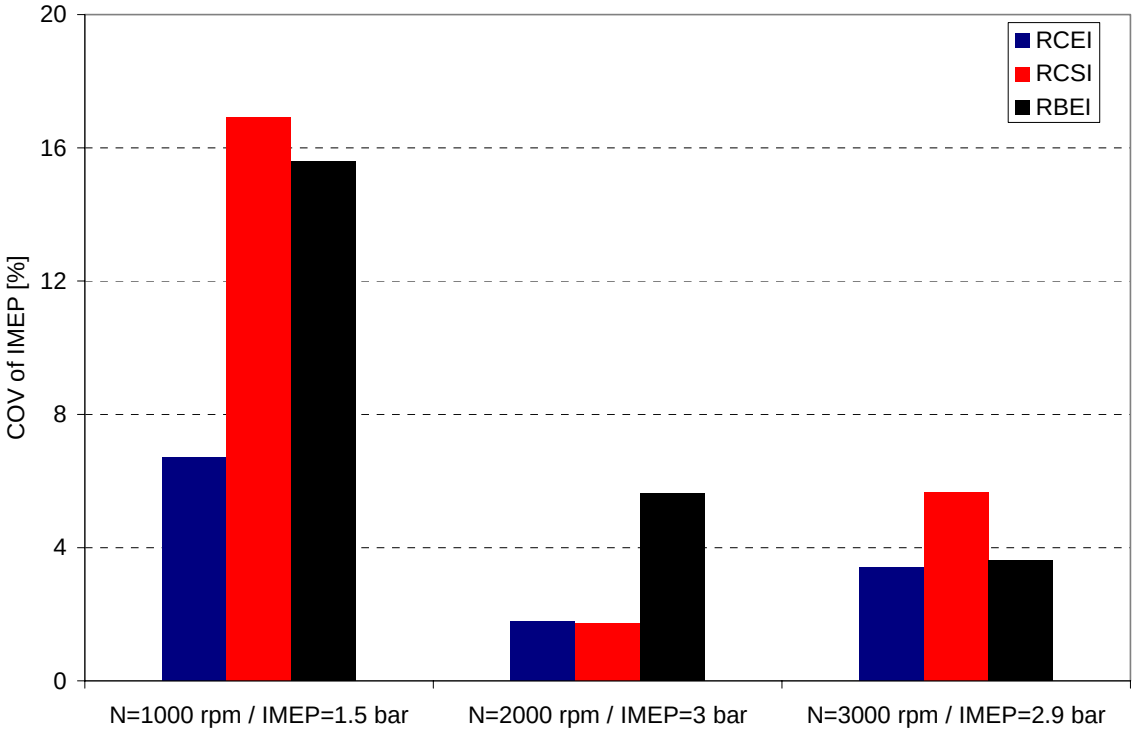

Figure 3.9: COVs of IMEP of HCCI combustion at the three different speed/load points.

At 3000 rpm, indicated thermal efficiencies are lower than those at 2000 rpm, although the IMEPs are near the same level. Shown in Table 3.6 are maximum rates of pressure rises at 2000 rpm and 3000 rpm. It is shown that the maximum rates of pressure rise in the cylinder are around 4 bar/deg at 2000 rpm, while those at 3000 rpm are 5.5 bar/deg, which generates higher peak cylinder pressures and peak cylinder temperatures at 3000 rpm leading to higher temperature gradients across the cylinder wall, more heat loss to the wall, and lower indicated thermal efficiencies compared to those at 2000 rpm. The calculated in-cylinder temperature traces for Re-compression Early Injection HCCI combustions at 2000 rpm and 3000 rpm are shown in Figure 3.10.

Table 3.6: MRPRs at different engine speeds

Speed [rpm]	HCCI Mode	MRPR [bar/deg]
2000	RCEI	4.0
	RCSI	3.7
	RBEI	3.2
3000	RCEI	5.5
	RCSI	5.5
	RBEI	5.5

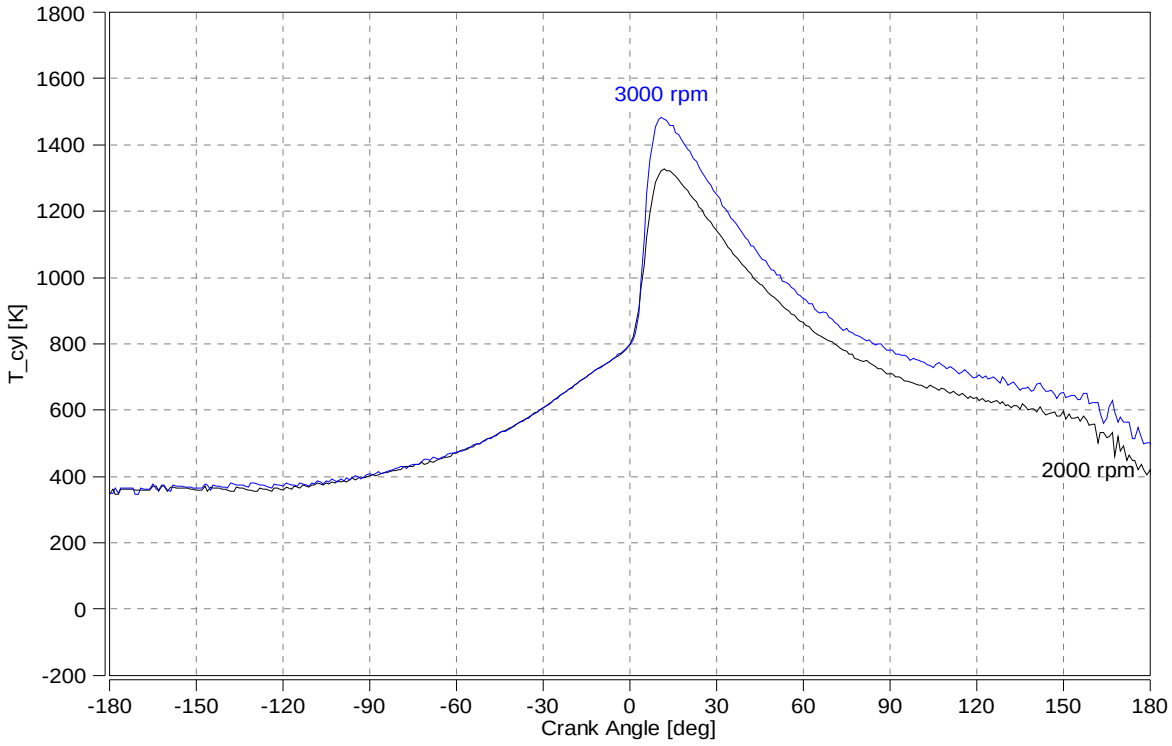

Figure 3.10: In-cylinder temperatures of RCEI HCCI combustions at 2000 rpm and 3000 rpm.

Indicated Specific Fuel Consumption

According to equation (3.1), indicated specific fuel consumptions are inversely proportional to indicated thermal efficiencies. It is shown in Figure 3.11 that Re-Compression Early Injection HCCI combustion has the lowest indicated specific fuel consumptions for all three speed/load points, while Re-Compression Split Injection mode has the highest fuel consumptions. For the RCSI HCCI combustions, around 30% of fuel is injected into the cylinder near the end of the compression stroke. Because of the short mixing time, part of fuel from the second injection was not well mixed with fresh air leading to incomplete combustion and higher fuel consumptions. The differences in fuel consumptions for RCEI and RCSI are significant at 3000 rpm, which is introduced by a shorter mixing time at higher engine speed.

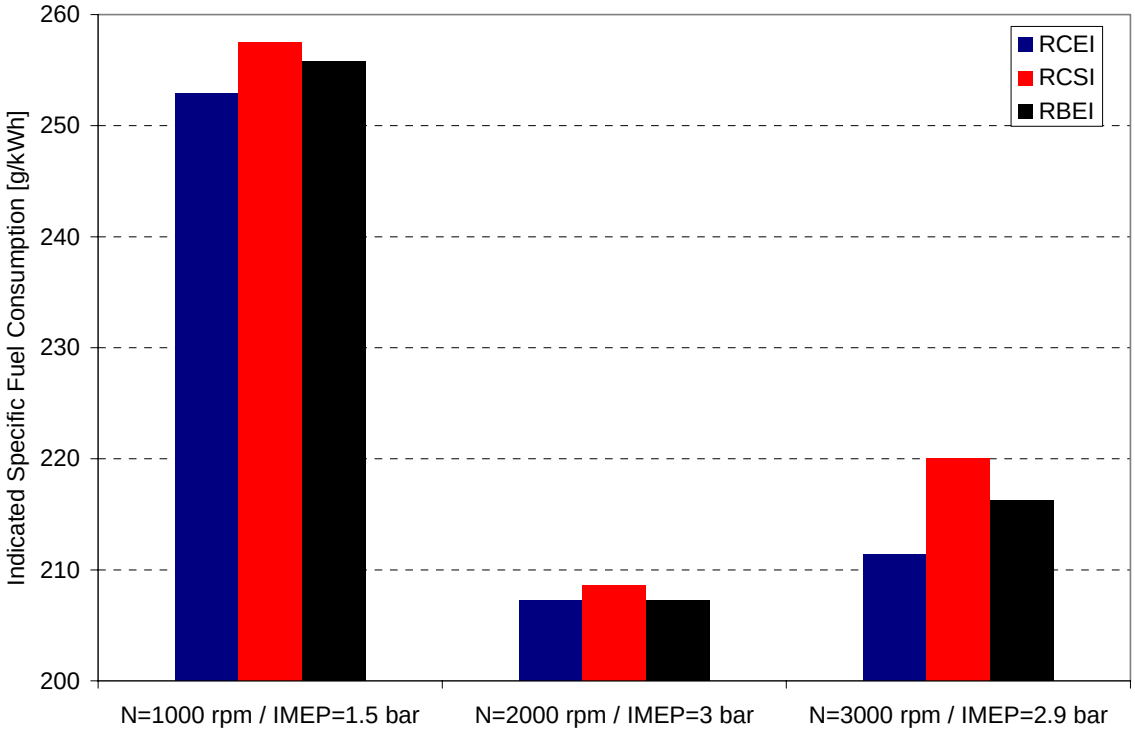

Figure 3.11: Indicated specific fuel consumptions of HCCI combustions at the three different speed/load points.

Fuel consumptions for Re-Breathing Early Injection HCCI combustion are higher than Re-Compression Early Injection HCCI combustion due to the heterogeneity introduced by the second exhaust valve opening during the intake stroke. In addition, more burnt gas was trapped in the combustion chamber with the second exhaust valve event, which leads to more incomplete combustion. Shown in Figure 3.12 are relative air/fuel ratios (λ) for all three speed/load points. It is shown in the figure that relative air/fuel ratios for RBEI HCCI combustions are the lowest among all three charge preparation modes, which indicates that the percentage of residual gas for RBEI HCCI combustions is the highest.

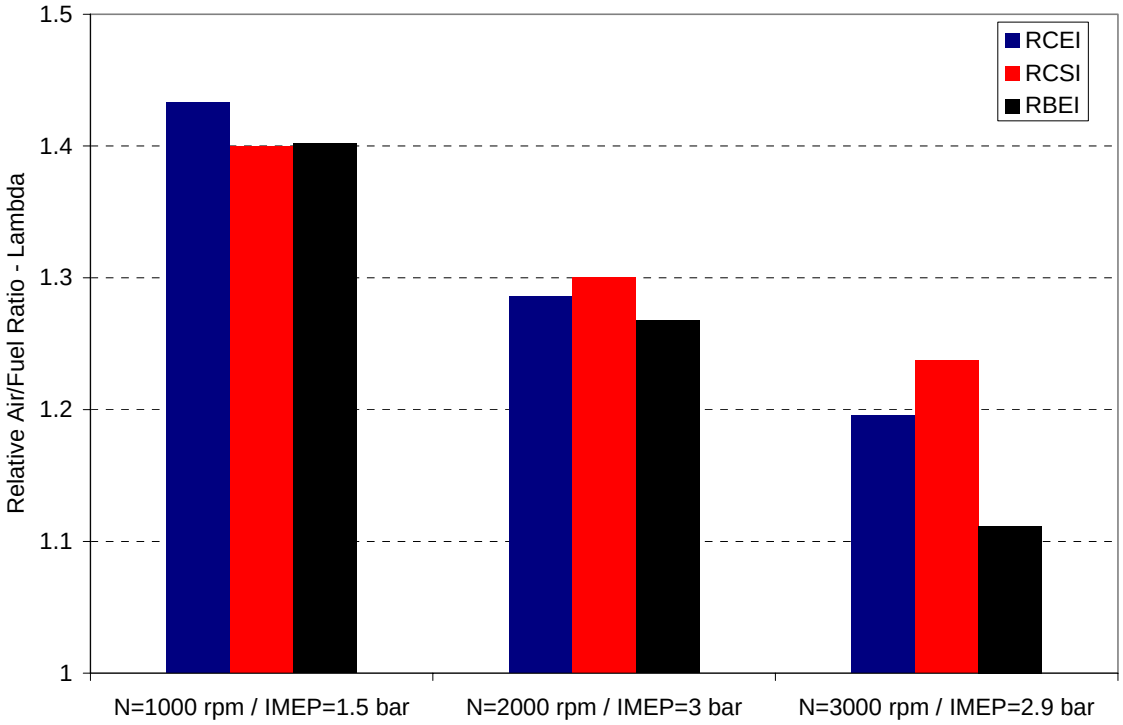

Figure 3.12: Relative air/fuel ratios (λ) of HCCI combustions at the three different speed/load points.

Rates of Heat Release

In this study, the combustion phasing, represented by 50% mass fraction burned location (CA50), was fixed at 5 degrees after top dead center (ATDC) for all testing points as shown in Figure 3.13.

To maintain constant combustion phasing, two parameters are changed from mode to mode. The primary parameter is the exhaust valve closing time. By adjusting the exhaust valve closing, the amount of residual gas and internal EGR are controlled to maintain the CA50 around 5 degrees ATDC. The secondary parameter used to control the combustion timing is the injection timing, which is controlled to fine tune the CA50 at 5 degrees ATDC. The best combinations of exhaust valve closing and injection timing are determined based on combustion stability. In this study, the coefficients of variation (COV) of IMEP are controlled to be less than or equal to 3%.

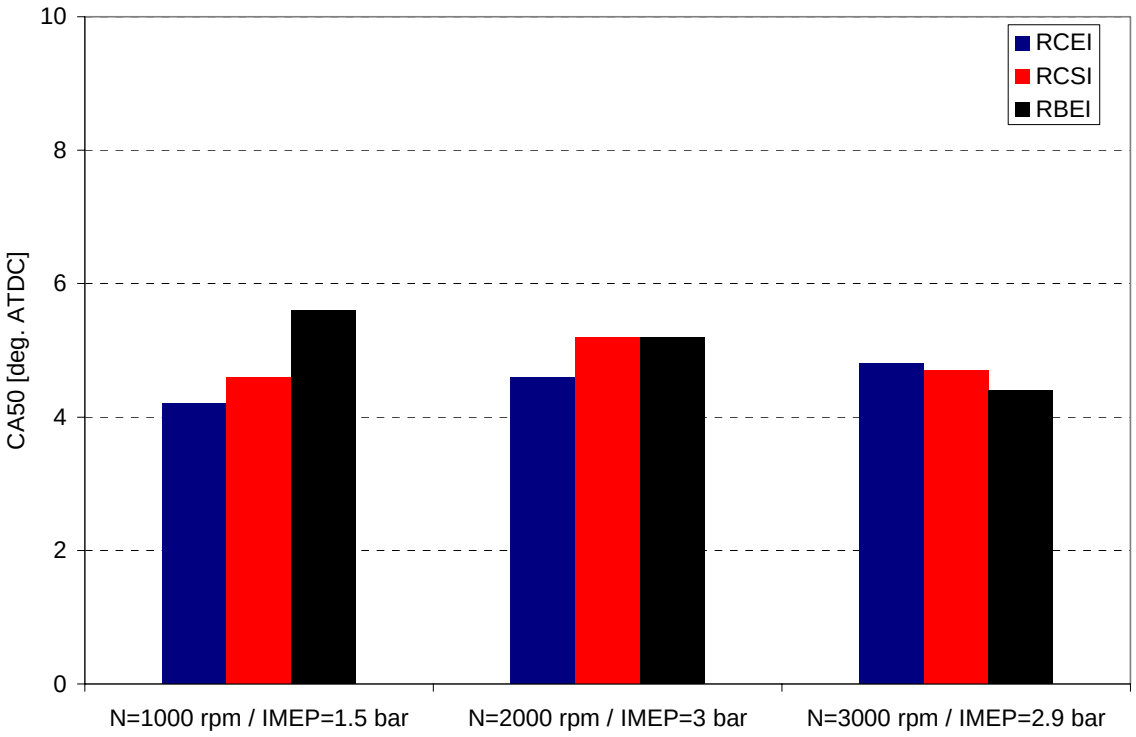

Figure 3.13: CA50 of HCCI combustion at the three different speed/load points.

The rates of heat release during the HCCI combustion for all three charge preparation modes at 2000 rpm are shown in Figure 3.14. It is shown that RCSI had the earliest heat release, which was triggered by the second injection near TDC. However, rates of heat release during the early stage of combustion for RCSI are lower than those for RCEI due to inhomogeneous mixing of the second injection fuel and fresh air. Due to the second exhaust valve opening during the intake stroke for RBEI mode, more exhaust gas was introduced into the combustion chamber and combustion was further damped, which was shown in Figure 3.14 with late and slow heat release.

During the heat release process, Figure 3.14, there is an inflection point in the heat release profile for RCSI mode. For RCSI HCCI combustion, the second injection introduced heterogeneity into the combustion chamber and initiated the combustion. With the combustion progressing, more and more homogeneous mixture of air and fuel from the first injection joined the combustion leading to a faster burn. For the other two charge preparation modes, fuel and air were more homogeneously mixed, leading to smoother combustion.

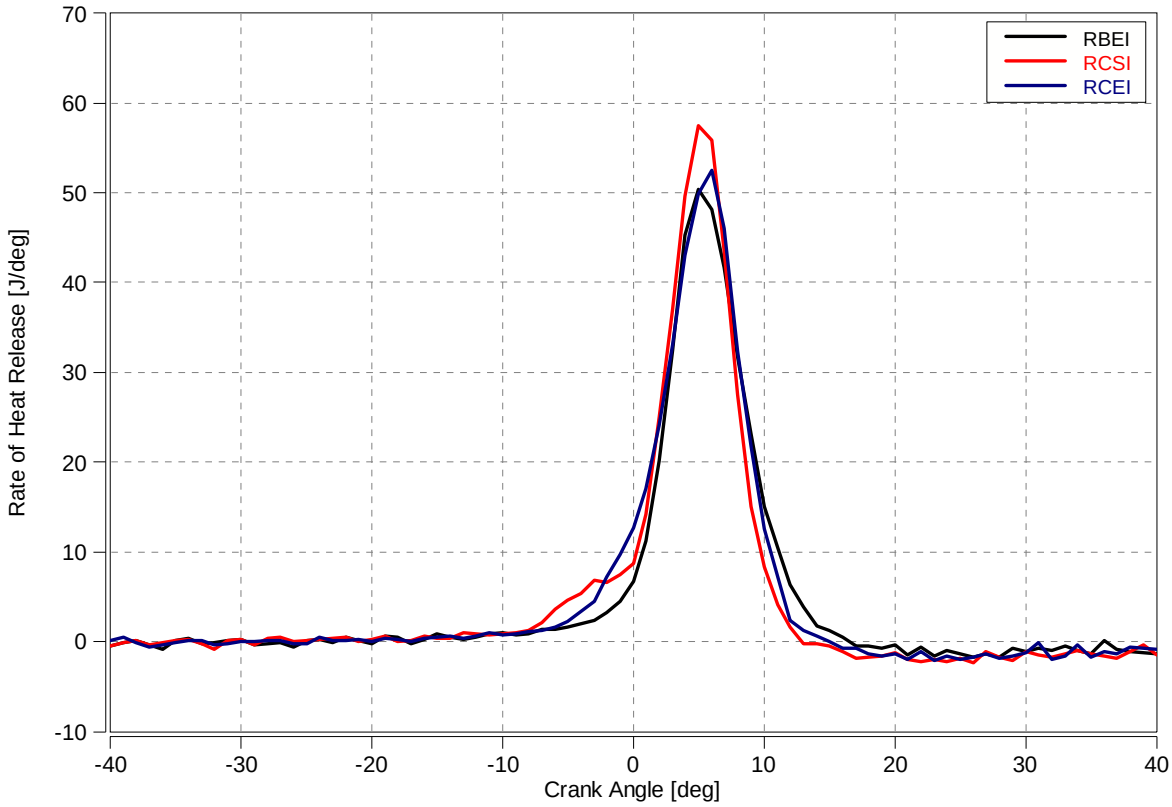

Figure 3.14: Rates of heat release during HCCI combustion for different charge preparation modes at 2000 rpm.

Shown in Figure 3.15 are cylinder pressure traces for all three charge preparation modes. It is shown that there are no significant differences between the RCEI and RCSI modes, while pressures during the combustion for RBEI mode are lower than both RCEI and RCSI modes due to the damping effect of internal EGR.

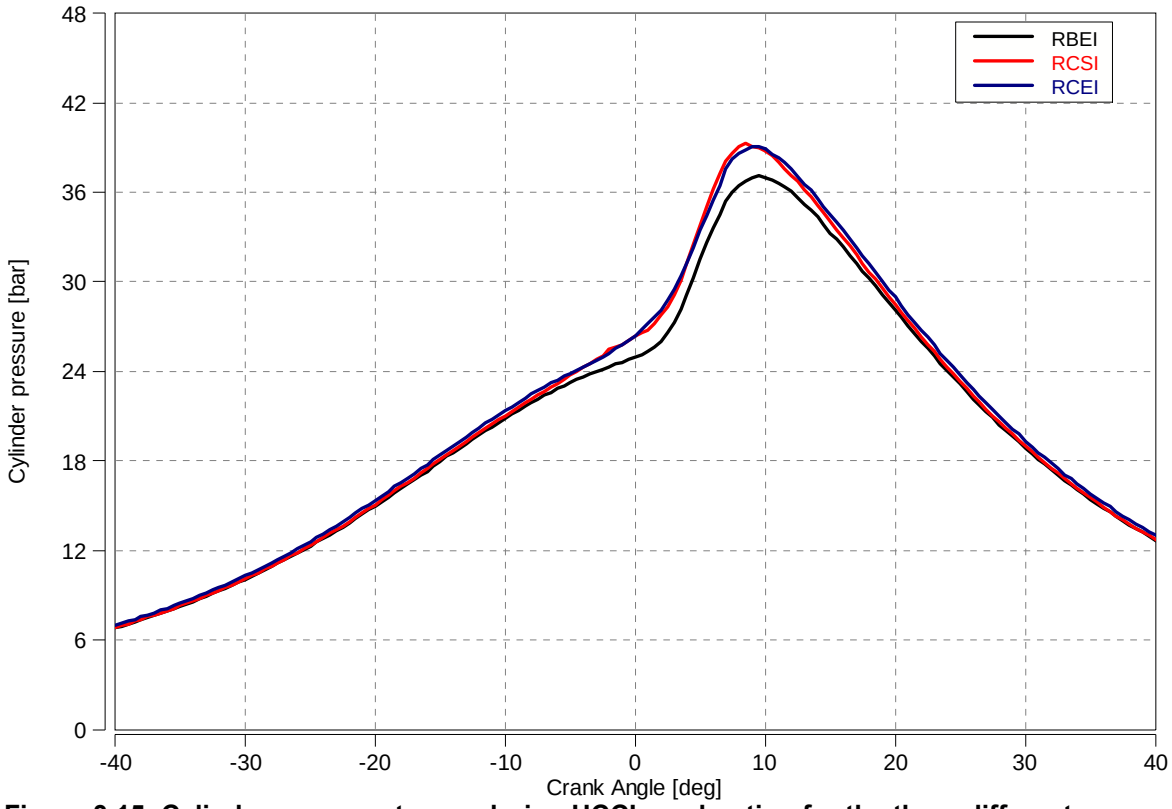

Figure 3.15: Cylinder pressure traces during HCCI combustion for the three different charge preparation modes.

3.2.4 Emissions

Indicated Specific HC

Figure 3.16 presents the indicated specific HC emissions for all three speed/load points. It is shown that HC emissions for RCEI and RCSI are comparable for all three speed/load conditions, while those for RBEI are the highest among the three charge preparation modes. Due to the second exhaust valve opening, RBEI introduces internal EGR to the combustion chamber resulting in more incomplete combustion and higher HC emissions than the regular-exhaust (RCEI and RCSI) modes.

Figure 3.16 also shows that HC emissions are much higher at 1000 rpm / 1.5 bar IMEP than the other two speed/load conditions, which was due to the unstable combustion at the idle operating point.

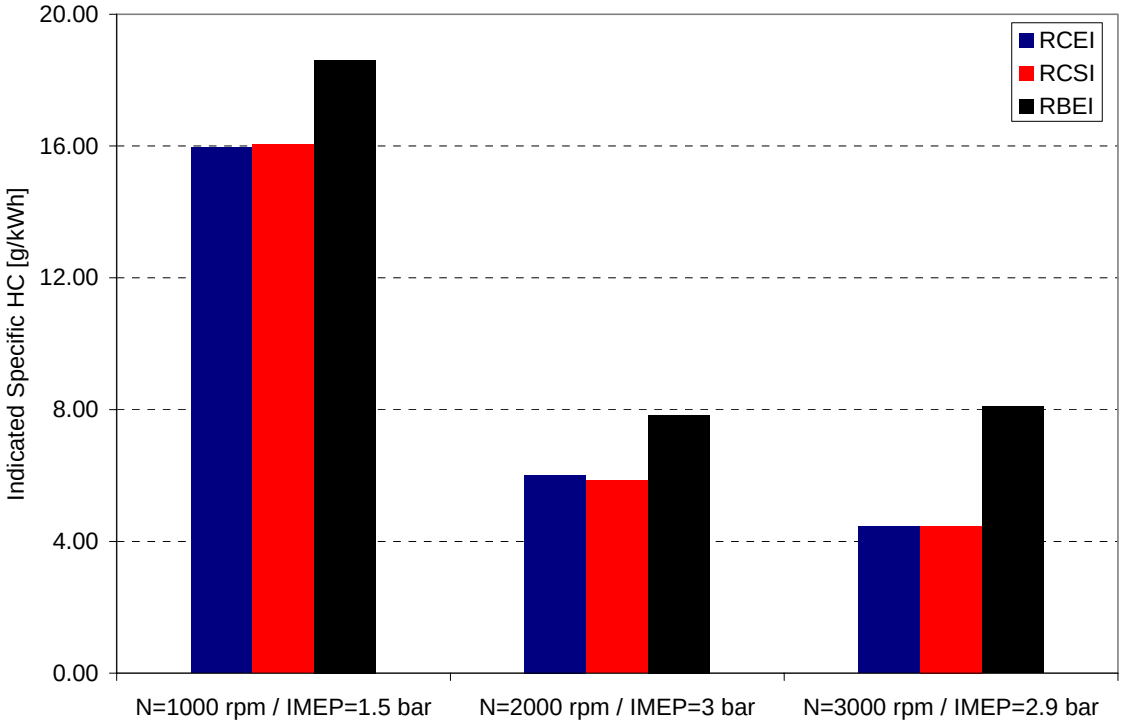

Figure 3.16: Indicated specific HC emissions for the three different charge preparation modes.

Indicated Specific CO

Indicated specific CO emissions for all three speed/load points are presented in Figure 3.17. It is shown that CO emissions for RCSI are the highest among three charge preparation modes. For the RCSI combustion, the second injection employed to trigger the combustion introduces local-rich combustion zones in the combustion chamber, generating more CO emissions than the single-injection (RCEI and RBEI) combustion modes. Similar to the HC emissions, CO emissions are much higher at the idle point than the other two operating conditions due to the unstable idle combustion.

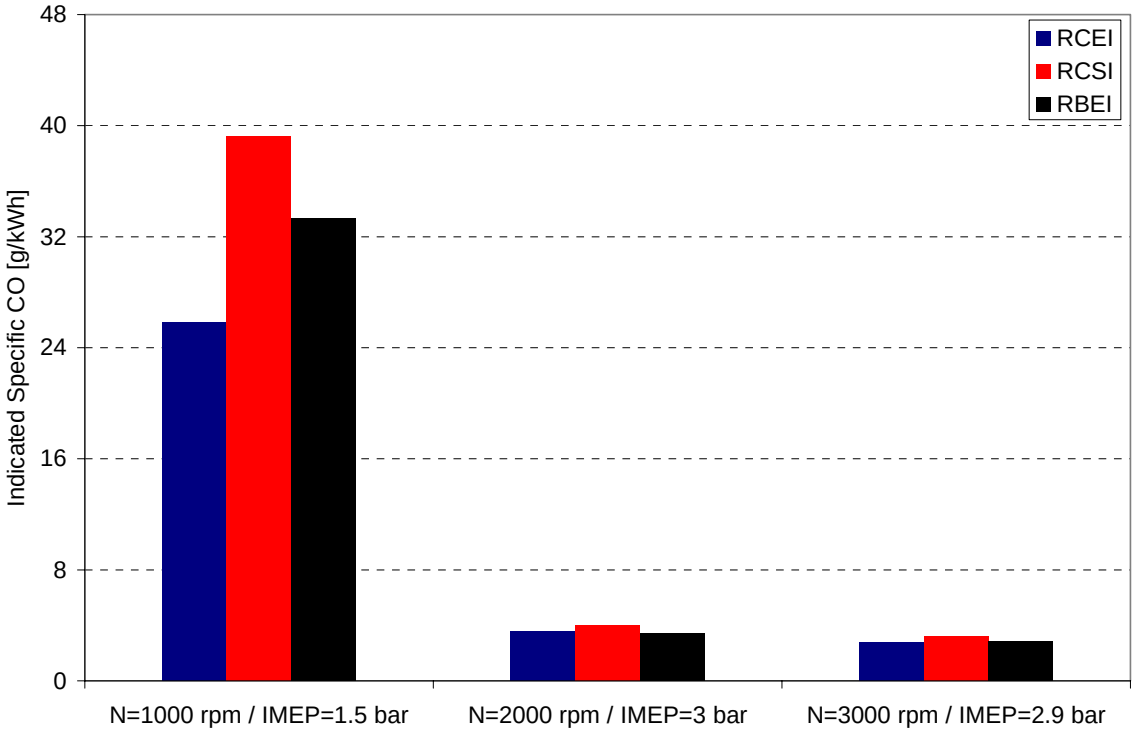

Figure 3.17: Indicated specific CO emissions for the three different charge preparation modes.

NOx Emissions

Figure 3.18 presents the NOx emissions for all three speed/load points. Due to higher maximum rate of pressure rise and higher in-cylinder temperatures at higher engine speed, NOx emissions increase with engine speed for all three HCCI combustion modes. In comparison to normal SI engine-out NOx emissions, these HCCI NOx emissions are incredibly low (<25 ppm).

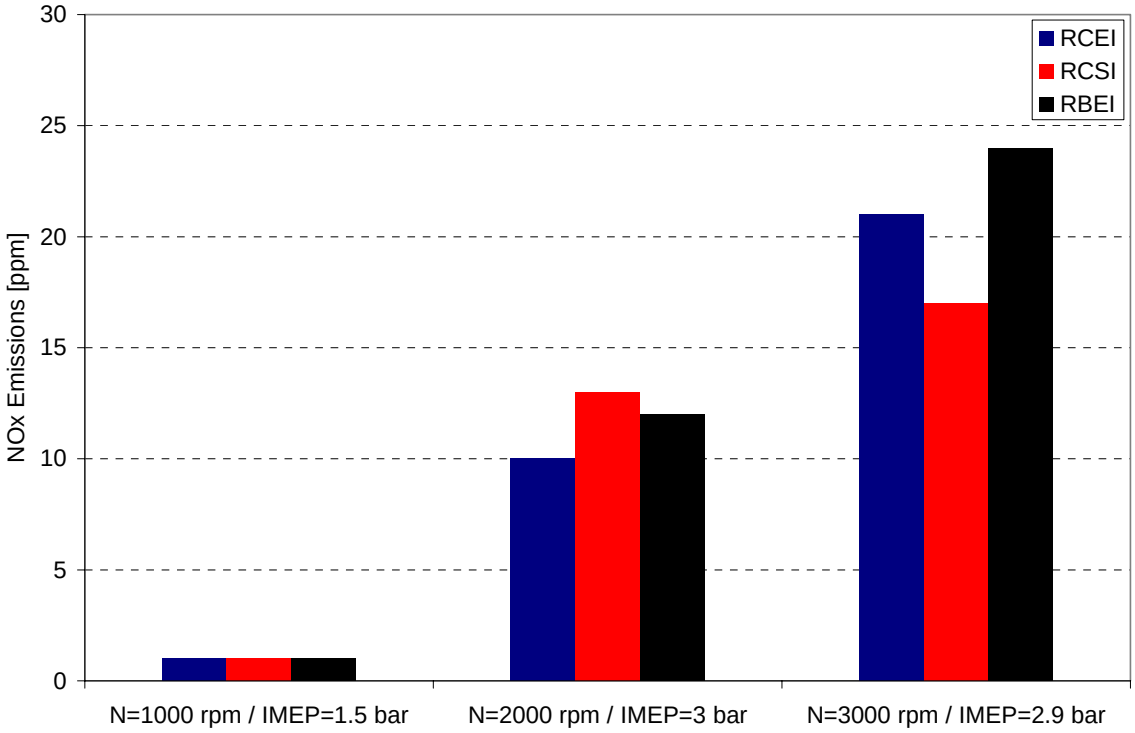

Figure 3.18: NOx emissions for the three different charge preparation modes.

3.3 Summary of baseline testing

Three different intake charge preparation modes, Re-Compression Early Injection (RCEI), Re-Compression Split Injection (RCSI), and Re-Breathing Early Injection (RBEI), on HCCI combustion in a single cylinder engine equipped with hydraulic variable valve train (VVT) and gasoline direction injection (GDI) system are studied with the baseline fuel indolene. For each intake charge preparation mode, three engine operating conditions are investigated: 1.5 bar IMEP at 1000 rpm, 3 bar IMEP at 2000 rpm, and 6 bar/deg of maximum rate of pressure rise at 3000 rpm.

With a fixed combustion phasing of CA50 at 5 degrees after TDC for all engine operating conditions and intake charge preparation modes, the following conclusions are deduced:

1. Re-Compression Early Injection (RCEI) mode exhibited the best thermal efficiency and fuel economy. It is also easy to implement, compared with Re-Compression Split Injection (two injection events in one cycle) and Re-Breathing Early Injection (two exhaust valve openings in one cycle);

2. Both re-compression split injection (RCSI) and re-breathing early injection (RBEI) modes introduce heterogeneity into the mixture in the combustion chamber leading to higher CO or HC emissions, compared to the re-compression early injection mode;

3. In the RCSI mode, local rich combustion introduced by the second injection generates more CO emissions than the RCEI mode;

4. With the second exhaust valve opening during the intake stroke in RBEI mode, internal EGR is introduced into the combustion chamber to dilute the intake charge and leads to more incomplete combustion and higher HC emissions than those of the RCEI mode;

5. The second fuel injection of the RCSI mode introduces two-stage combustion: a slower initial burn with the non-homogeneous mixture followed by a faster burn with homogeneous combustion. In contrast, there is only a single fast burn for both RCEI and RBEI modes.

4 Fuel tests

4.1 Fuel test order

A test order for fuel testing was randomized, based on the criterion of avoiding correlation between the test order and the most important fuel properties – especially RON and Sensitivity. The fuel test order is shown in Table 4.1, in which letters representing each fuel are also listed. The change of RON and sensitivity in the sequence of test order is shown in Figure 4.1. The changes of additional fuel properties are shown in Figure 4.2.

Table 4.1: Fuel test order

Order	Fuel (Code)
1	Indolene-Baseline (O)
2	C100 (C)
3	B30D70 (G)
4	Indolene-Baseline (O)
5	A100 (A)
6	B30D70 (G)
7	A79D21 (F)
8	Indolene-Repeat 1 (O)
9	B77D23 (I)
10	B100 (B)
11	C85D15 (K)
12	Indolene-Repeat 2 (O)
13	C50D50 (J)
14	C100 (C)
15	B50D50 (H)
16	A33D67 (E)
17	Indolene-Repeat 3 (O)

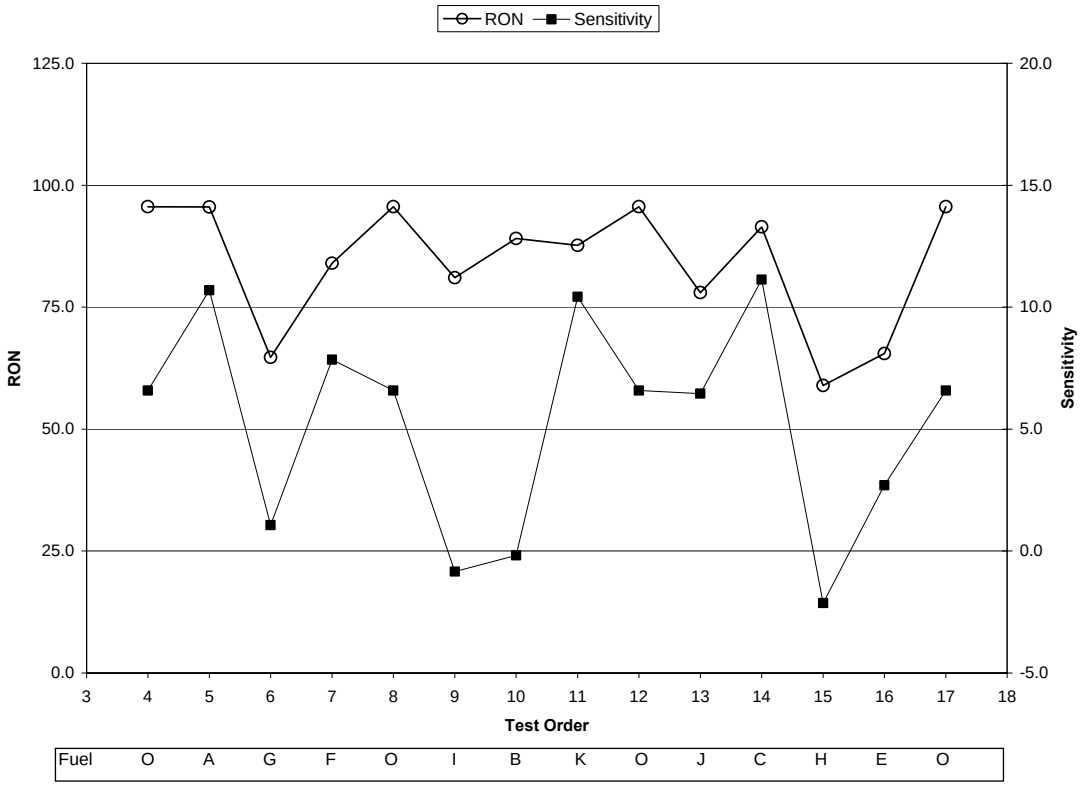

Figure 4.1: RON and sensitivity change in the sequence of test order

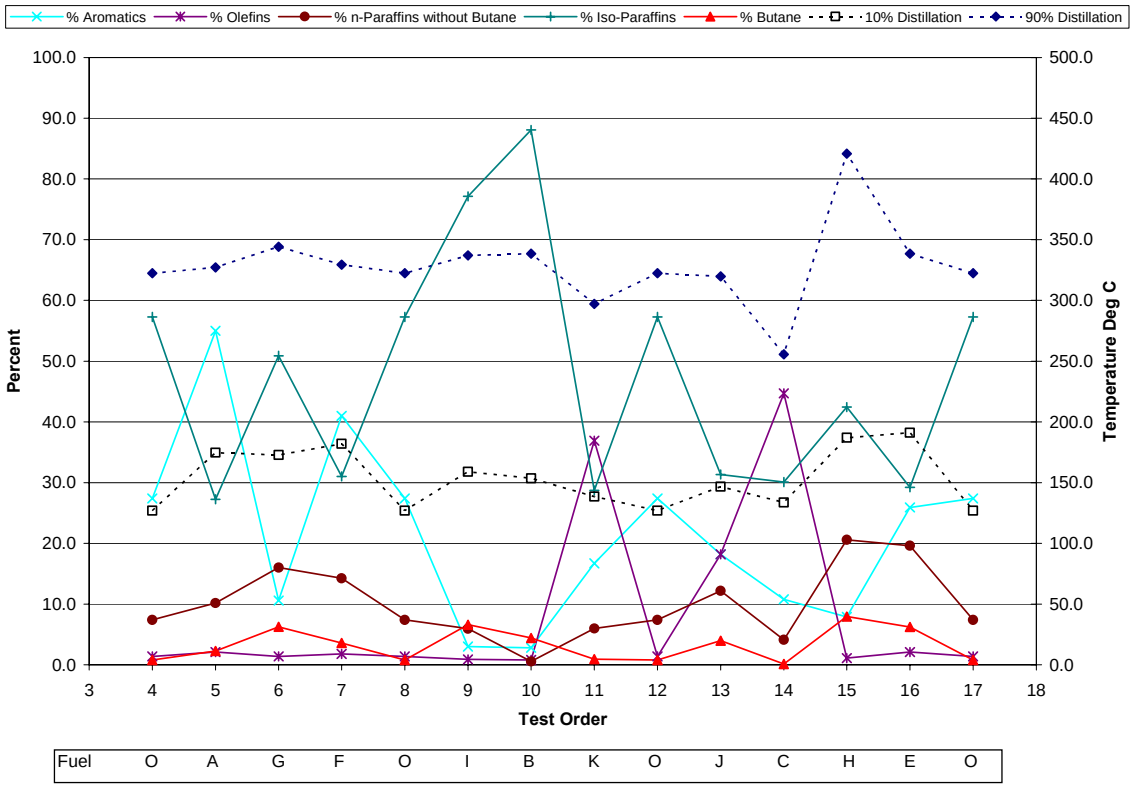

Figure 4.2: Changes of additional fuel properties in the sequence of test order

Engine tests with the baseline fuel Indolene at 2000 rpm and 3000 rpm for all three charge preparation modes were repeated throughout the fuel tests to ensure and monitor test repeatability. A set of baseline data were obtained after testing every three/four fuels. The detailed repeatability test plan is shown in Table 4.2. The results of these repeatability tests will be discussed shortly.

Table 4.2: Engine repeatability test plan

1	Baseline test in three HCCI modes at three speed/load points
2	The first three fuel tests (A, G, F)
3	Baseline test in three HCCI mode at 2000 rpm and 3000 rpm
4	The next three fuel tests (I, B, K)
5	Baseline test in three HCCI mode at 2000 rpm and 3000 rpm
6	The last four fuel tests (J, C, H, E)
7	Baseline test in three HCCI mode at 2000 rpm and 3000 rpm

4.2 Test procedure

In this study, the combustion phasing for every fuel is controlled at 5 degree after top dead center. To achieve this target, two parameters are changed from fuel to fuel. The primary parameter is the exhaust valve closing timing. If there are two exhaust valve events (RBEI mode), only the first exhaust valve closing timing is adjusted. The secondary parameter employed to control the combustion phasing is the (first) injection timing. Figure 4.3 presents the flow diagram of the procedure for the fuel tests.

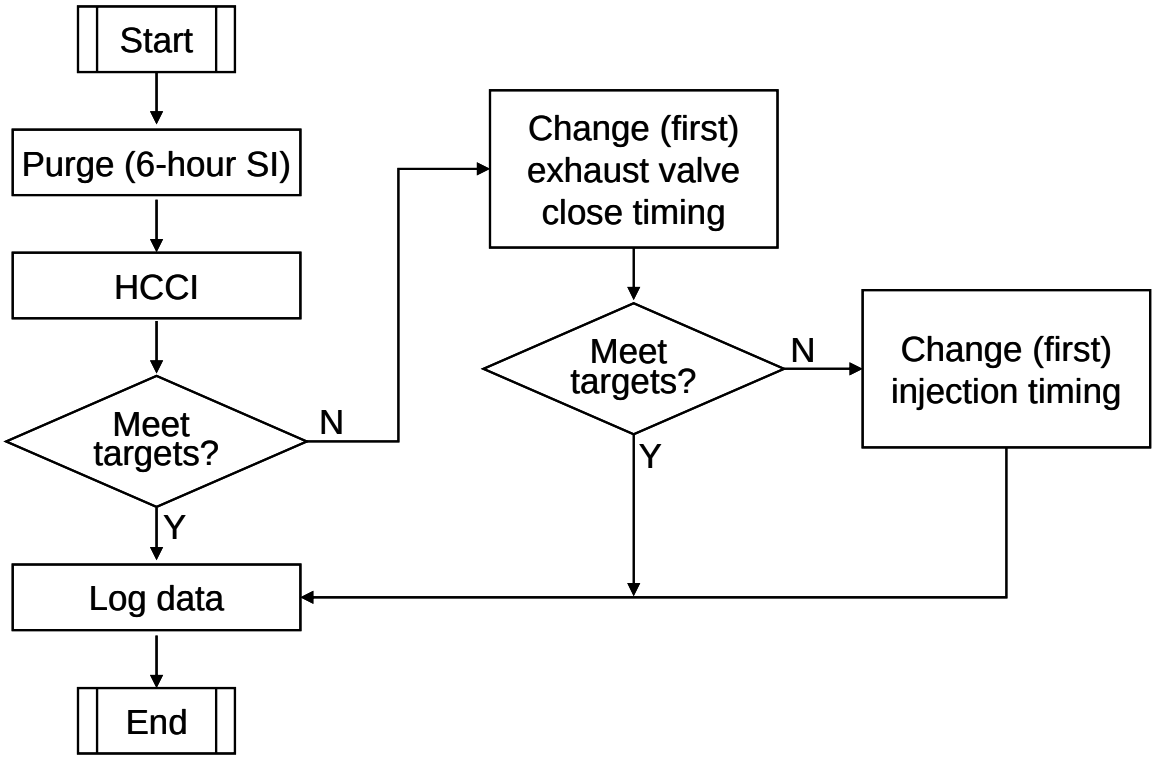

Figure 4.3: Fuel test procedure

Shown in Figures 4.4 and 4.5 are examples of changes of the first exhaust valve closing timing and the first injection timing at 2000 rpm, for RCEI and RCSI modes, respectively. It is shown that the first exhaust valve closing timing changed from fuel to fuel, while the first injection timing is almost constant.

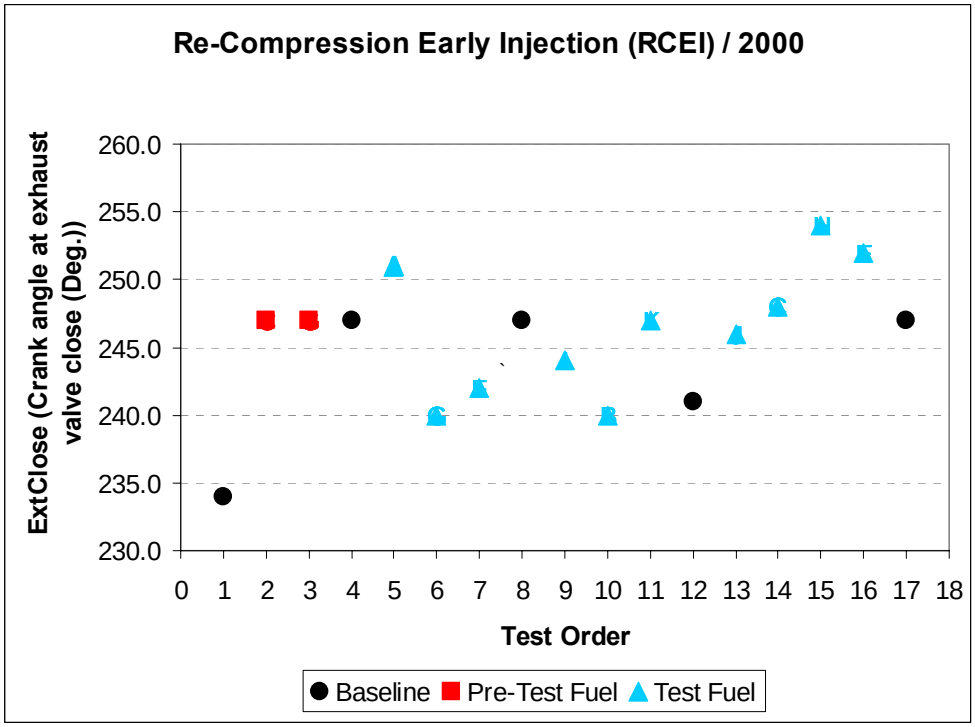

Figure 4.4: Variations of the first exhaust valve closing timing for the control of combustion phasing at 5 degrees ATDC.

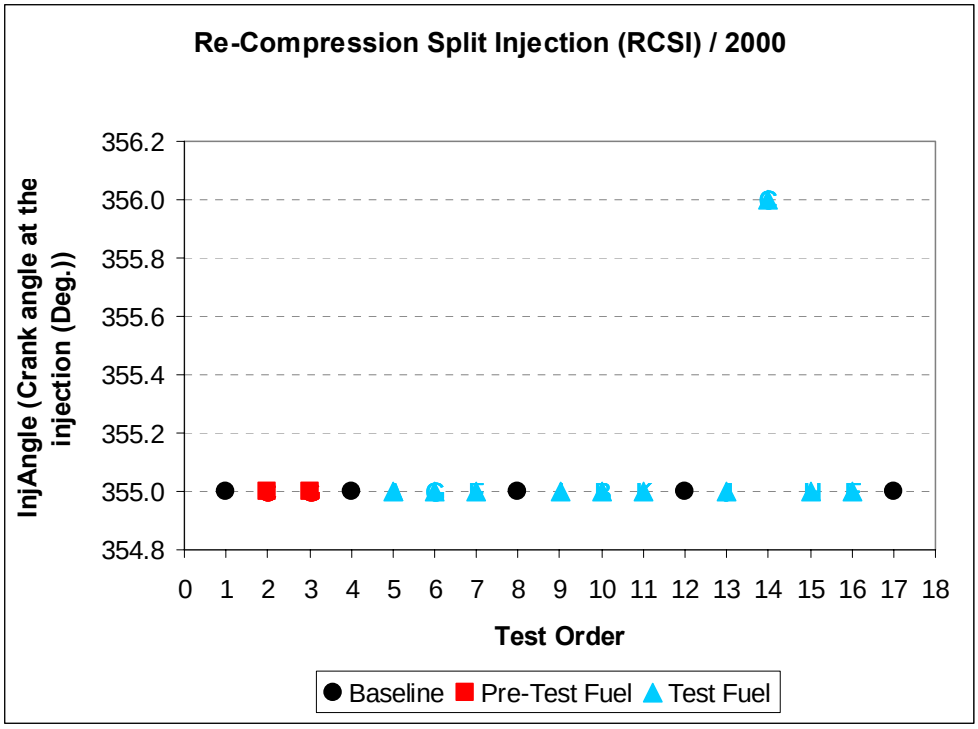

Figure 4.5: Variations of the first exhaust valve closing timing for the control of combustion phasing at 5 degrees ATDC.

4.3 Test results

Indicated specific fuel consumptions, indicated specific HC emissions, indicated specific CO emissions, and raw NOx emissions are presented in Figures 4.6 – 4.9. In the figures, the letters represent the individual data points, the triangles represent the average, and the bars the 95% confidence intervals of the means. In addition, the black symbols are the indolene repeatability tests, the red symbols are preliminary fuel tests, and the blue symbols are the test fuels.

Original plots of Figures 4.6 – 4.9 are attached to the report in the section of Appendix B.

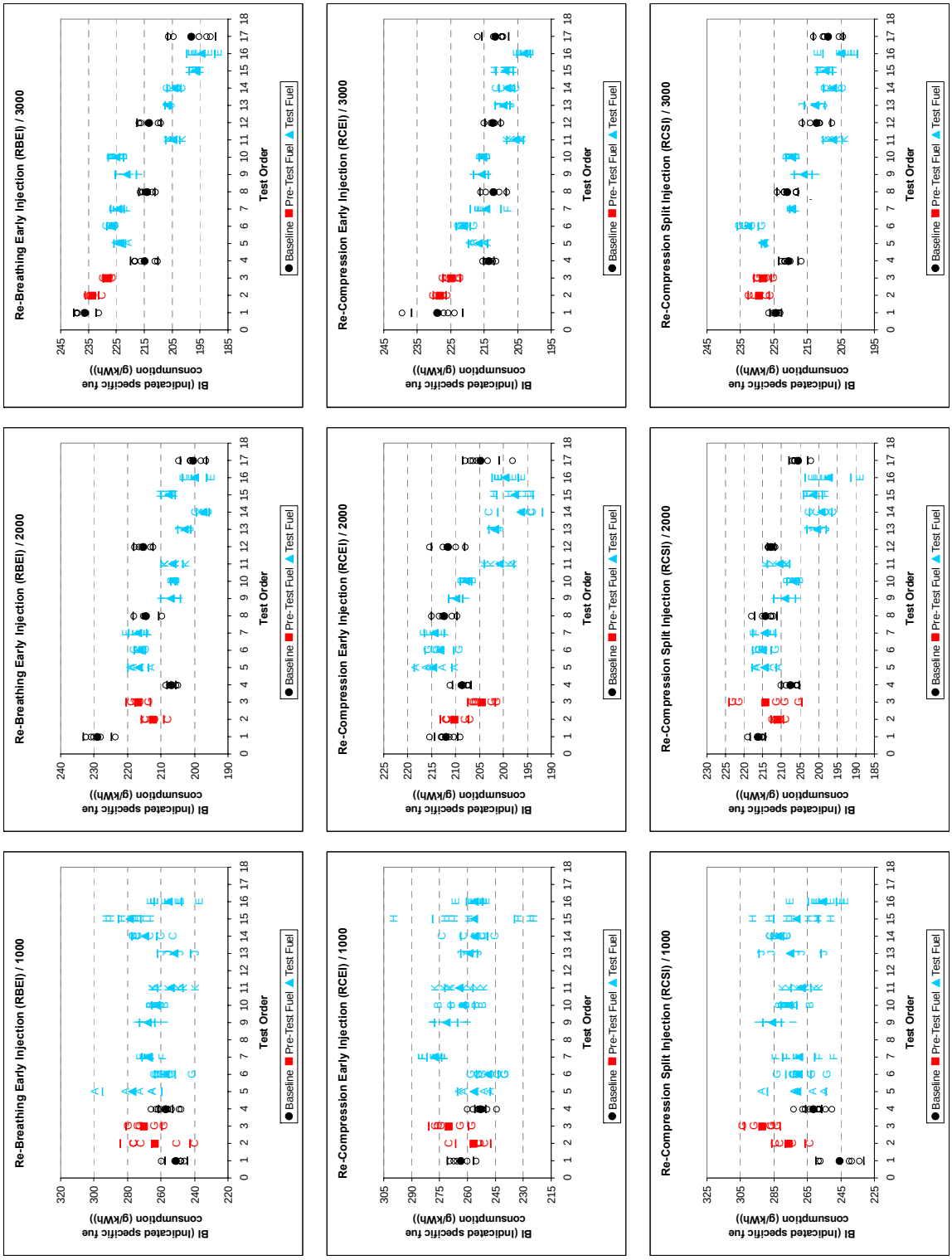

Figure 4.6: Indicated specific fuel consumptions for all fuel tests.

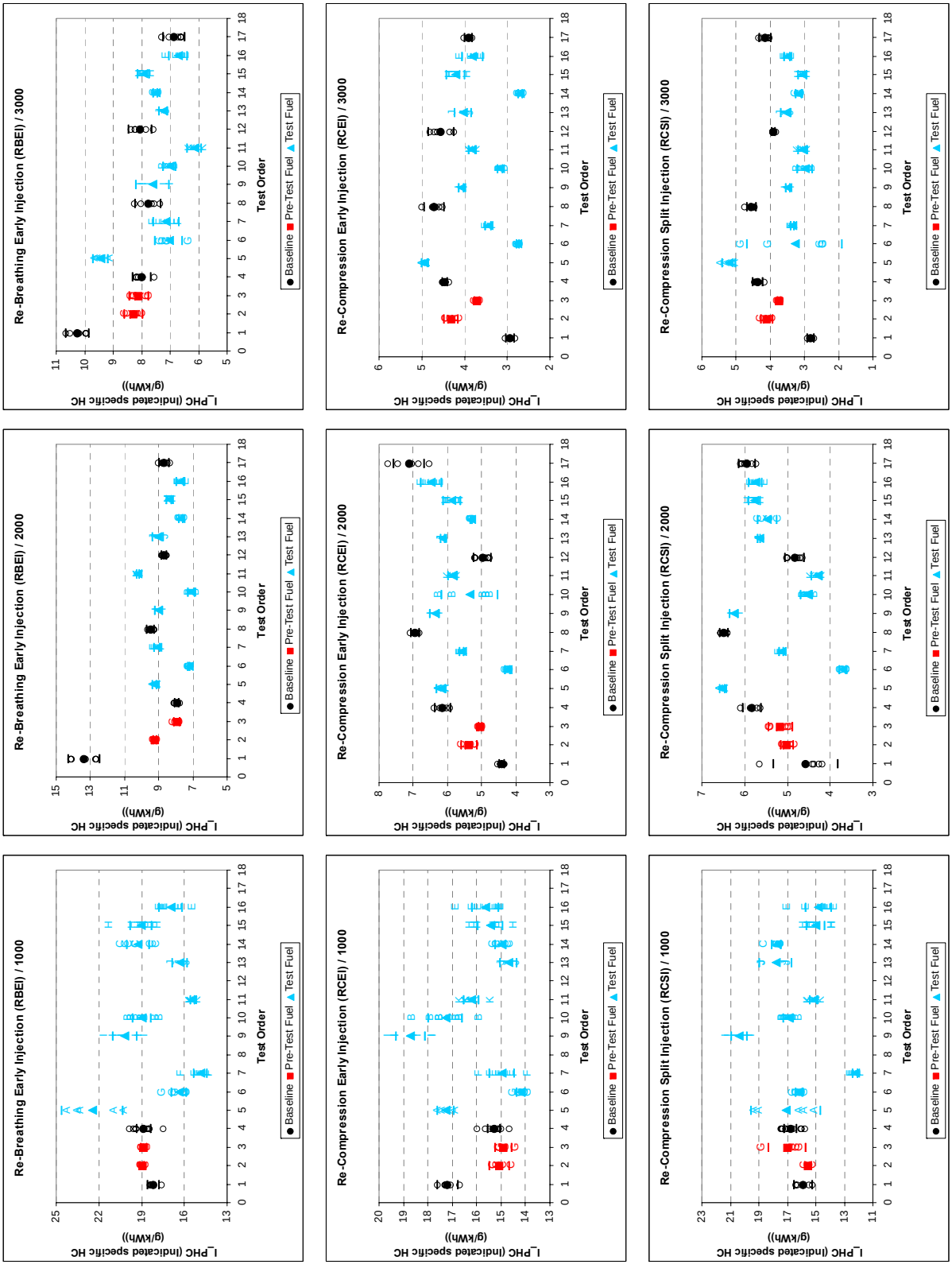

Figure 4.7: Indicated specific HC emissions for all fuel tests.

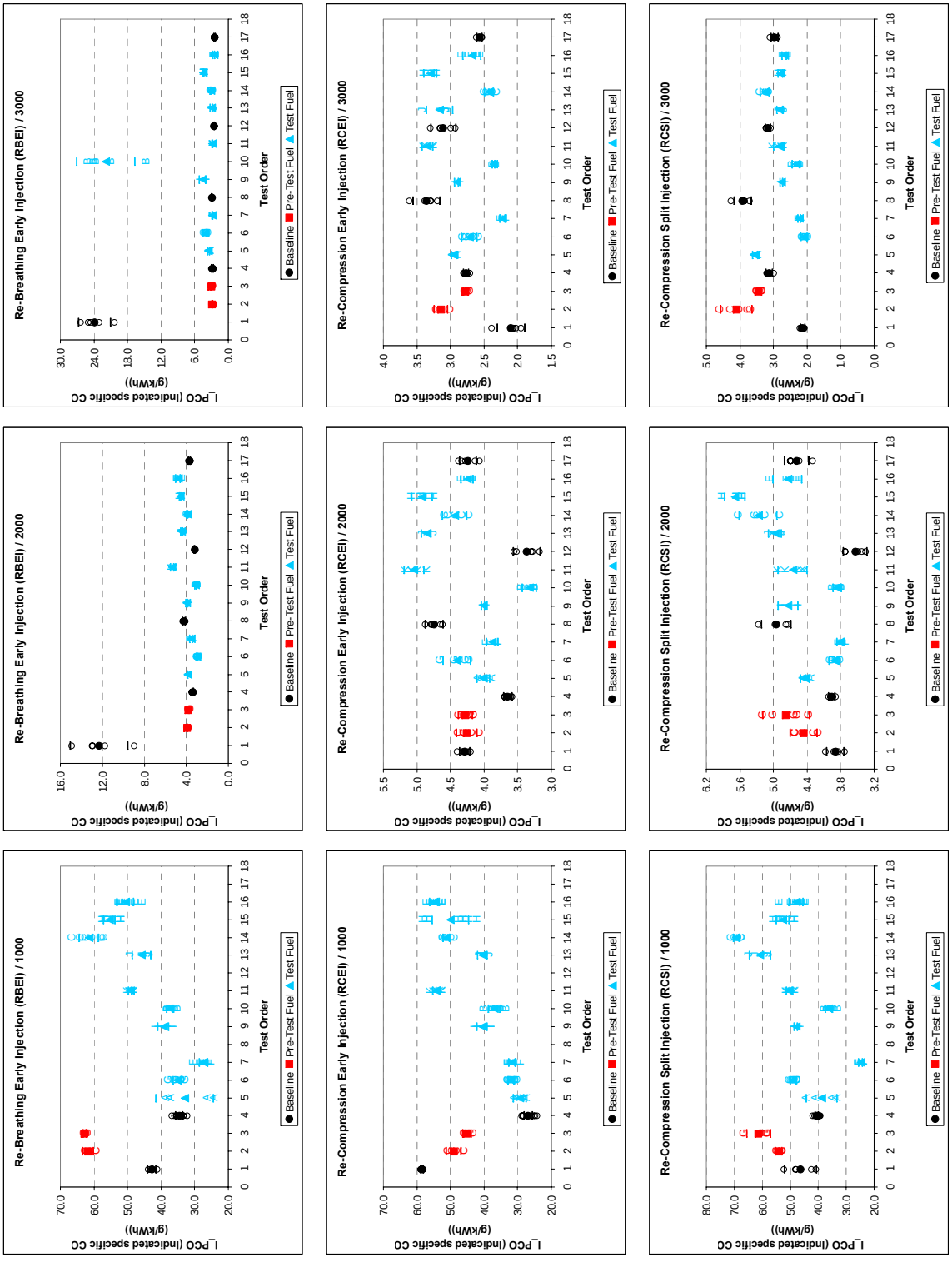

Figure 4.8: Indicated specific CO emissions for all fuel tests.

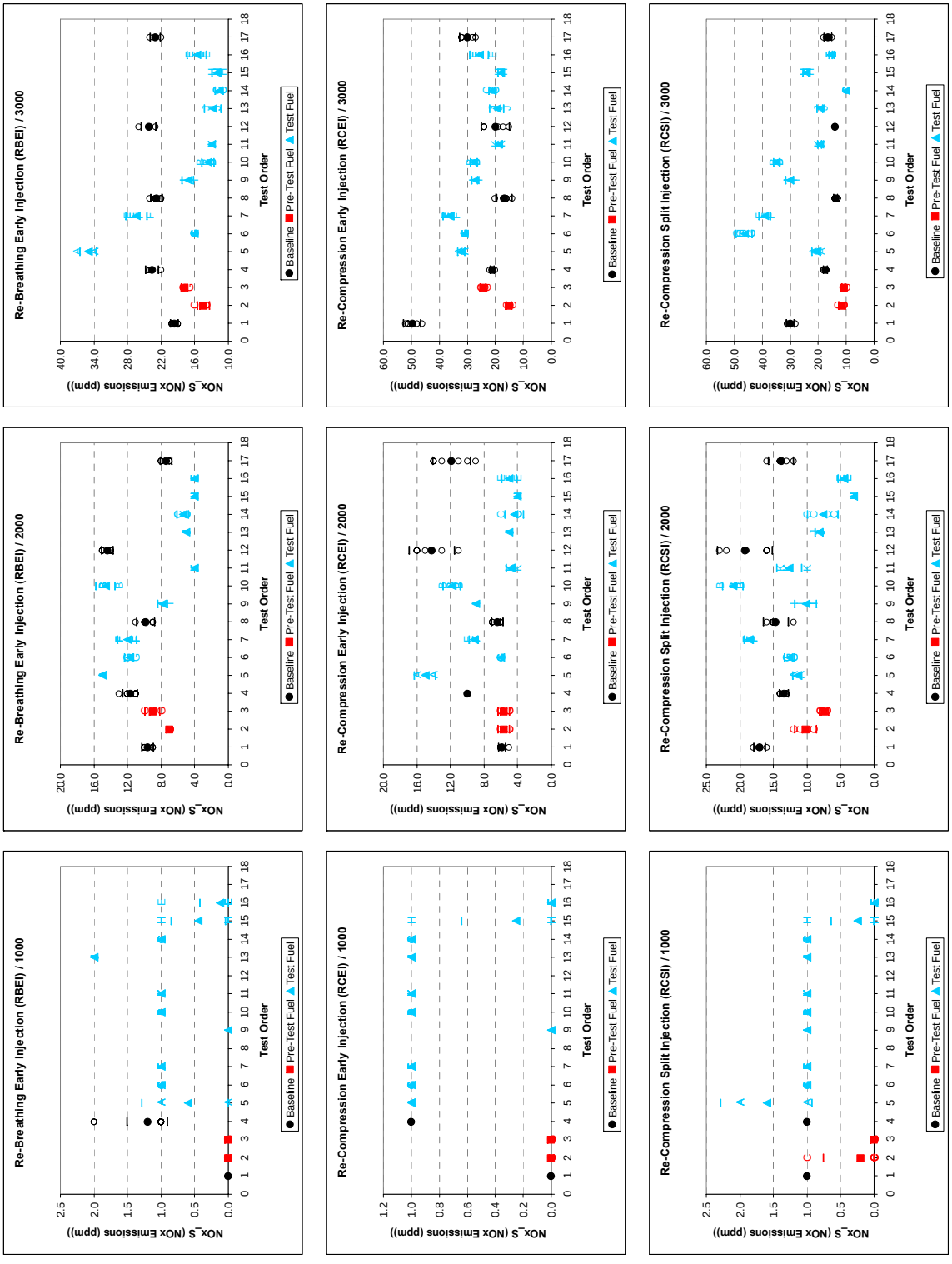

Figure 4.9: Raw NOx emissions for all fuel tests.

4.4 Data normalization based on indolene repeatability tests

It is expected that some of the observed variability of test results would be attributable to engine test repeatability. After examining the test results for all four repeatability tests, it was discovered that some of the observed variability in indolene results appeared to be due to causes that were measurable and potentially controllable. For example, each fuel test involved setting an engine speed, controlling the crank angle for 50% mass fraction burnt, and achieving a target engine load (for the 2000 rpm tests) or maximum rate of cylinder pressure rise (for the 3000 rpm tests). While it was possible to control the engine speed very precisely, there was more variability in the acceptable fluctuations of the other control parameters. Additionally, other uncontrolled conditions (e.g., ambient temperature) may impact the performance of the test engine on a particular test.

It was hypothesized that some of the observed variability in test fuel results may have been due to variation in attaining the controlled engine conditions. It was therefore suggested that the test fuel results be normalized to a consistent set of control conditions. The repeated tests of indolene throughout the test period provided an opportunity to make approximate corrections for variability in the 2000 and 3000 rpm test conditions (the 1000 rpm test condition results could not be normalized as the indolene baseline was performed only once at this condition). To do so, the following procedure was followed:

1. For each performance parameter, the average indolene performance $\bar{y}_{ij}$ was calculated for each of the *i* indolene tests (four in total) and each of the *j* engine operating modes (three in total). This yielded 12 data points.
2. A multiple regression model was fit to the indolene data with the $\bar{y}_{ij}$ as the response variable and a set of predictors that included:
    a. Engine operating mode (Mode) with values of RBEI, RCEI, and RCSI
    b. Mean crank angle at 50% burn (MFB_50)
    c. Mean load (PI) at 2000 rpm or maximum rate of cylinder pressure rise (PR_CYP) at 3000 rpm
    d. The interaction of b. and c.
    e. The intake air temperature (TL22)
3. Backward, stepwise regression was employed to reduce the model to the smallest set of significant predictors. This process was done by successively eliminating the predictor with the highest p-value greater than 0.05 (i.e., least significant) for the F-test of the Type III sum of squares for that factor. This continued until only factors with a p-value of 0.05 and below remained. The final result of this step was an equation:

$$Y_I = \beta_0 + \beta_1 * RBEI + \beta_2 * RCEI + \beta_3 * MFB\_50 + \beta_4 * PI(\text{or } PR\_CYP) +$$
$$\beta_5 * MFB\_50 * PI(\text{or } PR\_CYP) + \beta_6 * TL22$$
$$\text{where the } \beta_i \text{ terms equal zero for the non-significant predictors}$$

The value of β_i terms are shown in Table 4.3.

Table 4.3: Stepwise regression coefficients for data normalization

Response Variable	speed	FinalModel	Parameter							
			Intercept	Mode 1 RBEI	Mode 2 RCEI	MFB_50	PR CYP	PI	MFB_50 * PI	TL22
Indicated Specific Fuel Consumption (g/kWh)	2000	Mode	209.93	-0.77	-0.67					
	3000	Mode	215.58	-5.60	-3.16					
NO_x (ppm)	2000	Mode PI	-89.40	-3.75	-4.11			34.65		
	3000	Mode PR_CYP	-13.54	4.86	6.52		5.19			
Indicated Specific Hydrocarbons (HC) (g/kWh)	2000	Mode MFB_50 PI MFB_50*PI	384.53	3.53	1.65	-71.83		-129.35	24.52	
	3000	Mode PR_CYP	7.03	3.73	0.16		-0.50			
Indicated Specific Carbon Monoxide (CO) (g/kWh)	2000	Mode MFB_50 PI MFB_50*PI	257.90	-0.15	0.53	-47.67		-86.90	16.33	
	3000	Mode PR_CYP	5.96	-0.36	-0.35		-0.48			
Filter Smoke Number (size)	2000	Mode	0.04	0.02	0.01					
	3000	Mode	0.05	0.32	-0.01					
Combustion Duration (CA)	2000	Mode MFB_50	4.41	1.11	0.29	0.55				
	3000	Mode	9.53	0.00	-0.62					
Combustion Noise (dB)	2000	Mode TL22	72.31	-1.54	-0.43					0.63
	3000	Mode MFB_50 PR_CYP TL22	84.54	1.71	0.55	-0.31	0.66			0.22
Coefficient of Variance of IMEP (%)	2000	Mode	2.11	0.46	0.17					
	3000	Mode MFB_50 PR_CYP	-17.26	-2.21	-2.80	2.02	2.51			
Peak Cylinder Pressure (bar)	2000	Mode MFB_50 PI	24.50	-1.49	0.07	-0.90		6.44		
	3000	Mode PR_CYP	28.39	3.61	0.28		1.65			
Crank Angle at Exhaust Valve Close (deg)	2000	Mode	245.75	4.96	-0.25					
	3000	Mode	273.00	13.50	-5.96					
Maximum Rate of Cylinder Pressure Rise (bar)	2000	Mode MFB_50	5.58	-0.76	-0.26	-0.34				
Indicated Mean Effective Pressure (IMEP) (bar)	3000	Mode	2.65	0.38	0.11					

4. The relationship between the predictor variables and the responses as observed in the Indolene tests was used to adjust the test results of the test fuels as follows:

$$z'_k = z_k * \frac{Y_{I_{ref}}}{Y_{I_{act}}}$$

where

z'_k is the adjusted value of a measured parameter for a particular test fuel at replicate k

z_k is the unadjusted value of a measured parameter for a particular test fuel at replicate k

$Y_{I_{ref}}$ is the predicted indolene response at the mode of the test fuel data point and at the target control values of $MFB\_50 = 5$, $PI = 3\,(2000\ \text{rpm})$, or $PR\_CYP = 6\,(3000\ \text{rpm})$, and $TL22 = 25\ C$

$Y_{I_{act}}$ is the predicted indolene response at the mode of the test fuel data point and the observed control values for the z_k test fuel data point

Overall, these normalizations removed a portion of the observed variability in the data before continuing to the next step in the analysis and permitted a clearer analysis of the fuel property effects unclouded by variability from maintaining particular engine operating conditions.

One important limitation of this analysis is that the relationships derived from the indolene repeatability results are applied to every observed test fuel result. Therefore, the method supposes that the magnitude, direction, and significance of observed relationships in indolene testing would also hold for each of the other test fuels.

5 Statistical analysis

5.1 Methodology

Once the final data were obtained and normalizations were made to a common operating condition per the procedure described in Section 4.4, the performance data for the test fuels were ready to be modeled as a function of the fuel properties.

For each of the nine engine test conditions (1000 rpm, 2000 rpm, and 3000 rpm each tested for RCEI, RCSI, and RBEI), ten performance parameters were examined:

- Indicated specific fuel consumption (g/kWh)
- NO_x emission (ppm)
- Indicated specific hydrocarbon emission (g/kWh)
- Indicated specific carbon monoxide emission (g/kWh)
- Filter smoke number (size)
- Combustion duration (degrees)
- Noise (dB)
- Coefficient of Variance of IMEP (%)
- Peak cylinder pressure (bar)
- Exhaust valve closing angle (degrees)

Additionally, Maximum rate of cylinder pressure rise (bar) was examined for the 2000 rpm tests only and Indicated Mean Effective Pressure (bar) was examined for the 3000 rpm tests only. In all cases, the 1000 rpm results were non-normalized and the 2000 and 3000 rpm test results were normalized to reference engine operating conditions.

The performance data were modeled using the averages of the values of the repeated test points at each speed and mode. The averages were selected, rather than modeling the individual data values, since the measurements were expected to be correlated due to the fact that they represented repeated observations. This resulted in ten mean values, one for each test fuel, for each speed and mode, for each performance parameter.

In Section 2.3, seven independent fuel properties were presented and utilized to choose test fuels. For the statistical analysis, distillation temperature T90 was added to those 7 independent fuel properties to study impacts of both T10 and T90 on combustion. In addition, the percentages of n-butanes were separated from percentages of normal paraffins to study the effects of butane on the combustion. The nine fuel properties of interest as predictors were:

- RON
- Sensitivity
- T10
- T90
- % Aromatics
- % Iso Paraffins
- % Normal Paraffins without Butane
- % Butane
- % Olefins

Linear regression models were fit for each performance parameters as a function of each possible combination of two fuel properties and their interaction. With nine fuel properties, this resulted in 36 unique models of a performance parameter as a function of two of the nine fuel properties. For each of these models, the following data were tabulated:

- The correlation coefficient (r^2) for the model – the degree to which this model explains the overall variability seen in the data
- The mean square error – the remaining variation unexplained by the model
- The coefficients for each of the regression parameters and the corresponding p-values for whether they were significantly different from zero. The coefficients were for the intercept of the model, the first fuel property, the second fuel property and the interaction (i.e., product of the two fuel properties).

The two-factor models were fit in SAS v9.2 using the PROC GLM procedure. The two factor model with interaction was selected because it was felt that some significant interactions in fuel properties may exist. The number of two fuel properties at a time was driven by the modest number of fuels tested. With ten test fuels, the regression analysis of a response as a function of two factors and their interaction will require four degrees of freedom and will leave six degrees of freedom for estimating the error in the model. Adding a third factor and its interactions would raise the model degrees of freedom to eight and reduce the error degrees of freedom to two. This is judged to be too few degrees of freedom to reliably estimate the model error.

After fitting all possible models, the results were reviewed to identify the "best" model. Two different methods were considered for this process. First, the single two factor model with the highest r^2 value for each performance parameter was identified for every speed and mode condition. This method maximizes the explained variability but may ignore important consistency of results between modes and speeds. Therefore, a second approach was taken where each two-factor model for a particular performance parameter was evaluated across all nine operating conditions to determine a single "best" two factor model to explain the observed variability in that performance parameter. The first step in this process was to identify only models with an overall F-Test p-value of 0.1 or less. These may be considered potentially explanatory of the observed variability in the performance parameter. Then these models within each speed and mode condition were ranked from lowest to highest r^2 value and the two-factor model with the highest sum of ranks across the nine speed and mode conditions was identified as "best". This method placed strong weight on a two-factor model that was both highly explanatory of observed variability (i.e., high r^2) and consistently explanatory across speeds and modes (i.e., high sum of ranks).

5.2 Results

5.2.1 Reporting format

In this report section, final results for six performance parameters will be addressed, which are:

- Indicated specific fuel consumption (g/kWh)
- NO_x emission (ppm)
- Indicated specific hydrocarbon emission (g/kWh)

- Indicated specific carbon monoxide emission (g/kWh)
- Coefficient of Variance of IMEP (%)
- Exhaust valve closing

Results for the other four engine performance parameters are attached as Appendix E.

The final results from the statistical regression analysis are presented in tabular form for each of the performance parameters. For a select subset of parameters of most interest, the results are also shown in a graphic format using contour plots. Each of these is discussed below:

Tabular results: For each performance parameter, a table is presented that contains two sections. The top section shows the two-factor regression results resulting from the best r^2 model within each speed and mode combination. Each line of this block of the table contains the following values:

speed – 1000, 2000, or 3000 rpm
mode – 1, 2, or 3, denoting RBEI, RCEI, or RCSI, respectively
Predictor Variables
    P1 – the first fuel property predictor variable
    P2 – the second fuel property predictor variable
Model Coefficients
    Intercept – Intercept of the fitted regression function
    P1 – coefficient on the value of the first fuel property predictor variable
    P2 - coefficient on the value of the second fuel property predictor variable
    P1*P2 - coefficient on the interaction (product of the first and second fuel property predictor variables)
Standard Deviation – The mean square error of the fitted model
RSquare – the r^2 of the model or the percentage of the observed variability explained by the model
Overall Model p-Value – Probability associated with the F-test that the variability in results attributable to the model could be due to random chance. A low value (<0.1) indicates the model effectively explains variability in observed results.

The bottom block of the table utilizes the same format but shows the single two-factor with interaction model for a particular parameter that provides the best sum of ranked r^2 values among statistically significant (i.e., p-value<0.1) models. This can be thought of as the best explanatory model for all speed and mode conditions.

In both blocks, the model coefficients are asterisked once or twice if they are individually statistically significant at the 0.05 or 0.01 levels, respectively. This indicates a strong relationship between the predictor variable (or interaction) and the response variable. The overall model p-values of 0.05 and smaller are highlighted in yellow. This indicates that the subject model appears to explain the observed variability well.

Contour Plots: For the performance parameters Indicated Specific Fuel Consumption, NOx, Indicated Specific HC, and Indicated Specific CO emissions, the results of the best ranked two-factor model of performance parameter as a function of fuel properties are also illustrated graphically through the use of contour plots. These plots are provided on two pages. The first page shows the results for the three speeds (1000, 2000, and 3000) for mode=2 (RCEI). The second page shows the three modes (RBEI, RCEI, and

RCSI) at a speed of 2000 rpm. This permits a comparison in each case across an engine operation parameter of interest. A single page of contour plots for the three modes at 1000 rpm is provided for the response variable COV of IMEP because of its importance primarily at low power. A single page of contour plots for the three speeds under the RCEI modes is provided for the response variable Exhaust Valve Close Angle. Other contour plots appear in the section where valuable to understand test fuel performance results.

Each contour plot provides a means for assessing the region(s) of the fuel property values that optimize performance. The basic format of the contour plot is a set of lines, each representing a fixed response value of the performance parameter over the range of the two predictor variables used to create the regression relationship.

The contour plots have been augmented by superimposing the average response levels for each of the ten test fuels (with their corresponding values). This provides two valuable pieces of information. If the plotted points are close to the contour lines, it indicates that the observed data results match closely to the contour regression line results and hence that the proposed model appears to fit the observed data well. Second, it shows the span of the two predictor variables achieved in the test. This latter point is important since it is best to limit inferences in a two-factor regression model to the simultaneous range observed for both factors. One additional enhancement to the contour plots was the addition of the average indolene result in each case. This is provided strictly for reference and it should be noted that the indolene results were not used directly in the regression analysis.

In several cases, the best ranked r^2 model fit to the data was not effective at a particular speed and mode. In these cases, showing the contour plot might be misleading to indicate a relationship that does not appear statistically significant. In those cases where the overall model p-value was greater than 0.05 and none of the three predictor variable coefficients (P1, P2, or P1*P2) were statistically significant at the 0.05 level, the contour plot was replaced with a simple scatter plot of the observed mean response variable values as a function of P1 (y-axis) and P2 (x-axis).

For the reader interested in evaluating the regression results in a different manner than the best ranked r^2 criterion used here, a comprehensive list of all two-factor regression fits is provided for each performance parameter and for each speed and mode as Appendix D. The resulting models are sorted in descending order of their r^2 values.

5.2.2 Indicated specific fuel consumption

Table 5.1: Results for indicated specific fuel consumption

Best r-Square Model: Indicated Specific Fuel Consumption (g/kWh)

		Predictor Variables		Model Coefficients				Standard		Overall Model p
speed	mode	P1	P2	Intercept	P1	P2	P1 * P2	Deviation	RSquare	Value
1000	1	C4	RON	6.22	35.14 **	2.86 **	-0.38 **	4.927	82%	0.012
1000	2	C4	RON	281.10 *	-9.63	-0.27	0.13	8.246	36%	0.409
1000	3	i_Paraffins	n_Paraffins_woC4	287.44 **	-0.12	-2.46 *	0.04	5.534	70%	0.054
2000	1	Aromatics	i_Paraffins	192.36 **	-1.35	0.04	0.06 *	4.228	75%	0.031
2000	2	Aromatics	i_Paraffins	183.84 **	-0.93	0.19 *	0.05 *	3.204	87%	0.005
2000	3	Aromatics	i_Paraffins	192.08 **	-0.9	0.09	0.04	5.795	52%	0.188
3000	1	n_Paraffins_woC4	Distillation_10	9.3	12.18 *	1.40 **	-0.08 *	7.380	77%	0.023
3000	2	Aromatics	i_Paraffins	197.39 **	-0.99	0.13	0.04	3.821	70%	0.054
3000	3	Aromatics	i_Paraffins	192.98 **	-1.64	0.16	0.08	6.495	67%	0.067

Best Ranked r-Square Model: Indicated Specific Fuel Consumption (g/kWh)

		Predictor Variables		Model Coefficients				Standard		Overall Model p
speed	mode	P1	P2	Intercept	P1	P2	P1 * P2	Deviation	RSquare	Value
1000	1	Aromatics	i_Paraffins	254.20 **	0.78	0.18	-0.02	10.779	13%	0.823
1000	2	Aromatics	i_Paraffins	249.98 **	0.29	0.17	-0.004	9.619	13%	0.825
1000	3	Aromatics	i_Paraffins	269.61 **	0.62	0.18	-0.03	8.445	29%	0.523
2000	1	Aromatics	i_Paraffins	192.36 **	-1.35	0.04	0.06 *	4.228	75%	0.031
2000	2	Aromatics	i_Paraffins	183.84 **	-0.93	0.19 *	0.05 *	3.204	87%	0.005
2000	3	Aromatics	i_Paraffins	192.08 **	-0.9	0.09	0.04	5.795	52%	0.188
3000	1	Aromatics	i_Paraffins	175.83 **	-1.36	0.41	0.07	7.966	73%	0.037
3000	2	Aromatics	i_Paraffins	197.39 **	-0.99	0.13	0.04	3.821	70%	0.054
3000	3	Aromatics	i_Paraffins	192.98 **	-1.64	0.16	0.08	6.495	67%	0.067

Note: Response values have been adjusted by TL22, MFB 50, and PI at speeds = 2000 and by TL22, MFB 50, and PR_CYP at speeds = 3000.

* Significant at 0.05 Level of Significance

** Significant at 0.01 Level of Significance

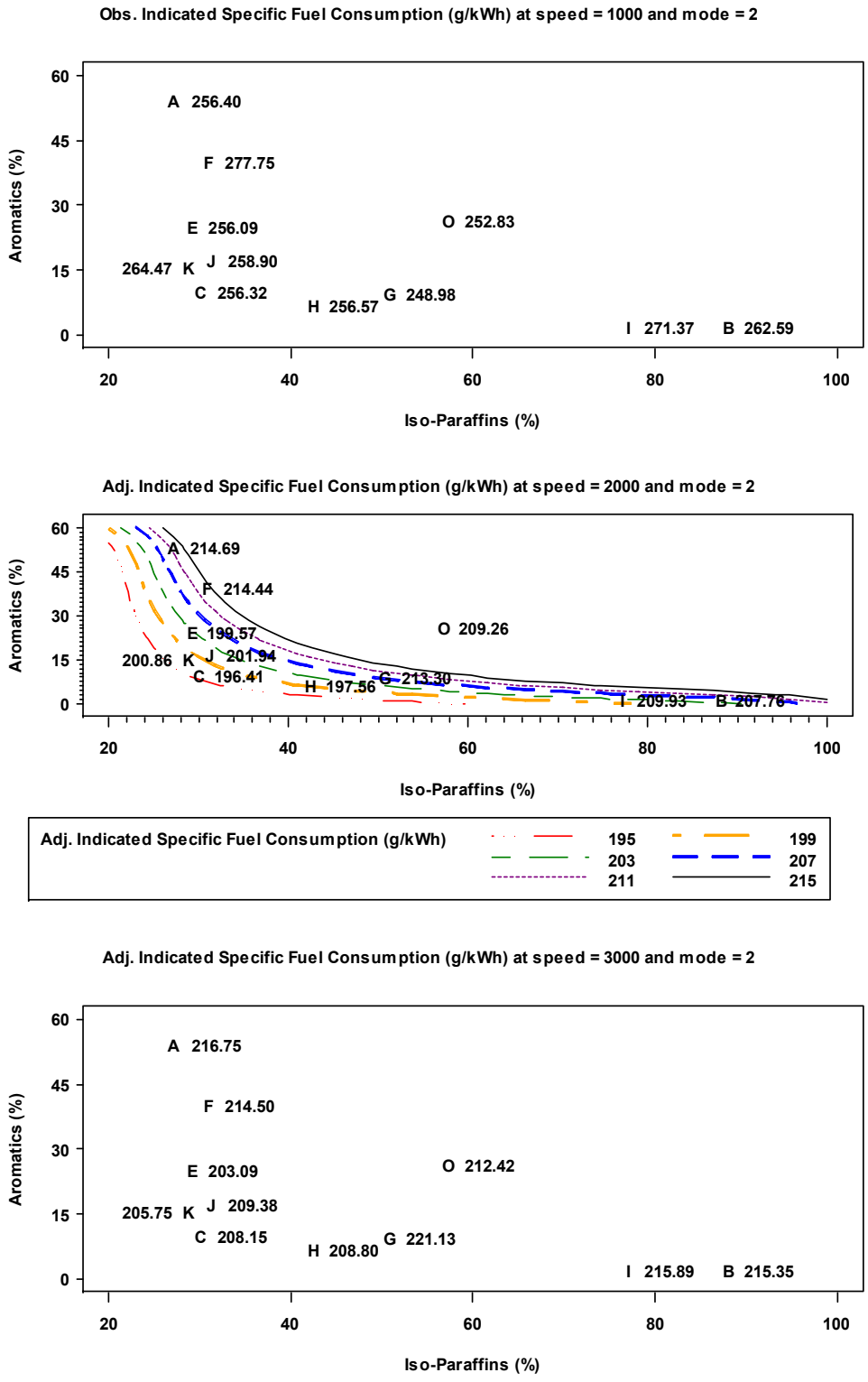

Figure 5.1: Contour Plots of indicated fuel consumption under best ranked r^2 model for RCEI (Mode=2)

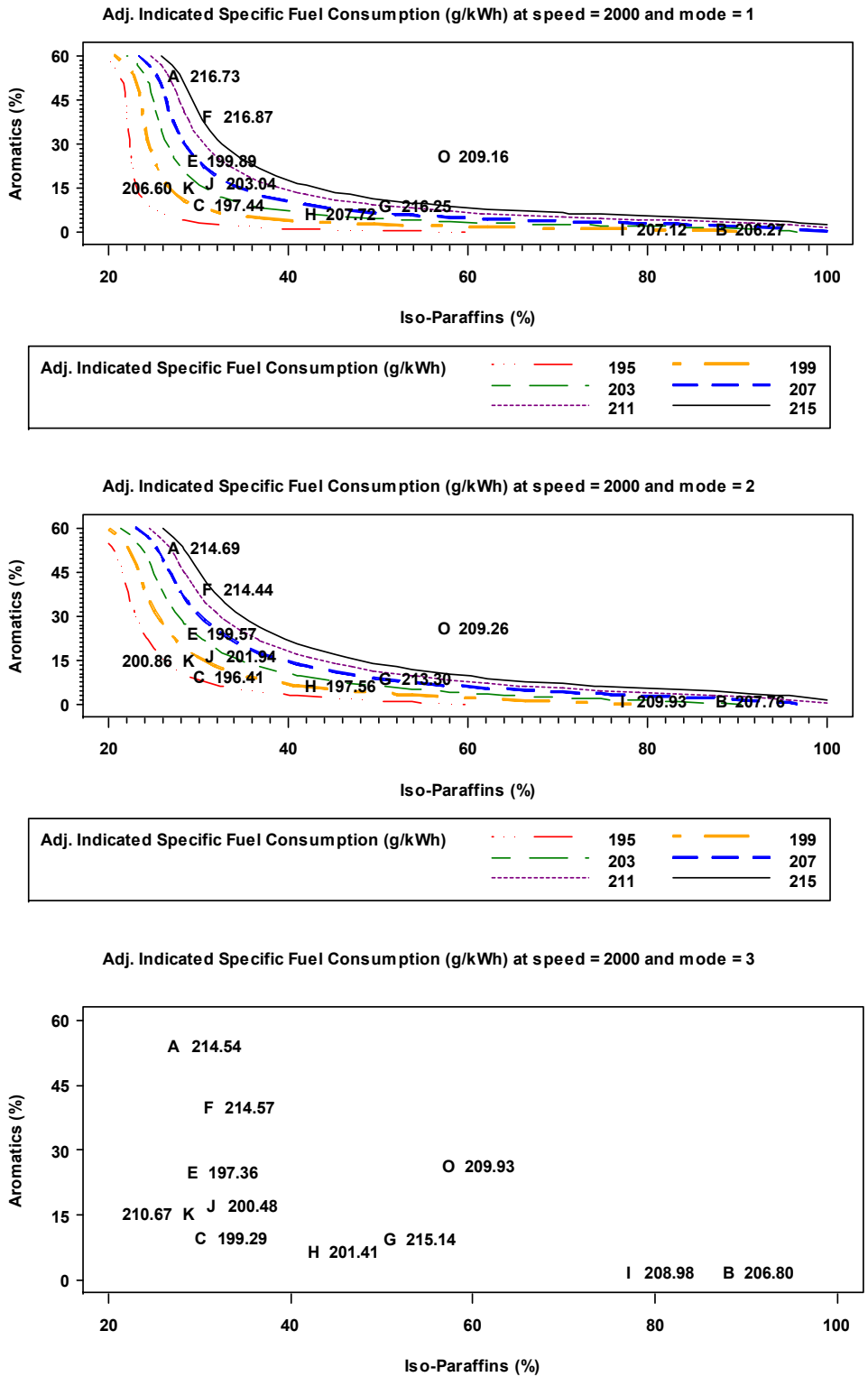

Figure 5.2: Contour Plots of indicated fuel consumption at 2000 rpm under best ranked r^2 model

It is observed from Figures 5.1 and 5.2 that higher aromatic or iso-paraffin levels lead to higher fuel consumption at 2000 and 3000 rpm. In Figures 5.3 and 5.4, it is shown that the high aromatic and iso-paraffin levels are associated with earlier exhaust valve close angle. This would be necessary if, for instance, these fuels were harder to ignite and earlier EVCA would be required to increase the amount of residual gas to increase the cylinder temperature at the beginning of compression and advance the combustion to maintain the constant combustion phasing at 5 degrees ATDC. More residual gas leads to more incomplete combustion in the cylinder resulting in higher fuel consumption.

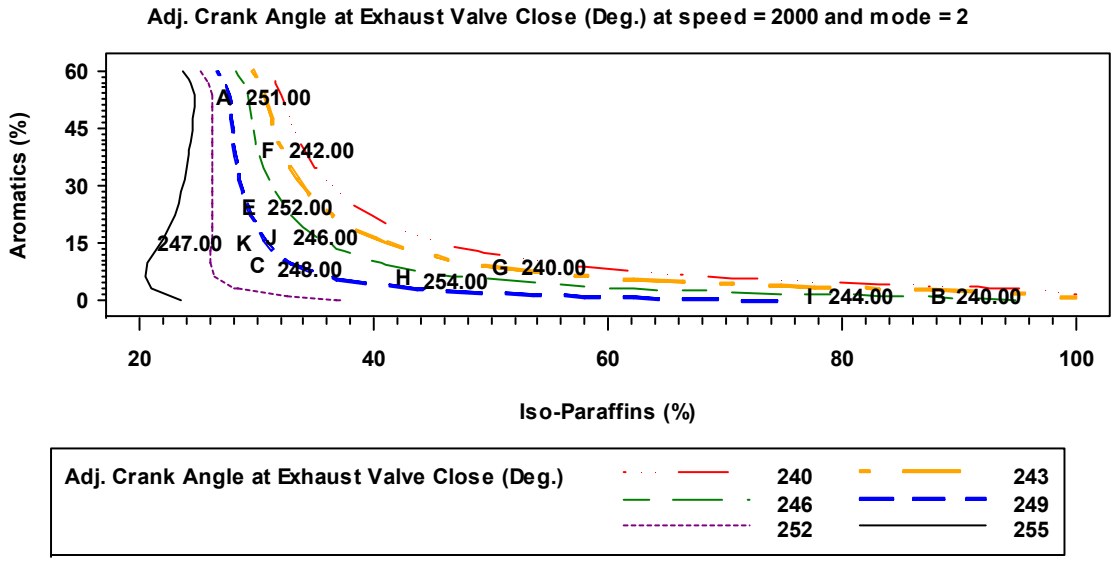

Figure 5.3: Contour Plots of exhaust valve close angle at 2000 rpm, RCEI (mode=2)

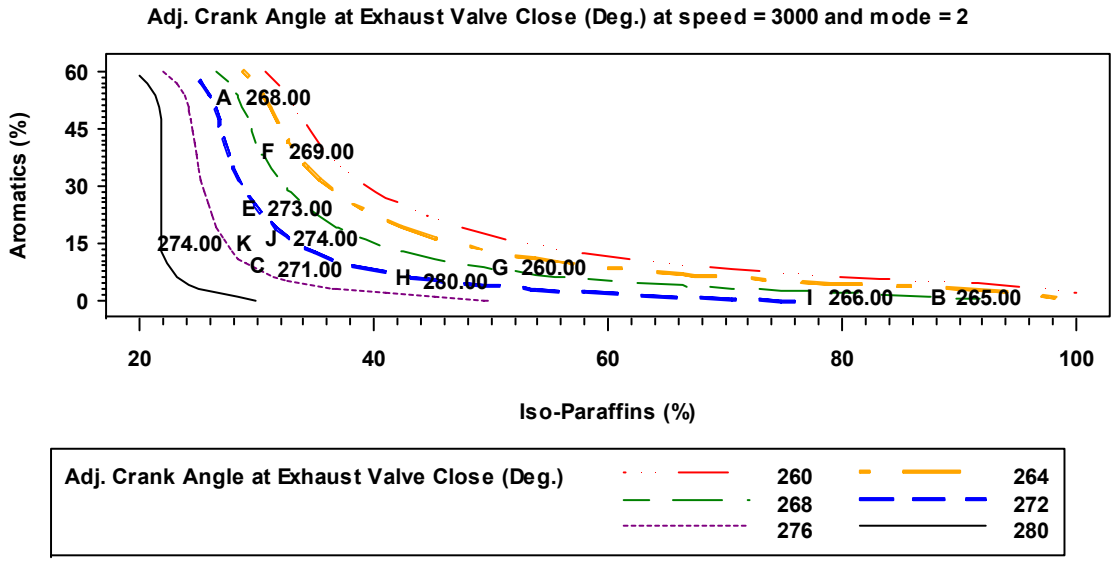

Figure 5.4: Contour Plots of exhaust valve close angle at 3000 rpm, RCEI (mode=2)

The trend in poorer fuel consumption for high aromatic and iso-paraffin fuels is also supported by the observed air/fuel ratios as shown for 2000 rpm RCEI and 3000 rpm RCEI in Figures 5.5 and 5.6, respectively.

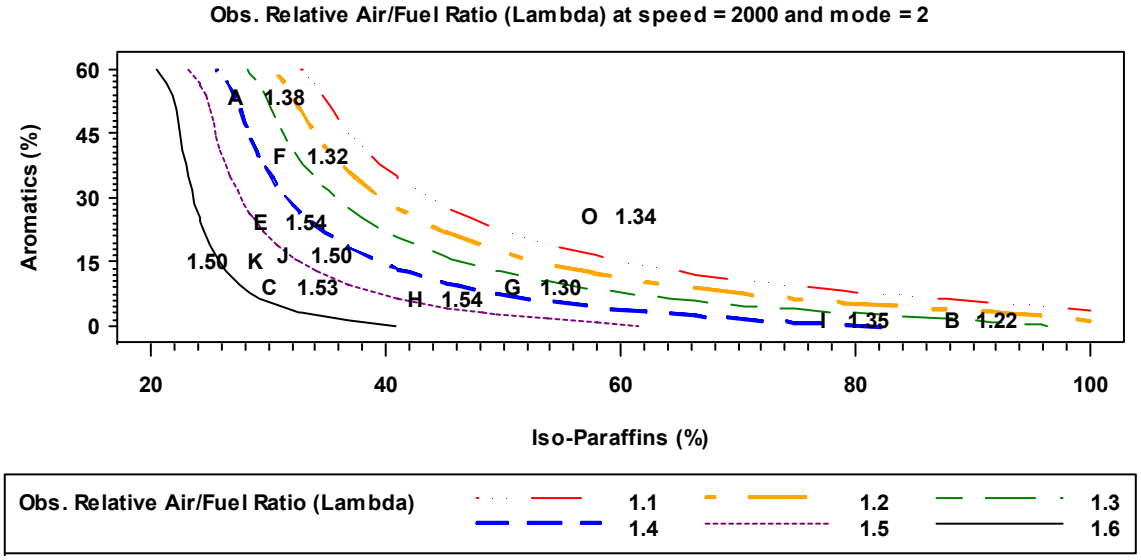

Figure 5.5: Contour Plots of observed air/fuel ratio (lambda) at 2000 rpm, RCEI (mode=2)

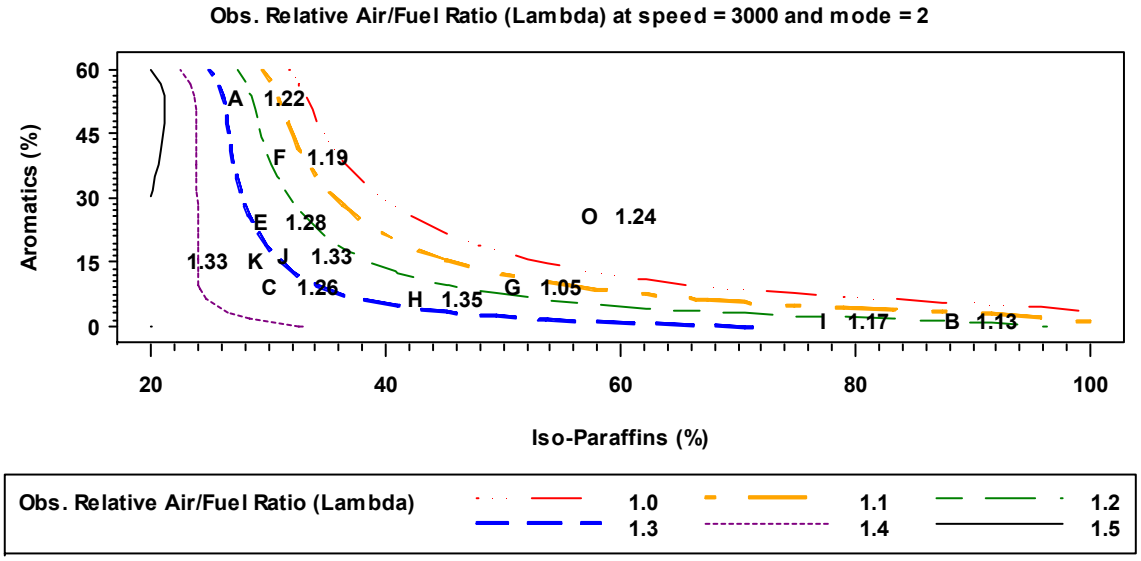

Figure 5.6: Contour Plots of observed air/fuel ratio (lambda) at 3000 rpm, RCEI (mode=2)

5.2.3 NOx emission

Table 5.2: Results for NO_x emission

Best r-Square Model: NOx Emissions (ppm)

		Predictor Variables		Model Coefficients				Standard		Overall Model p-
speed	mode	P1	P2	Intercept	P1	P2	P1 * P2	Deviation	RSquare	Value
1000	1	Olefins	C4	1.08	-0.01	-0.11	0.02 *	0.425	63%	0.097
1000	2	i_Paraffins	Sensitivity	-0.1	0.01	-0.26	0.01	0.302	70%	0.053
1000	3	i_Paraffins	RON	-6.50 *	0.13 *	0.09 **	-0.001 *	0.225	83%	0.010
2000	1	n_Paraffins_woC4	Distillation_10	-52.27 **	3.35 *	0.42 **	-0.02 **	1.698	86%	0.006
2000	2	Olefins	RON	-12.11 **	-0.14	0.27 **	-0.0006	1.121	94%	0.000
2000	3	n_Paraffins_woC4	Distillation_10	-48.79 *	3.46	0.42 *	-0.03 *	2.705	77%	0.023
3000	1	Aromatics	i_Paraffins	0.99	-0.6	0.12	0.04 *	2.785	88%	0.004
3000	2	Aromatics	i_Paraffins	4.79	-1.31 *	0.16	0.07 **	3.135	90%	0.002
3000	3	Aromatics	i_Paraffins	-1.21	-3.51 *	0.17	0.14 **	6.961	81%	0.013

Best Ranked r-Square Model: NOx Emissions (ppm)

		Predictor Variables		Model Coefficients				Standard		Overall Model p-
speed	mode	P1	P2	Intercept	P1	P2	P1 * P2	Deviation	RSquare	Value
1000	1	n_Paraffins_woC4	Distillation_10	0.84	0.45	-0.003	-0.002	0.467	55%	0.164
1000	2	n_Paraffins_woC4	Distillation_10	-0.31	0.26	0.01	-0.002	0.446	34%	0.445
1000	3	n_Paraffins_woC4	Distillation_10	-4.01	0.48 *	0.03 *	-0.003 *	0.257	78%	0.022
2000	1	n_Paraffins_woC4	Distillation_10	-52.27 **	3.35 *	0.42 **	-0.02 **	1.698	86%	0.006
2000	2	n_Paraffins_woC4	Distillation_10	-56.05 **	3.01 **	0.44 **	-0.02 **	1.128	94%	0.001
2000	3	n_Paraffins_woC4	Distillation_10	-48.79 *	3.46	0.42 *	-0.03 *	2.705	77%	0.023
3000	1	n_Paraffins_woC4	Distillation_10	-96.82 *	6.47 *	0.76 **	-0.04 *	4.034	74%	0.035
3000	2	n_Paraffins_woC4	Distillation_10	-98.64 *	4.86	0.86 *	-0.04	5.020	73%	0.037
3000	3	n_Paraffins_woC4	Distillation_10	-124.45	8.05	1.03	-0.06	13.094	34%	0.446

Note: Response values have been adjusted by TL22, MFB 50, and PI at speeds = 2000 and by TL22, MFB 50, and PR_CYP at speeds = 3000.
* Significant at 0.05 Level of Significance
** Significant at 0.01 Level of Significance

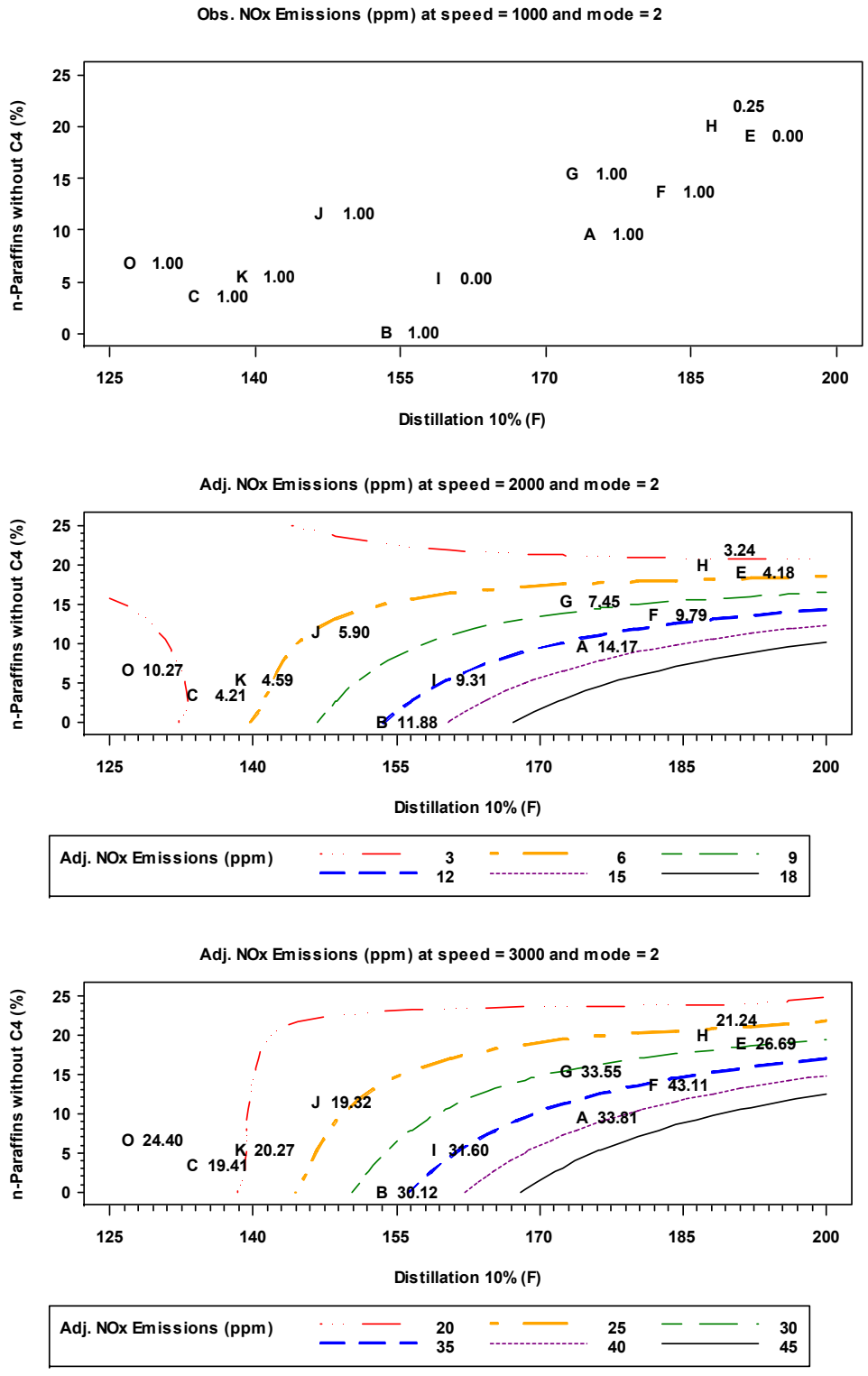

Figure 5.7: Contour plots of NO_x emission under best ranked r^2 model for RCEI (Mode=2)

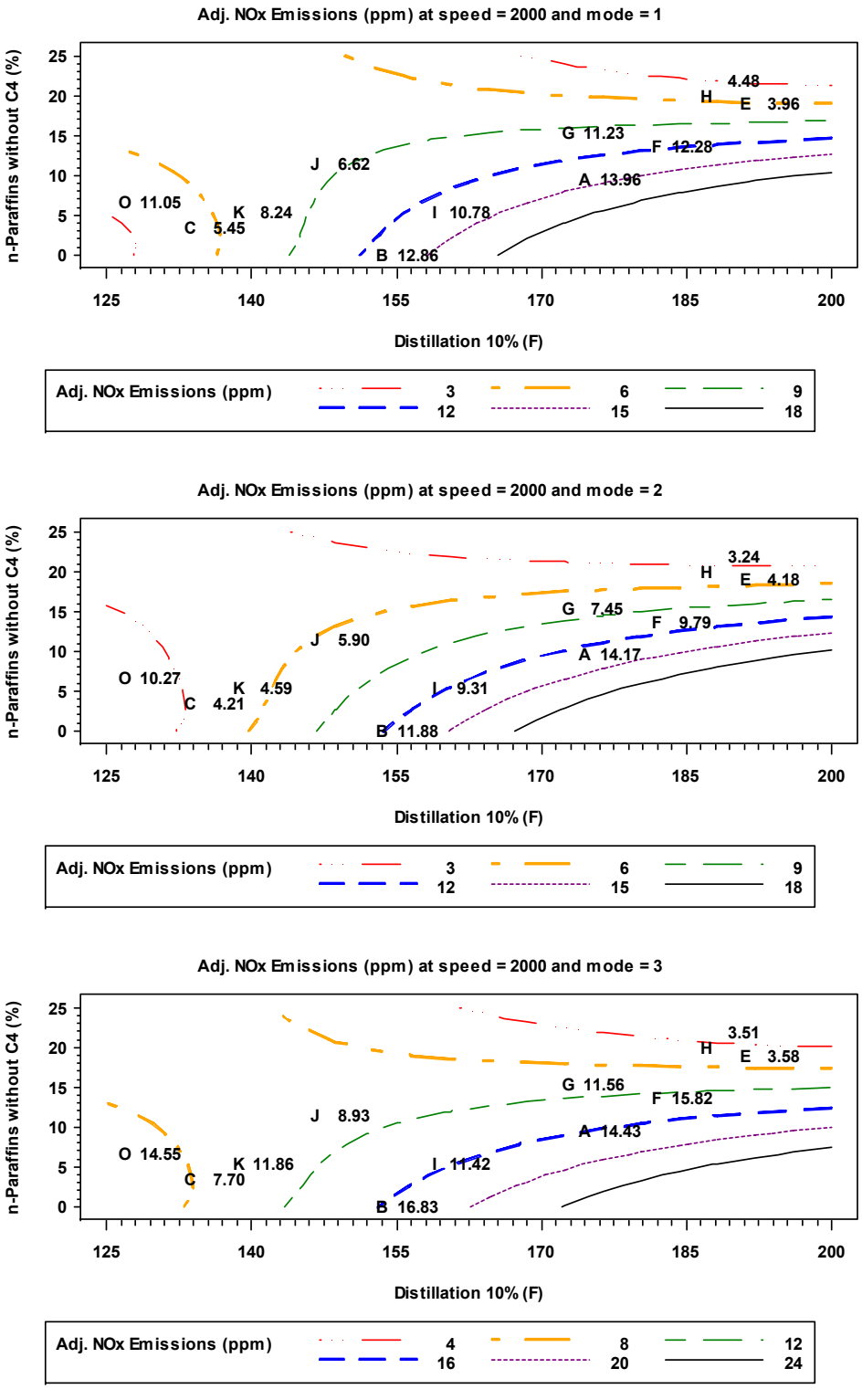

Figure 5.8: Contour plots of NO_x emission at 2000 rpm under best ranked r^2 model

The statistical analysis for NOx identified n-paraffins without butane and T10 as the best two factors to explain observed NOx performance. The contour plots for these results are shown in Figures 5.7 and 5.8 with the generalization that higher normal paraffin content resulted in lower NOx emissions (at a particular T10). Because of the T10 relationship, no simple generalization can be made about specific n-paraffins levels. Among the test fuels, there were those that showed all combinations of lower and higher n-paraffin content and lower and higher NOx emissions.

The detailed analysis of NOx is limited to the 2000 and 3000 rpm speeds since the observed NOx at 1000 rpm was extremely low (<2 ppm). Within each speed, the observed NOx levels were similar between the three engine test modes. NOx emission levels at the 3000 rpm test conditions were greater than that produced at the 2000 rpm test conditions, due to higher maximum rate of pressure rise.

NOx and specific fuel consumption performance appeared closely related. Specifically, test fuels with poorer specific fuel consumption were also most likely to exhibit higher NOx emissions. This is shown in Figures 5.9a and 5.9b for 2000 and 3000 rpm, RCEI, respectively.

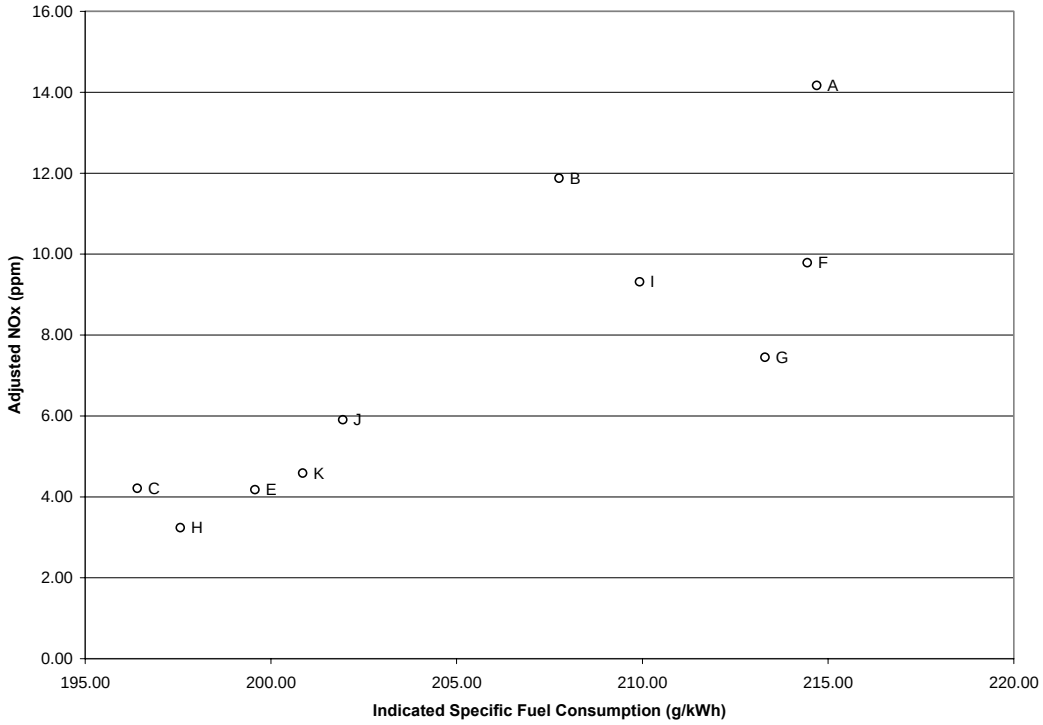

Figure 5.9a: The relationship between NOx emissions and specific fuel consumption for RCEI at 2000 rpm

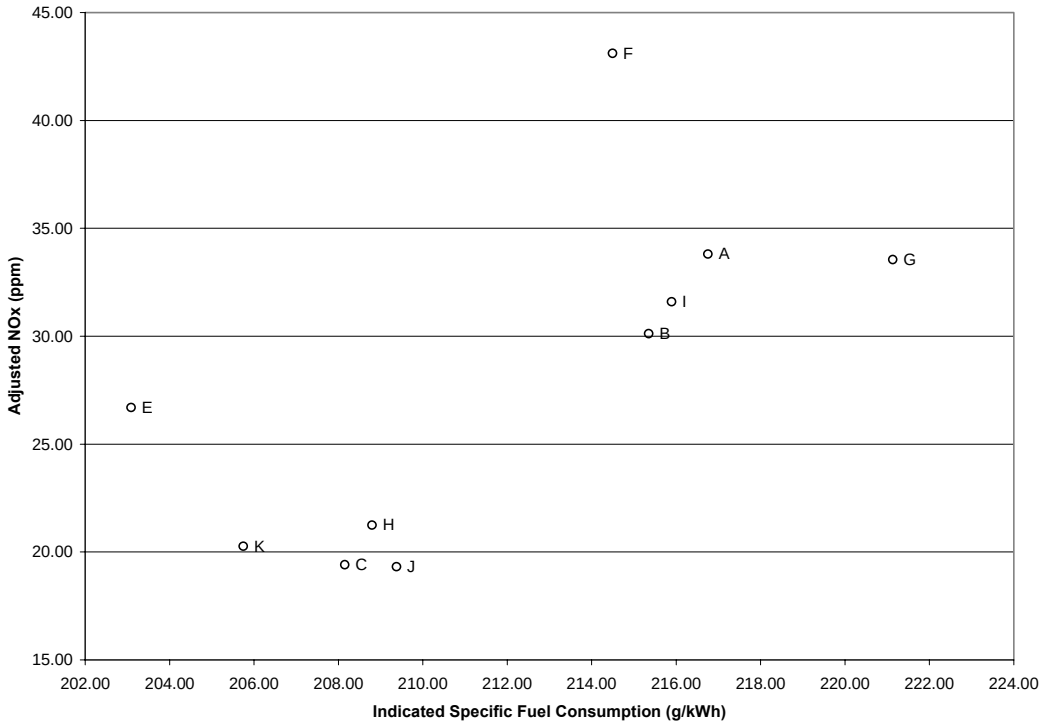

Figure 5.9b: The relationship between NOx emissions and specific fuel consumption for RCEI at 3000 rpm

Section 5.2.2 accounted for the poorer specific fuel consumption performance of some test fuels under the hypothesis that these fuels were harder to ignite and required earlier EVCA (with more high temperature residual gas) to maintain the constant 5 degree engine phasing. Ultimately, this resulted in more incomplete, and hence less efficient, combustion. Without measurements of the amount of residual gas or combustion temperatures, no definitive conclusion can be reached regarding how the earlier EVCA might affect NOx emissions. However, Figures 5.10a and 5.10b provide some insight, showing for the RCEI mode at 2000 and 3000 rpm that higher NOx levels are associated with shorter combustion durations. This suggests that the start of combustion was delayed with earlier EVCA for less efficient test fuels,. However, once started, the combustion proceeded more quickly to completion than for the more efficient fuels. This shorter combustion duration would likely feature a higher peak temperature where more NOx are produced.

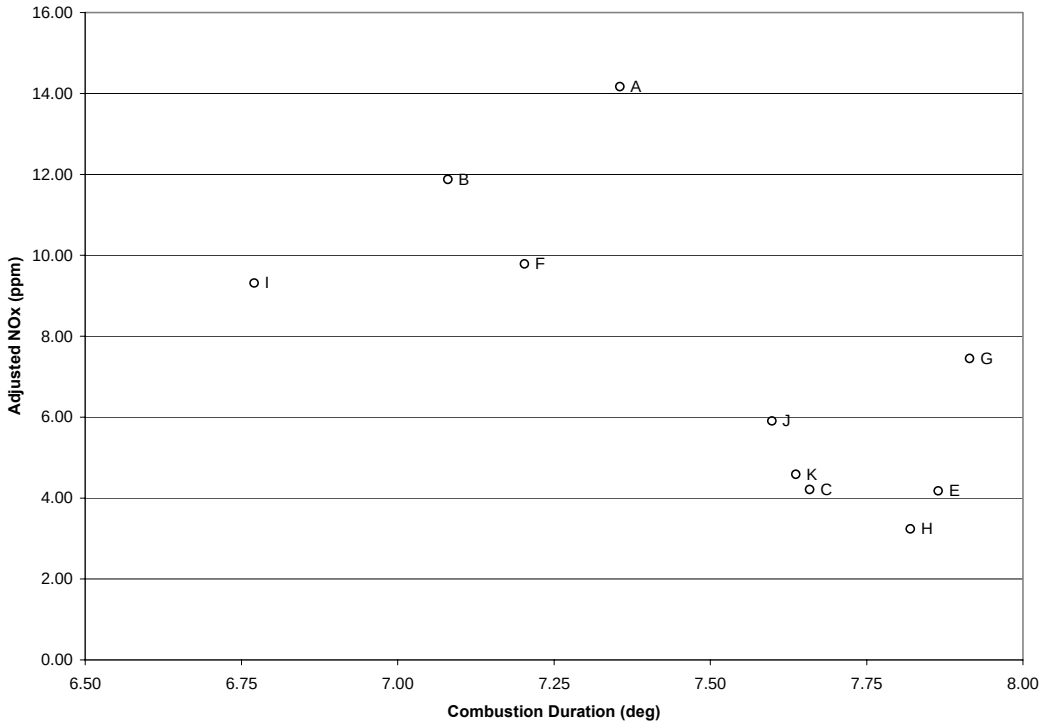

Figure 5.10a: The relationship between NOx emissions and combustion duration for RCEI at 2000 rpm

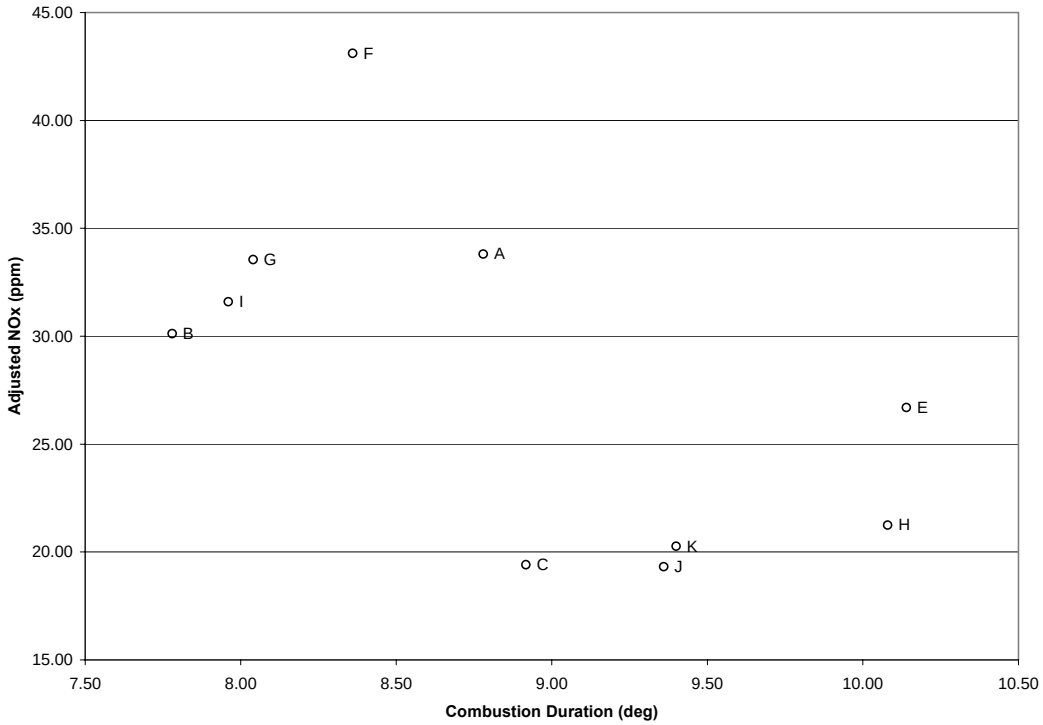

Figure 5.10 b: The relationship between NOx emissions and combustion duration for RCEI at 3000 rpm

5.2.4 Indicated specific HC emission

Table 5.3: Results for indicated specific HC emission

Best r-Square Model: Indicated Specific HC (g/kWh)

		Predictor Variables		Model Coefficients				Standard		Overall Model p
speed	mode	P1	P2	Intercept	P1	P2	P1 * P2	Deviation	RSquare	Value
1000	1	C4	RON	-44.37 *	7.62 **	0.69 **	-0.08 *	1.343	79%	0.019
1000	2	i_Paraffins	Sensitivity	13.28 **	0.04 *	1.74 **	-0.05 **	0.523	91%	0.002
1000	3	C4	Distillation_10	24.36 *	2.35	-0.06	-0.01	1.838	54%	0.175
2000	1	i_Paraffins	RON	-6.62	0.31	0.17	-0.003	0.822	54%	0.176
2000	2	i_Paraffins	Distillation_10	-36.71	1.07	0.28	-0.01	2.112	45%	0.276
2000	3	i_Paraffins	Sensitivity	5.82 **	-0.03 *	1.01 **	-0.03 **	0.487	81%	0.013
3000	1	Aromatics	RON	11.48 **	-0.33 *	-0.06	0.004 *	0.589	79%	0.020
3000	2	i_Paraffins	Sensitivity	4.26 **	-0.02	0.77 *	-0.03 *	0.472	65%	0.079
3000	3	Aromatics	RON	6.73 *	-0.15	-0.05	0.002	0.500	73%	0.037

Best Ranked r-Square Model: Indicated Specific HC (g/kWh)

		Predictor Variables		Model Coefficients				Standard		Overall Model p
speed	mode	P1	P2	Intercept	P1	P2	P1 * P2	Deviation	RSquare	Value
1000	1	i_Paraffins	Sensitivity	15.83 **	0.02	2.61	-0.08	2.012	53%	0.187
1000	2	i_Paraffins	Sensitivity	13.28 **	0.04 *	1.74 **	-0.05 **	0.523	91%	0.002
1000	3	i_Paraffins	Sensitivity	12.69 **	0.06	1.14	-0.03	2.173	35%	0.421
2000	1	i_Paraffins	Sensitivity	6.19 **	0.04	-0.39	0.02	0.845	51%	0.204
2000	2	i_Paraffins	Sensitivity	9.94 *	-0.07	0.81	-0.03	2.498	23%	0.634
2000	3	i_Paraffins	Sensitivity	5.82 **	-0.03 *	1.01 **	-0.03 **	0.487	81%	0.013
3000	1	i_Paraffins	Sensitivity	7.47 **	-0.01	1.06	-0.03	0.943	45%	0.278
3000	2	i_Paraffins	Sensitivity	4.26 **	-0.02	0.77 *	-0.03 *	0.472	65%	0.079
3000	3	i_Paraffins	Sensitivity	4.47 **	-0.02	0.51	-0.02	0.797	32%	0.470

Note: Response values have been adjusted by TL22, MFB 50, and PI at speeds = 2000 and by TL22, MFB 50, and PR_CYP at speeds = 3000.
* Significant at 0.05 Level of Significance
** Significant at 0.01 Level of Significance

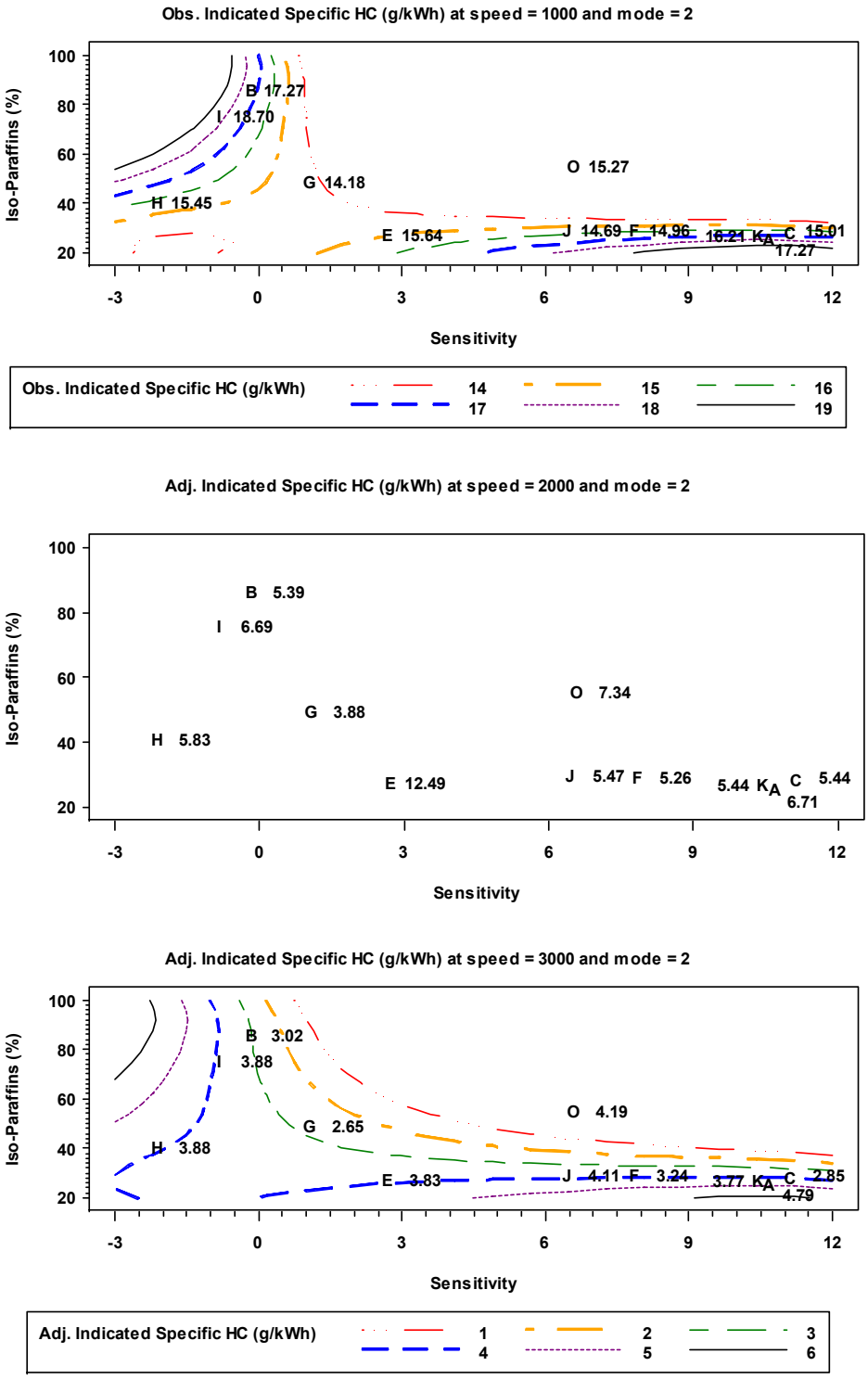

Figure 5.11: Contour plots of indicated specific HC emission under best ranked r^2 model for RCEI (Mode=2)

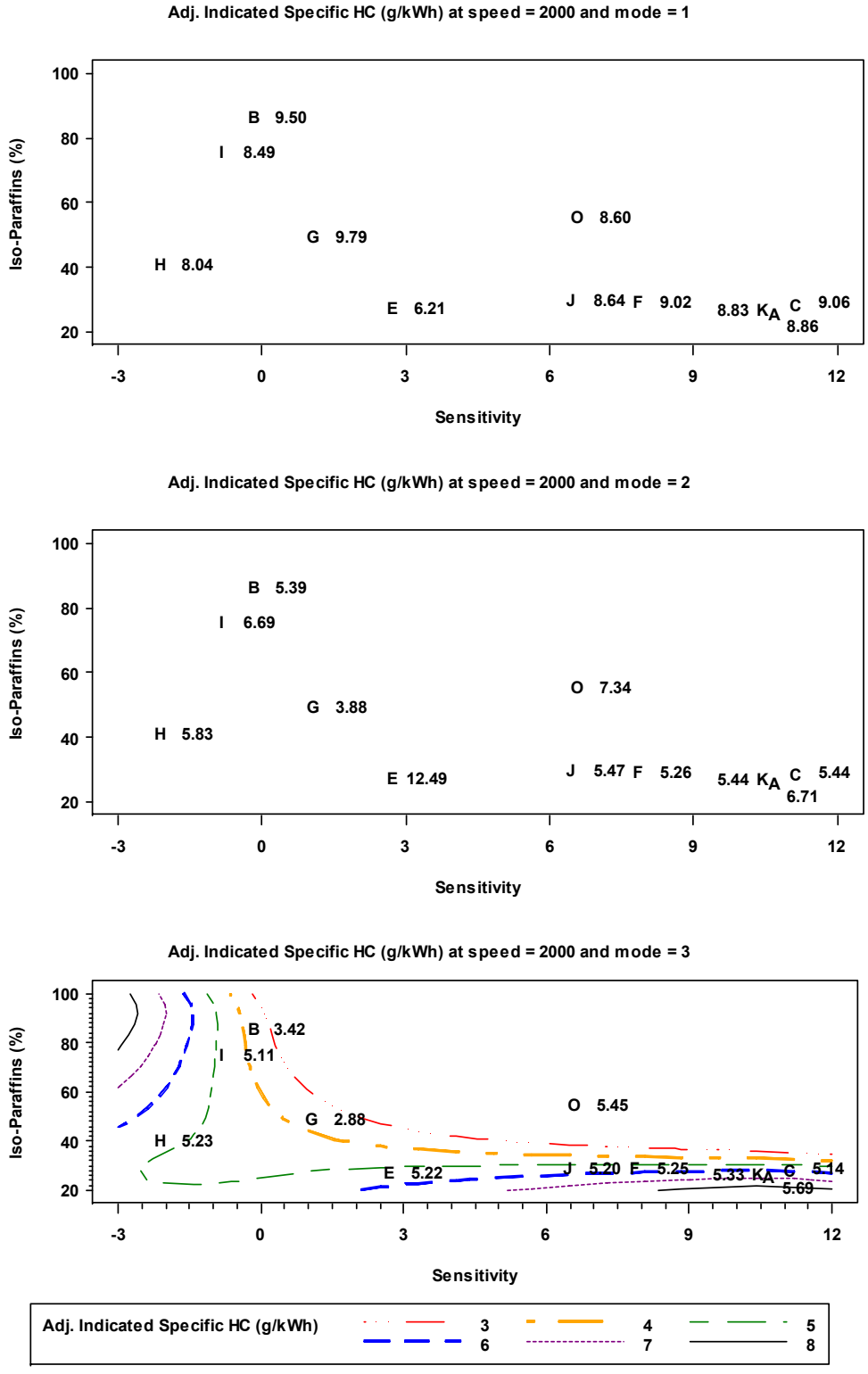

Figure 5.12: Contour plots of indicated specific HC emission at 2000 rpm under best ranked r^2 model

5.2.5 Indicated specific CO emission

Table 5.4: Results for indicated specific CO emission

Best r-Square Model: Indicated Specific CO (g/kWh)

		Predictor Variables		Model Coefficients				Standard		Overall Model p-
speed	mode	P1	P2	Intercept	P1	P2	P1 * P2	Deviation	RSquare	Value
1000	1	Aromatics	i_Paraffins	76.63 **	1.43	-0.28 *	-0.08 *	4.290	89%	0.002
1000	2	n_Paraffins_woC4	Distillation_10	225.66 **	-12.48 **	-1.21 **	0.08 **	5.316	80%	0.016
1000	3	Aromatics	i_Paraffins	84.33 **	0.87	-0.36	-0.06	7.560	76%	0.029
2000	1	i_Paraffins	Sensitivity	3.27	0.04	-1.54	0.05	1.254	53%	0.187
2000	2	i_Paraffins	RON	31.51 *	-0.54	-0.3	0.01	1.500	53%	0.185
2000	3	Aromatics	i_Paraffins	6.79 **	0.12	-0.03 *	-0.01	0.509	79%	0.020
3000	1	i_Paraffins	C4	-18.98 **	0.74 **	3.29 **	-0.11 **	1.608	93%	0.001
3000	2	Aromatics	Distillation_10	-2.39	0.41 *	0.03 *	-0.002 *	0.258	72%	0.042
3000	3	i_Paraffins	Sensitivity	3.89 **	-0.02	0.57	-0.02	0.462	62%	0.099

Best Ranked r-Square Model: Indicated Specific CO (g/kWh)

		Predictor Variables		Model Coefficients				Standard		Overall Model p-
speed	mode	P1	P2	Intercept	P1	P2	P1 * P2	Deviation	RSquare	Value
1000	1	Aromatics	i_Paraffins	76.63 **	1.43	-0.28 *	-0.08 *	4.290	89%	0.002
1000	2	Aromatics	i_Paraffins	69.62 **	1.36	-0.22	-0.07	5.631	78%	0.022
1000	3	Aromatics	i_Paraffins	84.33 **	0.87	-0.36	-0.06	7.560	76%	0.029
2000	1	Aromatics	i_Paraffins	4.82 *	-0.35	-0.02	0.01	1.379	43%	0.310
2000	2	Aromatics	i_Paraffins	6.75 *	0.15	-0.02	-0.01	1.973	18%	0.726
2000	3	Aromatics	i_Paraffins	6.79 **	0.12	-0.03 *	-0.01	0.509	79%	0.020
3000	1	Aromatics	i_Paraffins	-5.04	0.5	0.24 *	-0.02	3.806	63%	0.093
3000	2	Aromatics	i_Paraffins	3.62 **	0.06	-0.01	-0.003	0.344	51%	0.207
3000	3	Aromatics	i_Paraffins	3.40 **	0.13	-0.001	-0.005	0.547	47%	0.251

Note: Response values have been adjusted by TL22, MFB 50, and PI at speeds = 2000 and by TL22, MFB 50, and PR_CYP at speeds = 3000.

* Significant at 0.05 Level of Significance

** Significant at 0.01 Level of Significance

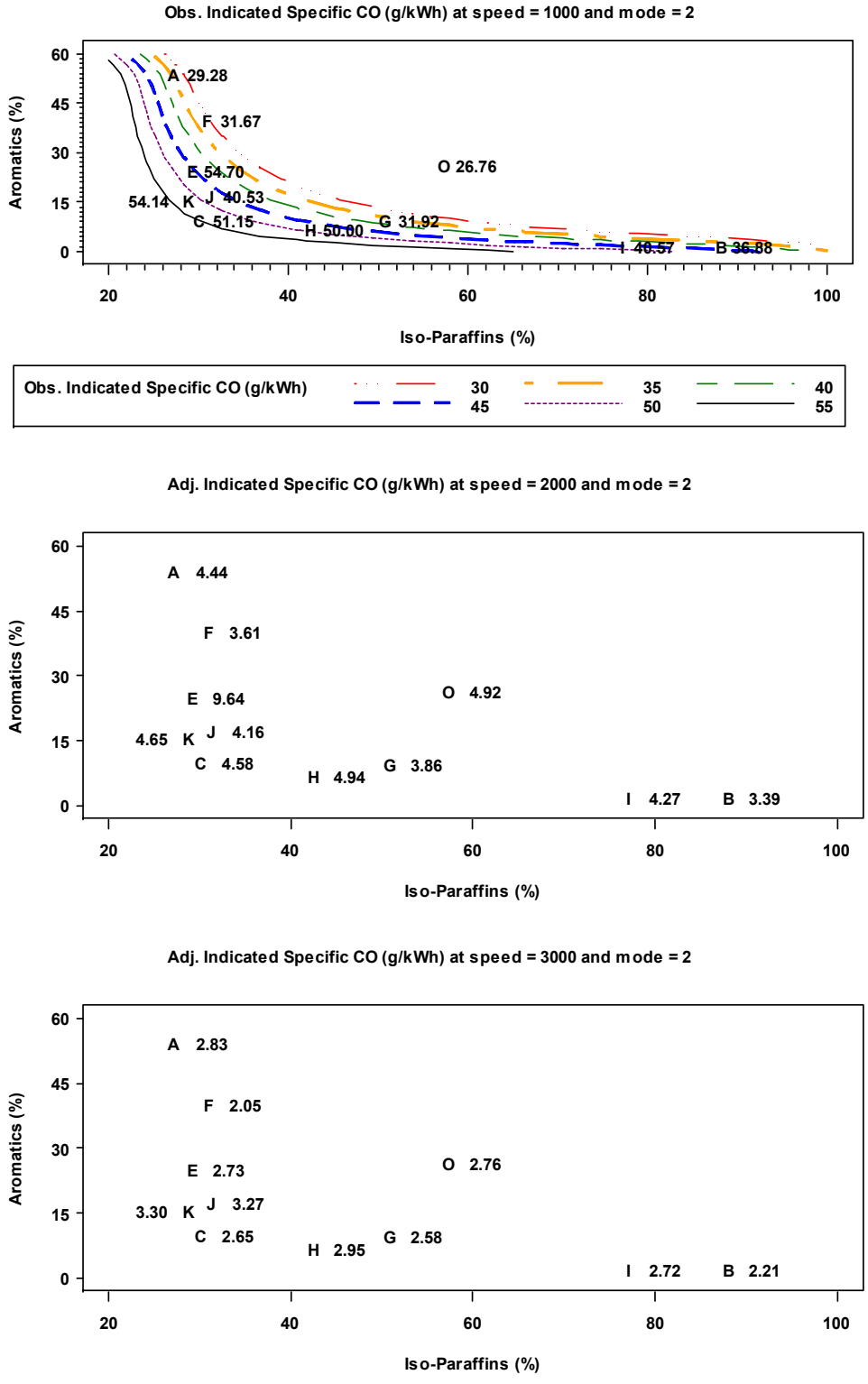

Figure 5.13: Contour plots of indicated specific CO emission under best ranked r^2 model for RCEI (Mode=2)

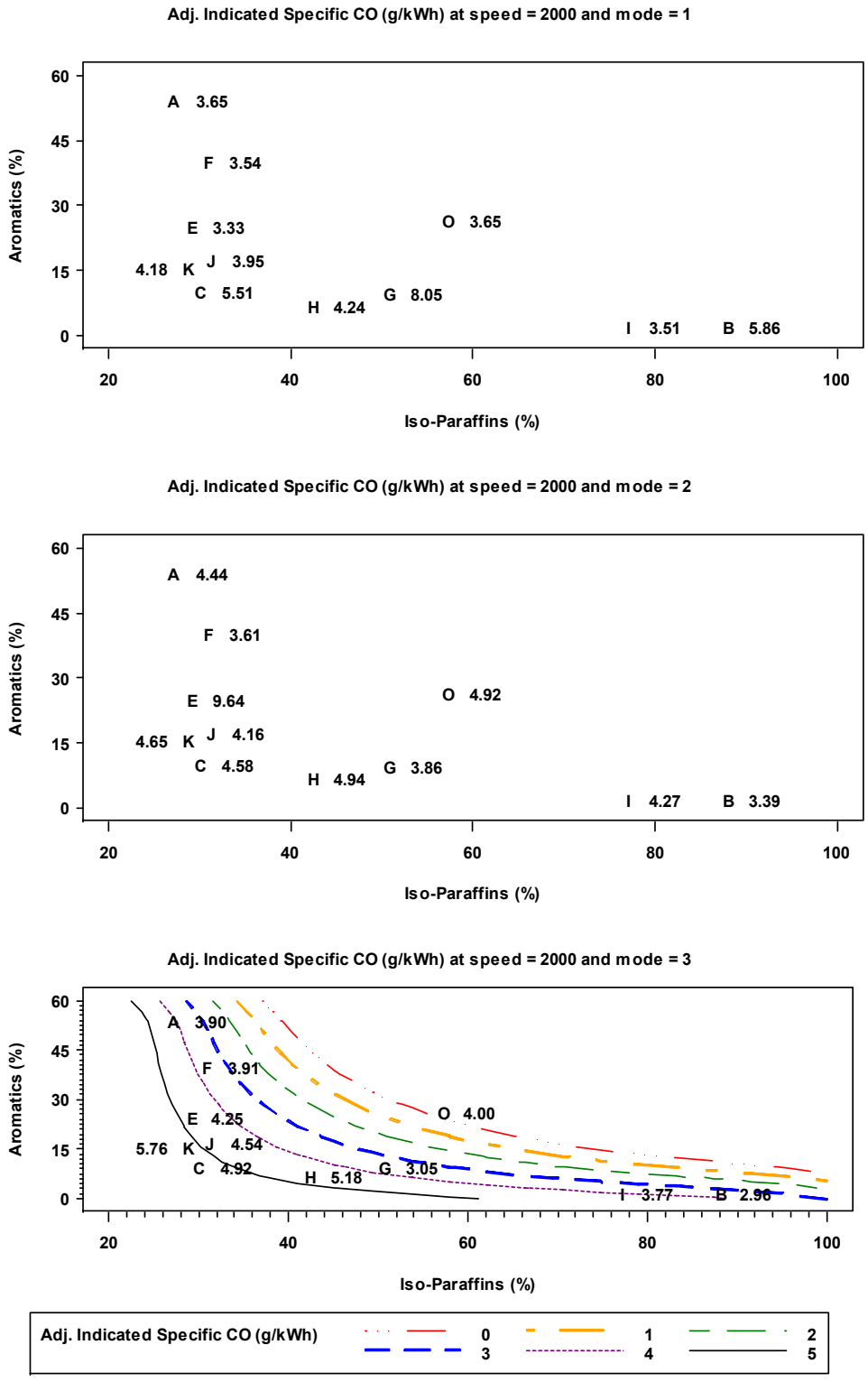

Figure 5.14: Contour plots of indicated specific CO emissions at 2000 rpm under best ranked r^2 model

It is observed that higher percentage of aromatics or iso-paraffins reduces CO emissions at 1000 rpm. Opposite results presented in Figures 5.5 and 5.6 at 2000 and 3000 rpm, higher percentage of aromatics or iso-paraffins at idle leads to less residual gas trapped in the cylinder and leaner combustion at 1000 rpm.

At 1000 rpm, an electrical intake heater is employed to increase the in-cylinder charge temperature at the beginning of compression to help ignite fuels, which makes the thermal effect of the residual gas a secondary factor. At low speed, there is more heat loss to the cylinder wall, which retards the combustion. To maintain constant combustion phasing at 5 degrees ATDC at 1000 rpm, less residual gas is required to advance the combustion, which is verified by the relationship between EVCA and lambda and percentage of aromatics and iso-paraffins in Figures 5.15 and 5.16, respectively. With less residual gas, the combustion in the cylinder is more complete, resulting in lower CO emissions.

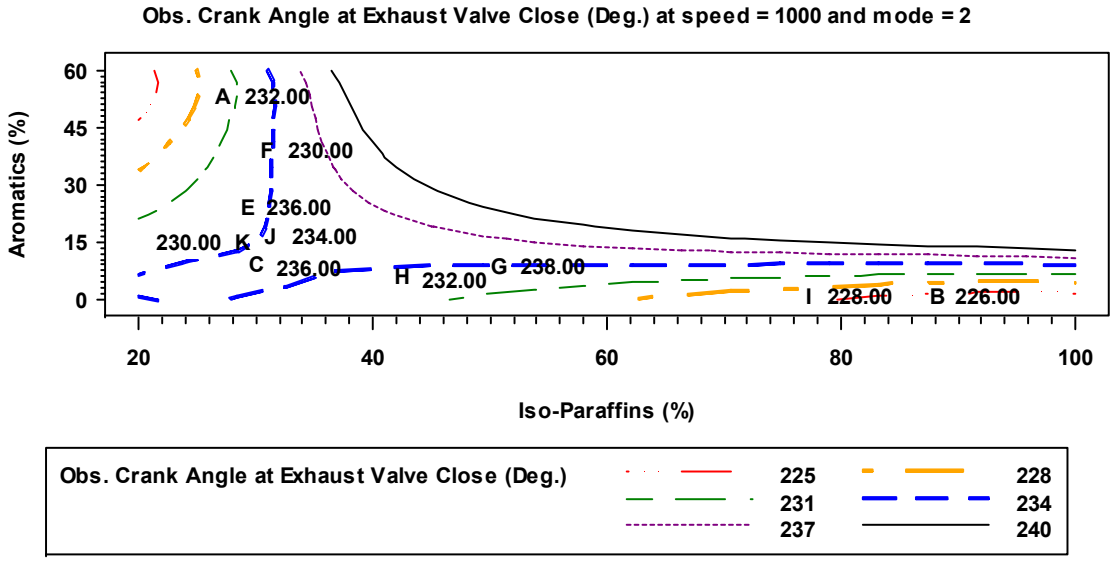

Figure 5.15: The relationship between EVCA and percentages of aromatics and iso-paraffins for RCEI at 1000 rpm

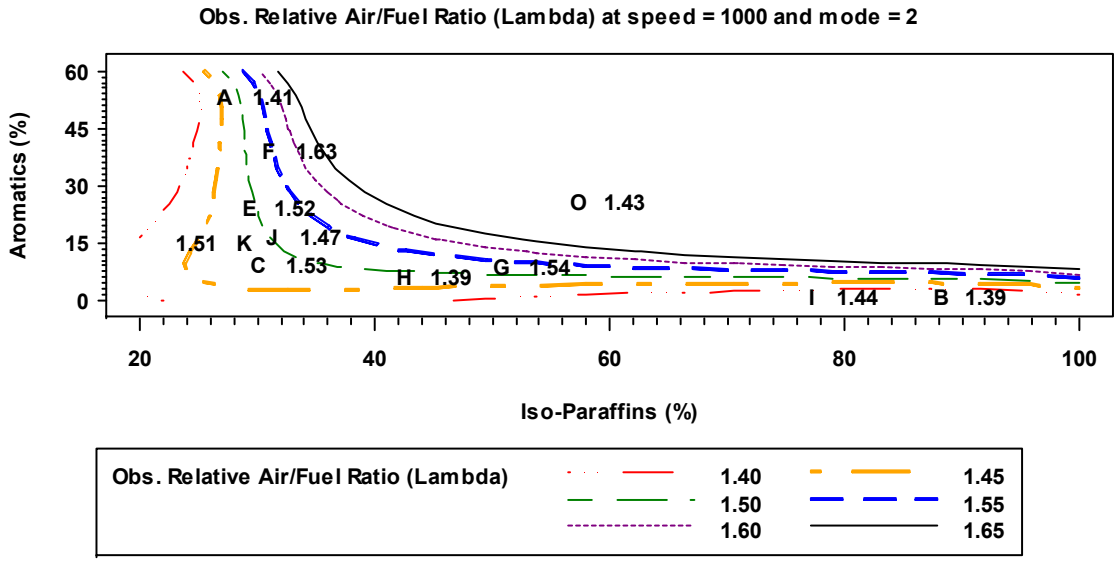

Figure 5.16: The relationship between Lambda and percentages of aromatics and iso-paraffins for RCEI at 1000 rpm

5.2.6 Fuel effects on expanding HCCI operating range

It is well understood that HCCI combustion delivers both high efficiency and low NOx, while its operation is limited to part-load operating conditions. At higher loads, the maximum rate of cylinder pressure rise is too large resulting in excessive combustion noise. Conversely at low loads, the combustion becomes unstable near the idle operation leading to high HC and CO emissions.

In this report, coefficients of variance (COV) of indicated mean effective pressures (IMEPs) were utilized to characterize the combustion stability of HCCI combustion. Higher COV of IMEP indicates more unstable HCCI combustion and a narrower operating range. Results for two-factor regression are shown in Table 5.5. The best model results from this analysis and the corresponding contour plots of fuel effects on the combustion stability (Figure 5.7) are limited to only the 1000 rpm test condition as this is most relevant to the evaluation of combustion stability.

Table 5.5: Results for coefficient of variance of IMEP

Best r-Square Model: Coefficient of Variance (COV) of IMEP (%)

		Predictor Variables		Model Coefficients				Standard		Overall Model p-
speed	mode	P1	P2	Intercept	P1	P2	P1 * P2	Deviation	RSquare	Value
1000	1	RON	Distillation_10	-427.70 **	5.43 **	2.60 **	-0.03 **	3.063	85%	0.008
1000	2	RON	Distillation_10	-252.93 *	3.16 *	1.49 *	-0.02 *	2.822	62%	0.101
1000	3	Olefins	i_Paraffins	13.40 **	-4.03	-0.05	0.14	3.023	66%	0.075
2000	1	i_Paraffins	n_Paraffins_woC4	2.08	0.002	0.33	-0.01	1.193	55%	0.158
2000	2	i_Paraffins	Sensitivity	2.77 **	-0.01	-0.24 *	0.01 *	0.149	75%	0.032
2000	3	Distillation_10	Distillation_90	17.17 **	-0.09 **	-0.05 **	0.0003 **	0.112	91%	0.001
3000	1	n_Paraffins_woC4	C4	6.23	-0.47	2.09 *	-0.04	2.098	86%	0.006
3000	2	Aromatics	Distillation_90	-21.33 *	1.48	0.07 *	-0.004	0.615	91%	0.002
3000	3	Aromatics	Olefins	2.72 **	0.09 *	0.31 **	-0.02 *	1.060	76%	0.027

Best Ranked r-Square Model: Coefficient of Variance (COV) of IMEP (%)

1000 RPM ONLY

		Predictor Variables		Model Coefficients				Standard		Overall Model p-
speed	mode	P1	P2	Intercept	P1	P2	P1 * P2	Deviation	RSquare	Value
1000	1	RON	Distillation_10	-427.70 **	5.43 **	2.6 **	-0.03 **	3.063	85%	0.008
1000	2	RON	Distillation_10	-252.93 *	3.16 *	1.49 *	-0.02 *	2.822	62%	0.101
1000	3	RON	Distillation_10	-8.46	0.59	0.17	-0.004	3.912	43%	0.310

Note: Response values have been adjusted by TL22, MFB 50, and PI at speeds = 2000 and by TL22, MFB 50, and PR_CYP at speeds = 3000.

* Significant at 0.05 Level of Significance

** Significant at 0.01 Level of Significance

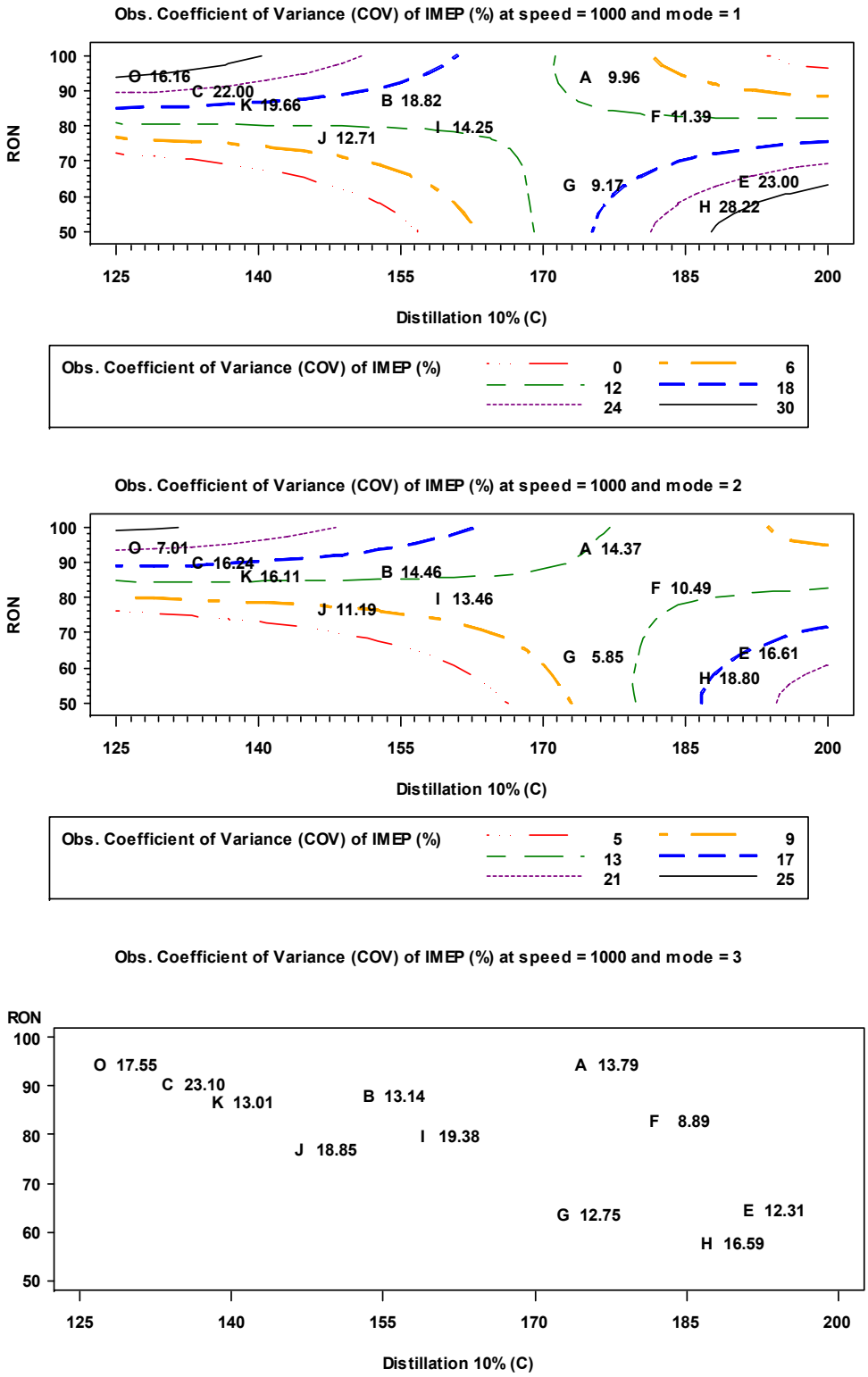

Figure 5.17: Contour plots of COV of IMEP at 1000 rpm under best ranked r^2 model

Figure 5.17 shows that COVs of IMEPs are influenced by RON and distillation temperature T10. The contour plots for modes 1 and 2 were both divided into four quadrants, which are defined as follows.

(I) T10 < 170 F & RON > 80;
(II) T10 > 170 F & RON > 80;
(III) T10 < 170 F & RON < 80;
(IV) T10 > 170 F & RON < 80.

In quadrants (I) and (III), where T10 is below 170 F, higher RON leads to higher COV of IMEP. In general, fuels with higher RON have lower tendency of auto-ignition, which leads to more difficult start of combustion for HCCI at idle and more unstable combustion. However, in quadrants (II) and (IV), where T10 is higher than 170 F, higher RON leads to lower COV of IMEP. There might be due to other fuel properties impacting the combustion stability.

In quadrants (I) and (II), where RON is higher than 80, higher distillation temperature T10 leads to lower COV of IMEP. Higher T10 results in more fuel mixed with the air near the end of compression, making start of combustion easier and more stable combustion. However, in quadrants (III) and (IV), where RON is less than 80, higher T10 leads to higher COV of IMEP, indicating more unstable HCCI combustion. It is might be due to other fuel properties having stronger influence than T10 on the combustion stability

Shown in Table 5.6 is the ability of HCCI combustion for each fuel at 800 rpm. Fuels able to ignite at 800 rpm have the potential to expand HCCI operating ranges at idle.

Table 5.6: Ability of HCCI combustion at 800 rpm

Test Order	ID	Fuel	RON	T10 [F]	Combustion
1	A	A100	95.5	174.6	NO
2	G	B30D70	64.7	172.8	YES
3	F	A79D21	84.0	181.9	YES
4	I	B77D23	81.0	158.9	NO
5	B	B100	89.1	153.5	NO
6	K	C85D15	87.7	138.6	YES
7	J	C50D50	78.0	146.7	YES
8	C	C100	91.5	133.7	NO
9	H	B50D50	58.9	187.0	NO
10	E	A33D67	65.5	191.1	YES

5.2.7 Exhaust valve close timing

To study the fuel impacts on the ignition timing, which is primarily controlled by the exhaust valve close timing, engine test data for Re-Compression Early Injection (RCEI) mode were investigated. The other two modes (RCSI and RBEI) are more difficult to interpret because of the influence of second injection (RCSI) and second exhaust valve open event (RBEI).

Table 5.7: Results for exhaust valve close timing

Best r-Square Model: Crank Angle at Exhaust Valve Close (Deg.)

		Predictor Variables		Model Coefficients				Standard		Overall Model p-
speed	mode	P1	P2	Intercept	P1	P2	P1 * P2	Deviation	RSquare	Value
1000	1	RON	Sensitivity	269.89 **	-0.50 **	-4.08	0.06 *	3.099	78%	0.020
1000	2	n_Paraffins_woC4	Distillation_90	259.68 **	-0.25	-0.1	0.002	2.533	71%	0.048
1000	3	RON	Sensitivity	262.56 **	-0.41 **	-0.83	0.02	2.112	82%	0.011
2000	1	i_Paraffins	Sensitivity	263.12 **	-0.26 *	4.87 *	-0.17 *	3.423	76%	0.027
2000	2	i_Paraffins	Sensitivity	258.55 **	-0.25 **	4.51 *	-0.17 **	2.412	84%	0.008
2000	3	i_Paraffins	Sensitivity	255.67 **	-0.19 *	3.48	-0.13 *	2.861	69%	0.059
3000	1	i_Paraffins	Distillation_90	425.10 **	-4.05	-0.39	0.01	3.423	73%	0.040
3000	2	Olefins	Distillation_90	220.05 **	-0.04	0.14	0.001	4.467	58%	0.130
3000	3	i_Paraffins	Sensitivity	283.62 **	-0.24 *	3.75	-0.14	3.181	73%	0.038

Best Ranked r-Square Model: Crank Angle at Exhaust Valve Close (Deg.)

		Predictor Variables		Model Coefficients				Standard		Overall Model p-
speed	mode	P1	P2	Intercept	P1	P2	P1 * P2	Deviation	RSquare	Value
1000	1	i_Paraffins	Sensitivity	249.59 **	-0.28 *	0.33	-0.03	3.819	67%	0.068
1000	2	i_Paraffins	Sensitivity	240.18 **	-0.13	-2.99	0.09	2.871	62%	0.098
1000	3	i_Paraffins	Sensitivity	245.75 **	-0.22 **	-1.58	0.04	2.274	79%	0.018
2000	1	i_Paraffins	Sensitivity	263.12 **	-0.26 *	4.87 *	-0.17 *	3.423	76%	0.027
2000	2	i_Paraffins	Sensitivity	258.55 **	-0.25 **	4.51 *	-0.17 **	2.412	84%	0.008
2000	3	i_Paraffins	Sensitivity	255.67 **	-0.19 *	3.48	-0.13 *	2.861	69%	0.059
3000	1	i_Paraffins	Sensitivity	299.26 **	-0.25 *	1.28	-0.06	4.050	62%	0.105
3000	2	i_Paraffins	Sensitivity	282.52 **	-0.25 *	3.33	-0.13	4.662	55%	0.165
3000	3	i_Paraffins	Sensitivity	283.62 **	-0.24 *	3.75	-0.14	3.181	73%	0.038

Note: Response values have been adjusted by TL22, MFB 50, and PI at speeds = 2000 and by TL22, MFB 50, and PR_CYP at speeds = 3000.
* Significant at 0.05 Level of Significance
** Significant at 0.01 Level of Significance

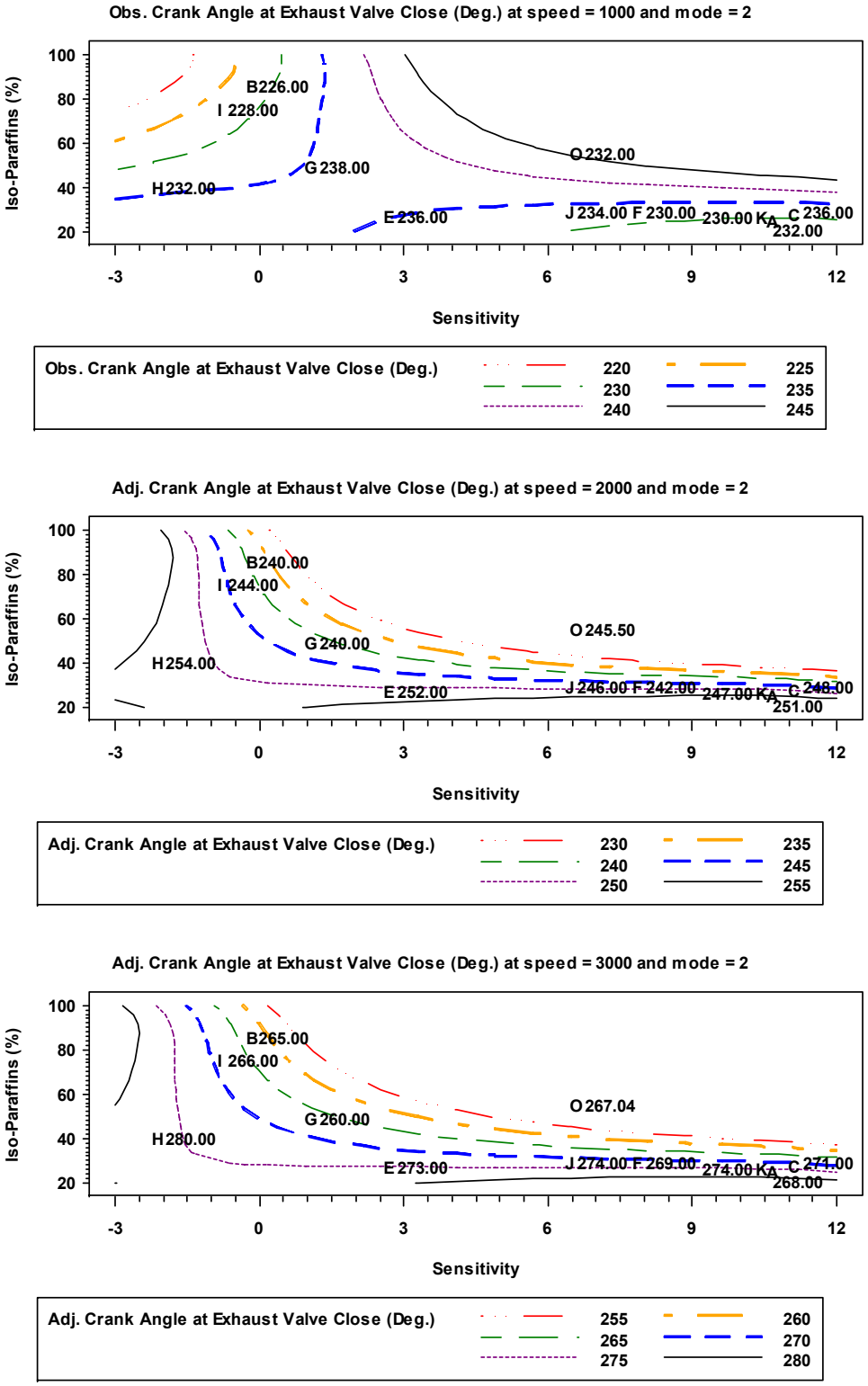

Figure 5.18: Contour plots of exhaust valve close timing under best ranked r^2 model for RCEI (Mode=2)

Figure 5.18 shows that higher percentages of iso-paraffins (when the sensitivity is positive) lead to earlier exhaust valve close timing at 2000 rpm and 3000 rpm and later exhaust valve close timing at 1000 rpm. The exhaust valve close timing results for 2000 and 3000 rpm were discussed in further detail in Sections 5.2.2 and 5.2.3 in conjunction with indicated specific fuel consumption and NOx performance, respectively. The results for 1000 rpm were discussed in further detail in Section 5.2.5 relating to CO emissions.

5.3 Conclusions and recommendations – statistical analysis

The regression analysis of performance variables against fuel properties yielded some potential relationships between HCCI performance and fuel properties; however, there were no unambiguous and consistent fuel effects across all speeds and operating modes.

1. For speeds above idle, specific fuel consumption performance appeared statistically related to fuel aromatic and iso-paraffin content. Best specific fuel consumption was associated with fuels having low aromatic and iso-paraffin content. Increases in either fuel property were associated with decreased SFC performance.
2. For speeds above idle, NOx emissions appeared statistically related to n-paraffin content (excluding butane) and the temperature at which 10 percent of the fuel distils. Lowest NOx was associated with fuels having low n-paraffins and high T10. Though not completely consistent, increases in n-paraffins were generally associated with lower NOx and increases in T10 with higher NOx.
3. At idle, CO emissions appeared statistically related to fuel aromatic and iso-paraffin content. Lowest CO was associated with fuels having high aromatics and low iso-paraffins. Increases in either fuel parameter were associated with decreased CO emission levels.
4. At all speed and mode conditions, smoke appeared statistically related to aromatic content and RON. Lowest smoke was associated with low aromatics and RON of at least 75.

However, the above results need further study before they can be considered definitive. Recommendations for further analysis of the existing data and additional testing are as follows:

1. Explore other potential models (e.g., non-linear, three-factor) that might better explain the observed variability in the test fuel performance;
2. Repeat the current analyses with a more restricted set of fuel properties that are not highly correlated. Some of these properties will serve as surrogates for other (excluded) properties; however, the resulting analysis might reveal properties that produce consistent effects across operating conditions and modes;
3. Expand the regression model by combining the data from different operating conditions and modes. This may provide stronger statistical evidence regarding the effects of fuel properties while simultaneously accounting for the effects of these operating conditions;
4. Conduct targeted testing of additional fuel blends in areas of potential interest relative to the results observed in this evaluation.

6 Acknowledgement

AVL Powertrain Engineering, Inc. (AVL) would like to acknowledge Coordinating Research Council (CRC) for funding the project. AVL would also like to thank Dr. John Orban, Robert Krile, and Elizabeth Slone from Battelle for their statistical modeling and data analysis. Through the program, Ken Wright from ConocoPhillips, William Leppard retired from GM Research and Development Center, and Dr. Bruce Bunting from Oak Ridge National Laboratory provided valuable ideas and suggestions, which AVL very much appreciated.

7 References

1. Morrison, D.F. (1976) Multivariate Statistical Methods. McGraw Hill Series in Probability and Statistics.
2. Orban, J.E.; Tsai, H; and Whitacre, S.D. (2003) "Statistical Design and Analysis Methods for Evaluating the Effects of Lubricant Formulations on Diesel Engine Emissions." JSAE 20030201 and SAE 2003-01-2022.
3. Zheng, J., Yang, W., et al, "A Skeletal Chemical Kinetic Model for the HCCI Combustion Process," SAE Technical Paper 2002-01-0423.
4. Law, D., Allen, J., et al, "Controlled combustion in an IC-Engine with a fully variable valve train," SAE Technical Paper 2001-01-0251.
5. Sun, R., Thomas, and R., Gray, C., "An HCCI Engine: Power Plant for a Hybrid Vehicle," SAE Technical Paper 2004-01-0933.
6. Marriott, C. and Reitz, R., "Experimental Investigation of Direct Injection Gasoline for Premixed Compression-Ignited Combustion-Phasing Control," 2002-01-0418.
7. Peng, Z., Zhao, H., and Ladommatos, N., "Effects of Air/Fuel Ratios and EGR Rates on HCCI Combustion of n-heptane, a Diesel Type Fuel," SAE Technical Paper 2003-01-0747.
8. Sjoberg, M., Edling, L., et al, "GDI HCCI: Effects of Injection Timing and Air Swirl on Fuel Stratification, Combustion and Emissions Formation," SAE Technical Paper 2002-01-0106.
9. Olsson, J., Tunestal, P., et al, "The Effect of Cooled EGR on Emissions and Performance of a Turbocharged HCCI Engine," SAE Technical Paper 2003-01-0743.
10. Kaneko, M., Morikawa, K., et al, "Study on Homogeneous Charge Compression Ignition Gasoline Engine," *The Fifth International Symposium on Diagnostics and Modeling of Combustion in Internal Combustion Engines* (*COMODIA 2001*), Nagoya, Japan, July, 2001.
11. Milovanovic, N., Chen, R. and Turner, J., "Influence of the Variable Valve Timing Strategy on the Control of a Homogeneous Charge Compression (HCCI) Engine," SAE Technical Paper 2004-01-1899.
12. Fuerhapter, A., Piock, W.F. and Fraidl, G.K., "CSI – Controlled Auto Ignition – The Best Solution for the Fuel Consumption – Versus Emission Trade-Off?" SAE Technical Paper 2003-01-0754.
13. Kaahaaina, N.B., Simon, A.J., et al, "Use of Dynamic Valving to Achieve Residual-Affected Combustion," SAE Technical Paper 2001-01-0549.
14. Nehmer, D.A., Fluechinger, L., et al, "Development of a Fully Flexible Hydraulic Valve Actuation Engine, Part I: *Hydraulic Valve Actuation System Development," Proceedings of the 2002 Global Powertrain Congress* (*GPC*) *on Advanced Engine Design and Performance*, Ann Arbor, Michigan, September 24 – 26, 2002.
15. Schock, H. J., Shen, Y., et al, "The Measurement and Control of Cyclic Variations of Flow in a Piston Cylinder Assembly," SAE Technical Paper 2003-01-1357.

16. Urushihar, T., Murayama, T., et al, “Turbulence and Cycle-by-cycle Variations of Mean Velocity Generated by Swirl and Tumble Flow and Their Effects on Combustion,” SAE Technical Paper 950813.
17. Heywood, J.B., *Internal Combustion Engine Fundamentals*, McGraw-Hill, 1988.

Appendix A: Literature review

The appendix is an independent technical report written by James Szybist and Bruce Bunting, Oak Ridge National Laboratory. The Microsoft Word file “AVFL-13 Gasoline HCCI Literature Review.doc” is sent with the final report.

Appendix B: Summary of measured data

Appendix B is a set of plots and data summaries for all tested fuels. This appendix is contained in a WinZip file named, “AVFL-13 Appendix B_Summary_Plots_20060716.zip” sent with this final report. The file is composed of five separate Excel workbooks.

Appendix C: Measured fuel properties

This appendix is contained in the worksheet, “AVFL-13 Appendix_C_Fuel_Analysis.xls,” sent with this final report.

Appendix D: All 2-factor regression models sorted by R^2

This appendix is contained in the Excel file, “AVFL 13 Appendix_D_Models_Sorted_by_R-Square_with_Overall_Pvalue_20060716.xls,” sent with this final report.

Appendix E: Statistical analysis results: smoke, combustion duration, noise, and peak cylinder pressure

E.1. SMOKE

Best r-Square Model: Filter Smoke Number (sz)

		Predictor Variables		Model Coefficients				Standard		Overall Model p
speed	mode	P1	P2	Intercept	P1	P2	P1 * P2	Deviation	RSquare	Value
1000	1	Aromatics	C4	0.04	-0.003	-0.01	0.001 *	0.029	68%	0.060
1000	2	Aromatics	Sensitivity	0.01 *	-0.00009	-0.001	0.0001 *	0.005	93%	0.001
1000	3	RON	Distillation_10	0.03	-0.002	-0.0007	0.00002	0.007	91%	0.001
2000	1	Aromatics	RON	0.83 **	-0.04 **	-0.01 **	0.0005 **	0.057	89%	0.003
2000	2	Aromatics	RON	0.54 *	-0.03 *	-0.01 *	0.0004 *	0.048	85%	0.007
2000	3	Aromatics	RON	0.11	-0.01	-0.0009	0.0001	0.028	77%	0.024
3000	1	n_Paraffins_woC4	RON	-9.69 *	0.46 *	0.11 *	-0.004	0.275	88%	0.004
3000	2	i_Paraffins	Distillation_90	0.84	-0.04	-0.002	0.0001	0.038	92%	0.001
3000	3	Sensitivity	Distillation_90	-2.67 **	0.16 **	0.01 **	-0.0004 **	0.055	95%	0.000

Best Ranked r-Square Model: Filter Smoke Number (sz)

		Predictor Variables		Model Coefficients				Standard		Overall Model p
speed	mode	P1	P2	Intercept	P1	P2	P1 * P2	Deviation	RSquare	Value
1000	1	Aromatics	RON	-0.11	0.02 *	0.001	-0.0002 *	0.030	66%	0.071
1000	2	Aromatics	RON	-0.004	-0.0008	0.0001	0.00002	0.006	91%	0.002
1000	3	Aromatics	RON	-0.003	-0.00009	0	0.00001	0.013	75%	0.032
2000	1	Aromatics	RON	0.83 **	-0.04 **	-0.01 **	0.0005 **	0.057	89%	0.003
2000	2	Aromatics	RON	0.54 *	-0.03 *	-0.01 *	0.0004 *	0.048	85%	0.007
2000	3	Aromatics	RON	0.11	-0.01	-0.0009	0.0001	0.028	77%	0.024
3000	1	Aromatics	RON	3.61 *	-0.04	-0.04 *	0.0009	0.346	80%	0.015
3000	2	Aromatics	RON	0.90 *	-0.02	-0.01 *	0.0002	0.081	65%	0.080
3000	3	Aromatics	RON	1.75 *	-0.06	-0.02 *	0.0008	0.167	57%	0.144

Note: Response values have been adjusted by TL22, MFB 50, and PI at speeds = 2000 and by TL22, MFB 50, and PR_CYP at speeds = 3000.

* Significant at 0.05 Level of Significance

** Significant at 0.01 Level of Significance

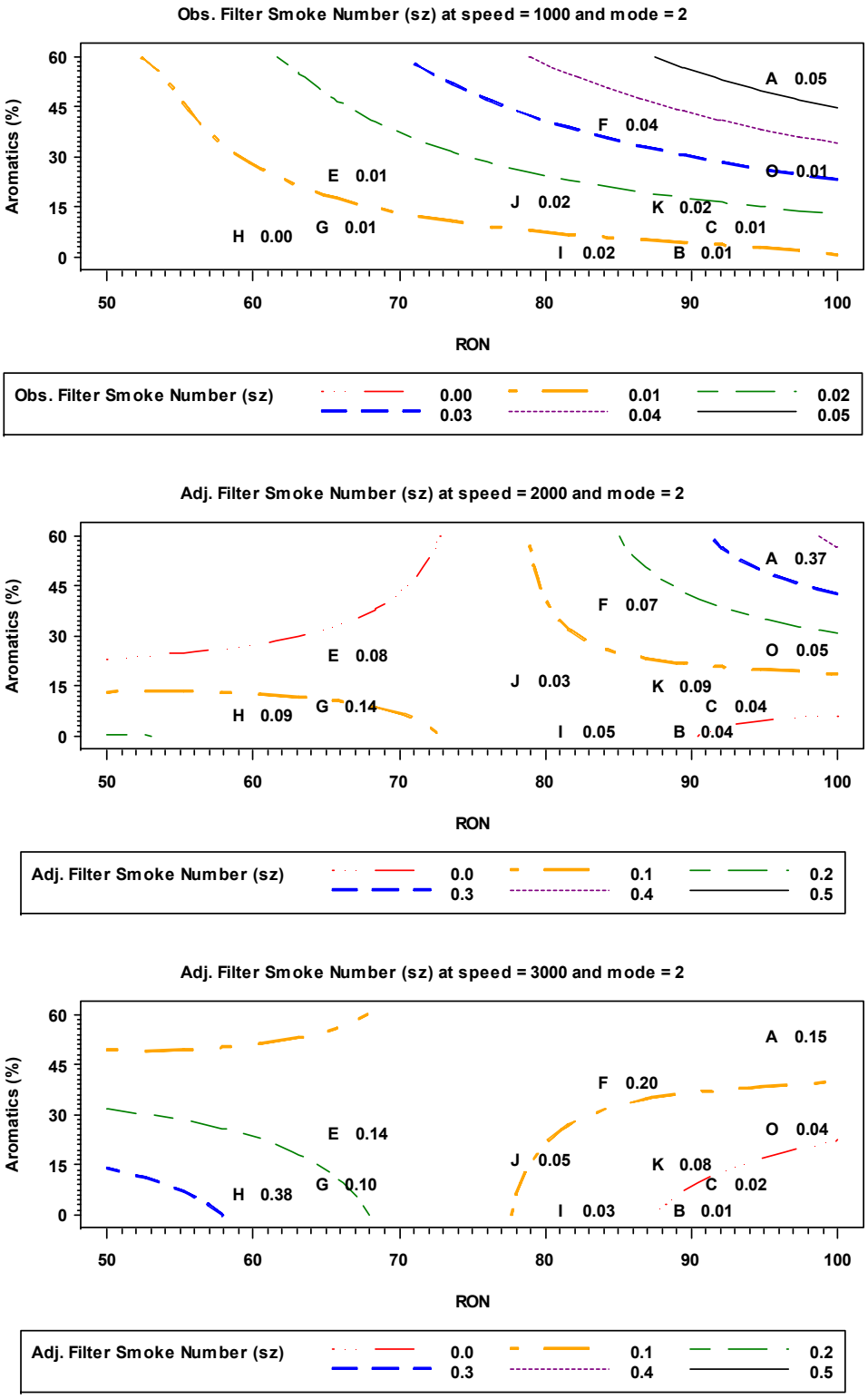

Figure Appendix E.1.1: Contour plots of filter smoke number under best ranked r^2 model for RCEI (Mode=2)

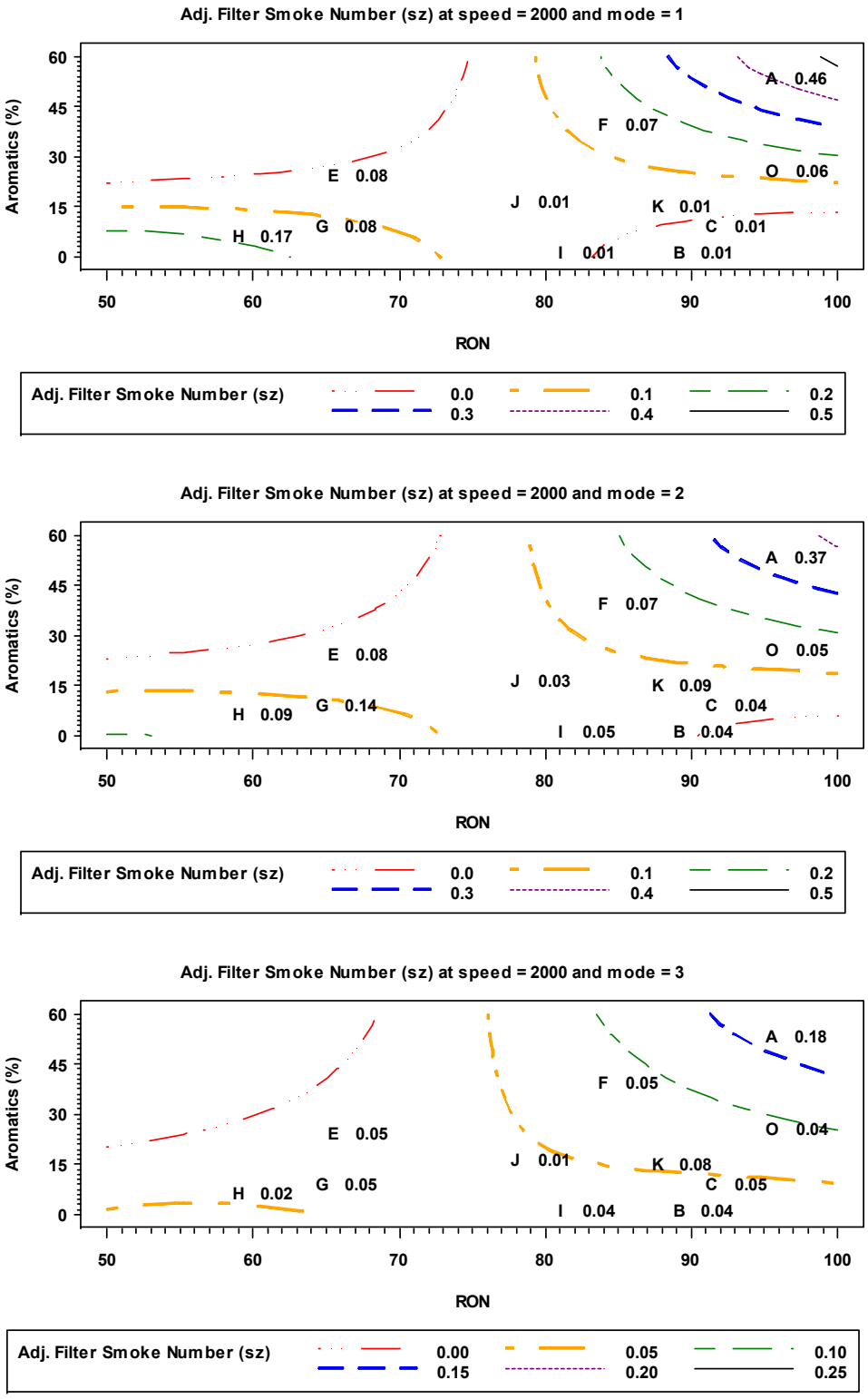

Figure Appendix E.1.2: Contour plots of adjusted filter smoke number under best ranked r2 model for 2000 RPM

Fuels in the range of less than 20 percent aromatics and greater than 75 RON showed lowest average smoke across all speed/modes. Fuels with either higher aromatics or lower RON (there were no fuels with both), displayed higher average smoke level.

E.2 COMBUSTION DURATION

Best r-Square Model: Combustion Duration (CA)

		Predictor Variables		Model Coefficients				Standard		Overall Model p-
speed	mode	P1	P2	Intercept	P1	P2	P1 * P2	Deviation	RSquare	Value
1000	1	Aromatics	i_Paraffins	17.12 **	0.07	-0.04 **	-0.004	0.421	88%	0.004
1000	2	Aromatics	i_Paraffins	15.50 **	0.2	-0.02	-0.01 *	0.606	71%	0.049
1000	3	Olefins	i_Paraffins	14.12 **	-0.88	-0.04	0.03	0.820	54%	0.176
2000	1	Olefins	Distillation_90	4.58 **	-0.02	0.01 *	0.0002	0.232	74%	0.036
2000	2	C4	RON	10.55 **	0.06	-0.03	-0.003	0.157	88%	0.003
2000	3	n_Paraffins_woC4	Sensitivity	6.29 **	0.08 **	0.15 **	-0.01 **	0.268	85%	0.007
3000	1	n_Paraffins_woC4	Distillation_10	27.09 **	-2.03 **	-0.12 **	0.01 **	0.592	94%	0.000
3000	2	i_Paraffins	Sensitivity	11.44 **	-0.05 **	0.26	-0.01	0.519	75%	0.029
3000	3	n_Paraffins_woC4	RON	-0.93	0.61 *	0.11 *	-0.01 *	0.361	72%	0.043

Best Ranked r-Square Model: Combustion Duration (CA)

		Predictor Variables		Model Coefficients				Standard		Overall Model p-
speed	mode	P1	P2	Intercept	P1	P2	P1 * P2	Deviation	RSquare	Value
1000	1	n_Paraffins_woC4	Distillation_10	31.65 **	-0.93 *	-0.12 **	0.01 **	0.482	84%	0.008
1000	2	n_Paraffins_woC4	Distillation_10	26.87 **	-1.04	-0.09 *	0.01 *	0.721	58%	0.131
1000	3	n_Paraffins_woC4	Distillation_10	22.12 *	-0.16	-0.06	0.002	0.972	35%	0.429
2000	1	n_Paraffins_woC4	Distillation_10	13.16 **	-0.25	-0.03 *	0.002	0.288	59%	0.123
2000	2	n_Paraffins_woC4	Distillation_10	11.47 **	-0.14	-0.03 *	0.001	0.238	73%	0.037
2000	3	n_Paraffins_woC4	Distillation_10	12.50 **	-0.2	-0.04	0.002	0.412	65%	0.080
3000	1	n_Paraffins_woC4	Distillation_10	27.09 **	-2.03 **	-0.12 **	0.01 **	0.592	94%	0.000
3000	2	n_Paraffins_woC4	Distillation_10	18.30 **	-0.52	-0.07	0.004	0.602	67%	0.069
3000	3	n_Paraffins_woC4	Distillation_10	13.61 **	-0.42	-0.03	0.003	0.446	57%	0.143

Note: Response values have been adjusted by TL22, MFB 50, and PI at speeds = 2000 and by TL22, MFB 50, and PR_CYP at speeds = 3000.
* Significant at 0.05 Level of Significance
** Significant at 0.01 Level of Significance

E.3 COMBUSTION NOISE

Best r-Square Model: Combustion Noise (dB)

		Predictor Variables		Model Coefficients				Standard		Overall Model p-
speed	mode	P1	P2	Intercept	P1	P2	P1 * P2	Deviation	RSquare	Value
1000	1	Aromatics	n_Paraffins_woC4	72.63 **	0.12	0.21 *	-0.01	0.850	61%	0.108
1000	2	Aromatics	n_Paraffins_woC4	71.99 **	0.12	0.24 *	-0.01	0.910	63%	0.097
1000	3	i_Paraffins	RON	59.30 **	0.44 *	0.18	-0.01 *	0.873	61%	0.106
2000	1	Olefins	Sensitivity	86.23 **	-0.28	0.09	0.03	0.996	49%	0.230
2000	2	i_Paraffins	Sensitivity	87.50 **	-0.01	1.29	-0.04	1.680	25%	0.600
2000	3	Aromatics	Distillation_10	99.39 **	-0.83	-0.07	0.005	1.433	29%	0.529
3000	1	i_Paraffins	C4	96.14 **	-0.07 *	-0.34	0.01	0.345	73%	0.037
3000	2	i_Paraffins	C4	95.90 **	-0.08 *	-0.5	0.02 *	0.438	56%	0.151
3000	3	i_Paraffins	C4	96.42 **	-0.10 *	-0.67 *	0.02 *	0.544	58%	0.135

Best Ranked r-Square Model: Combustion Noise (dB)

		Predictor Variables		Model Coefficients				Standard		Overall Model p-
speed	mode	P1	P2	Intercept	P1	P2	P1 * P2	Deviation	RSquare	Value
1000	1	Aromatics	n_Paraffins_woC4	72.63 **	0.12	0.21 *	-0.01	0.850	61%	0.108
1000	2	Aromatics	n_Paraffins_woC4	71.99 **	0.12	0.24 *	-0.01	0.910	63%	0.097
1000	3	Aromatics	n_Paraffins_woC4	72.46 **	0.13	0.21 *	-0.01	0.956	54%	0.175
2000	1	Aromatics	n_Paraffins_woC4	86.07 **	0.03	-0.02	-0.001	1.313	11%	0.861
2000	2	Aromatics	n_Paraffins_woC4	88.32 **	-0.08	-0.12	0.01	1.794	15%	0.796
2000	3	Aromatics	n_Paraffins_woC4	88.27 **	-0.09	-0.14	0.01	1.453	27%	0.565
3000	1	Aromatics	n_Paraffins_woC4	93.27 **	0.01	0.02	0.00003	0.541	34%	0.436
3000	2	Aromatics	n_Paraffins_woC4	93.21 **	-0.0006	0.01	0.0003	0.647	5%	0.959
3000	3	Aromatics	n_Paraffins_woC4	92.95 **	0.01	0.02	-0.001	0.827	3%	0.981

Note: Response values have been adjusted by TL22, MFB 50, and PI at speeds = 2000 and by TL22, MFB 50, and PR_CYP at speeds = 3000.
* Significant at 0.05 Level of Significance
** Significant at 0.01 Level of Significance

E.4 PEAK CYLINDER PRESSURE

Best r-Square Model: Peak Cylinder Pressure (bar)

		Predictor Variables		Model Coefficients				Standard		Overall Model p-
speed	mode	P1	P2	Intercept	P1	P2	P1 * P2	Deviation	RSquare	Value
1000	1	Aromatics	RON	25.06 **	0.18	0.04	-0.002	0.633	29%	0.534
1000	2	Aromatics	i_Paraffins	30.44 **	-0.06	-0.03 **	0.001	0.233	87%	0.005
1000	3	Olefins	Distillation_10	18.94 **	-0.06	0.05	0.0009	0.878	48%	0.241
2000	1	Aromatics	C4	39.24 **	-0.03 *	-0.17 **	0.004	0.176	88%	0.004
2000	2	Aromatics	RON	36.23 **	0.07	0.04 **	-0.001	0.243	84%	0.008
2000	3	Olefins	i_Paraffins	38.29 **	0.26 *	0.02 **	-0.01	0.167	91%	0.002
3000	1	n_Paraffins_woC4	Distillation_90	42.04 **	-0.46	-0.0008	0.001	0.476	71%	0.046
3000	2	i_Paraffins	Distillation_10	44.88 **	-0.3	-0.05	0.002	0.515	58%	0.132
3000	3	Olefins	i_Paraffins	37.74 **	0.79 *	0.01	-0.03 *	0.515	68%	0.062

Best Ranked r-Square Model: Peak Cylinder Pressure (bar)

		Predictor Variables		Model Coefficients				Standard		Overall Model p-
speed	mode	P1	P2	Intercept	P1	P2	P1 * P2	Deviation	RSquare	Value
1000	1	Olefins	i_Paraffins	27.88 **	0.36	0.01	-0.01	0.657	23%	0.636
1000	2	Olefins	i_Paraffins	28.95 **	-0.17	-0.01	0.01	0.448	51%	0.201
1000	3	Olefins	i_Paraffins	28.73 **	0.81	0.002	-0.03	0.944	40%	0.351
2000	1	Olefins	i_Paraffins	37.48 **	-0.002	0.01	0.0009	0.225	80%	0.016
2000	2	Olefins	i_Paraffins	38.34 **	0.22	0.02 **	-0.01	0.247	83%	0.009
2000	3	Olefins	i_Paraffins	38.29 **	0.26 *	0.02 **	-0.01	0.167	91%	0.002
3000	1	Olefins	i_Paraffins	41.19 **	0.11	0.01	-0.004	0.863	5%	0.950
3000	2	Olefins	i_Paraffins	38.08 **	0.49	0.01	-0.02	0.619	40%	0.354
3000	3	Olefins	i_Paraffins	37.74 **	0.79 *	0.01	-0.03 *	0.515	68%	0.062

Note: Response values have been adjusted by TL22, MFB 50, and PI at speeds = 2000 and by TL22, MFB 50, and PR_CYP at speeds = 3000.
* Significant at 0.05 Level of Significance
** Significant at 0.01 Level of Significance